Effects of A Gap Junction Inhibitor on Stem Cell Retention and Efficacy During Early Myocardial Ischemia

BY

SANTIPONGSE CHATCHAVALVANICH
M.D., Mahidol University, 2002

THESIS

Submitted as partial fulfillment of the requirements
for the degree of Doctor of Philosophy in Physiology and Biophysics
in the Graduate College of the
University of Illinois at Chicago, 2012

Chicago, Illinois

Defense Committee:

R. John Solaro, Chair
David L. Geenen, Advisor
Kathrin Banach
Ahlke Heydemann
Mark M. Rasenick
Nadim Mahmud, Bioengineering

This thesis is dedicated to the memory of my grandparents,

Charoen and Duangkamol Chatchavalvanich,

who appreciated the importance of education,

for without them I would not be who I am today.

ACKNOWLEDGEMENT

This dissertation would not have been possible without the support from many wonderful people throughout the course of my study. First and foremost, I would like to tremendously thank Dr. David Geenen, my mentor and thesis advisor, for his continued support, guidance, and encouragement. Despite his busy schedule, he always makes himself available for his students. I could not stress enough how grateful I am to him for everything he has done.

I sincerely thank all members of my thesis committee which includes my thesis advisor Dr. Geenen as well as Dr. Kathrin Banach, Dr. Ahlke Heydemann, Dr. Nadim Mahmud, Dr. Mark Rasenick, Dr. John Solaro; and additionally Dr. John Kennedy who was part of the committee, for all their time, support and advice over the past years.

I would like to thank member of Geenen lab especially Dr. Liliana Grajales and Dr. Shamim Chowdhury who have become my 'best friends' and are like my older sisters over the years; Dr. Robert Boomsma for his friendship and help in the gap junction study.

Furthermore, I would like to thank all past and present members of Department of Physiology and Biophysics and Section of Cardiology research labs for providing such a wonderful environment to work with. Specifically, Dr. Beata Wolska for her support, advice, compassion, and friendship. Dr. Jaime DeSantiago for his friendship and help with heart digest study. Dr. Paul Goldspink who provided his expertise and advice on adenoviral works.

ACKNOWLEDGEMENT (continued)

I especially thank all the administrative staff (past and present) of Department of Physiology and Biophysics, particularly Kathleen Engstorm, Janice Gentry, Jennifer Guthrie, Elzbieta Klapczynska, Laura Scott, and Marian Johnson-Powell, for all their patience, assistant, and friendship through the program.

I am thankful for all of my friends here in the United States for their friendship, especially Dr. Sudarat Nimitvilai and Dr. Witchuda Saengsawang. Moreover, I truly appreciate Steven Altman for his friendship, company and tremendous patience and support during the last few years. Lastly, I would like to thank my family for their unwavering love, support, understanding and encouragement for all these years.

SC

TABLE OF CONTENTS

TABLE OF CONTENTS (continued)

TABLE OF CONTENTS (continued)

LIST OF TABLES

LIST OF FIGURES

LIST OF FIGURES (continued)

FIGURE PAGE

LIST OF ABBREVIATIONS

11β-HSD1	11 beta-hydroxysteroid dehydrogenase type 1
αSMA	alpha sarcomeric actinin
BM-MSC	Bone marrow-derived mesenchymal stromal/stem cells
CBX	Carbenoxolone
cTnI	Cardiac troponin I
cTnT	Cardiac troponin T
Cx	Connexin
CXCR4	CXC-chemokine receptor 4
CVEC	Canine vascular endothelial cells
dP/dt	Derivative pressure product
EDPVR	End-diastolic pressure–volume relation
E_{es}	End-systolic elastance
eGFP	Enhanced green fluorescent protein
E_{max}	Maximum elastance
ESPVR	End-systolic pressure–volume relationship
FBS	Fetal bovine serum
HGF	Hepatocyte growth factor
G-CSF	Granulocyte colony stimulating factor
GFP	Green fluorescent protein
G_i	Inhibitory regulative G-proteins
GPCR	G protein-coupled receptor

LIST OF ABBREVIATIONS (continued)

GRK	G protein-coupled receptor kinase
HIF-1	Hypoxia-inducible factor-1
HSC	Hematopoietic stem cells
IFN	Interferon
IGF	Insulin-like growth factor
iNOS	Inducible nitric oxide synthase
IL	Interleukin
LV	Left ventricular
MCP	Monocyte chemoattractant protein
MI	Myocardial infarction
MIG	Monokine induced by interferon gamma
MIP	Macrophage inflammatory protein
MOI	Multiplicity of infection
MSC	Mesenchymal stromal/stem cells
M-CSF	Macrophage colony stimulating factor
NMVM	Neonatal mouse ventricular myocytes
PBS	Phosphate buffered saline
PCR	Polymerase chain reaction
PDGF	Platelet-derived growth factor
PGE2	Prostaglandin E2
PI	Propidium iodide

LIST OF ABBREVIATIONS (continued)

PI3K	Phosphoinositide-3 kinase
PLC-β	Phospholipase C-beta
RT-PCR	Reverse transcriptase polymerase chain reaction
SDF-1	Stromal cell-derived factor-1
TGF	Transforming growth factor
TNF	Tumor necrosis factor
TTC	2,3,5-triphenyltetrazolium chloride
TUNEL	Terminal deoxynucleotidyl transferase dUTP nick end labeling
VEGF	Vascular endothelial growth factor

SUMMARY

Myocardial infarction is one of the major causes of morbidity and mortality worldwide. Death of cardiomyocytes caused by disruption of blood supply and further exacerbated by restoration of blood flow results in remodeling of cardiac architecture and deterioration of cardiac function. Cardiac regenerative therapy using stem/progenitor cells has increasingly gained considerable attention over the past decade. Several cell types have been proposed as suitable sources to be used and extensive studies reported varying degrees of beneficial effects. Bone marrow-derived mesenchymal stromal cell (BM-MSC) is one of the potential cell types due to its relative ease of harvesting and minimal ethical controversy. Nevertheless, our laboratory and others have demonstrated a dramatic loss of the transplanted cells within hours of administration. Since the number of cells in treatment correlates with their beneficial effects, prevention of the loss of stem cells should enhance their effectiveness and augment their benefits. To achieve this goal, we examined the role of CXC-chemokine receptor 4 (CXCR4) and its cognate ligand, stromal cell-derived factor-1 (SDF-1) on BM-MSC migration and retention. Additionally, we also investigated the involvement of gap junction communication in inducing death of newly transplanted BM-MSCs.

We used adenoviral expression of CXCR4 in our BM-MSC culture to study the effects of CXCR4 overexpression on BM-MSC migration and retention in the heart after ischemic injury, Contrary to our expectation cells overexpressing CXCR4 demonstrated markedly

lower migration toward an SDF-1 gradient when compared to MSCs transduced with control AdGFP. Interestingly, AdCXCR4-transduced BM-MSCs treated with AMD3100 (a CXCR4 antagonist) displayed increased migration when compared to SDF-1- and SDF-1+AMD3100-treated groups under normoxic conditions. Nevertheless, the overexpression of CXCR4 in BM-MSC showed a trend in increasing retention of BM-MSCs in the heart suffering from ischemia–reperfusion injury.

We also demonstrated that coculturing BM-MSCs with hypoxic HL-1 myocytes could induce death and apoptosis of BM-MSC when compared to BM-MSCs cocultured with normoxic HL-1s. Although it is worth mentioning that the conditions under which the cells were cultured affected the ratio between dead and apoptotic cells. Coculturing under hypoxic conditions resulted in a higher number of dead cells while normoxic cocultures had more apoptotic cells. The presence of the gap junction uncoupler carbenoxolone (CBX) in the coculture significantly reduced the number of both dead and apoptotic cells in both groups.

To further determine the beneficial effects of CBX—treated MSCs, we performed *in vivo* experiments using a mouse model of ischemia–reperfusion injury. Digests from whole hearts with injected MSCs demonstrated a trend toward increased BM-MSCs in the hearts that received CBX-treated cells compared to the hearts that received untreated cells. The change in cell number could not be attributed to increased cell proliferation as indicated by

our *in vitro* experiments. Hemodynamic studies recapitulated the beneficial effects of MSC as reported previously and were consistent with our *in vitro* studies. End-systolic elastance, maximum elastance, and ±dP/dt were enhanced in animals treated with CBX-treated BM-MSCs compared to untreated controls. The protective effects of CBX-treated BM-MSC could not be achieved by the administration of vehicle with CBX alone. Lastly, we did not observe any significant difference in area-at-risk or infarct size in this study.

Overall, our data indicate that early massive loss of transplanted stem cells may be mediated in part by coupling of stem cells with hypoxic cardiomyocytes and interfering with this gap junction-mediated intercellular communication results in a significant improvement of cardiac function after ischemia–reperfusion injury.

I. INTRODUCTION

1. Background

1. Myocardial Infarction

Myocardial infarction (MI) is "cell death of cardiac myocytes caused by ischemia, which is the result of a perfusion imbalance between supply and demand", resulting in the loss of cardiomyocytes which is one of the major causes of morbidity and mortality worldwide (Thygesen, Alpert, & White, 2007). Consequent depressed contractility leads to impaired cardiac function which if left untreated will result in heart failure and eventual death of the patient. Current American Heart Association guidelines for management of MI mainly focus on medical treatment followed by lifestyle adjustment and coronary artery revascularization(Antman, et al., 2004; Kushner, et al., 2009). Although rates of death attributable to cardiovascular diseases, including MI, have declined in the recent years, MI still has a significant impact with overall prevalence of 3.1% in US adults age 20 years and above and estimated annual incidences of 610,000 new and 325,000 recurrent attacks. (Roger, et al., 2012).

Death of cardiomyocytes affected by MI occurs through all three pathways of cell death; autophagy, apoptosis, and necrosis (Chiong, et al., 2011). After the onset of ischemia, the death of cardiomyocytes develops over a finite period, the length of which is affected by several factors such as collateral circulation to ischemic area, type of coronary occlusion,

and sensitivity of myocytes (Thygesen, Alpert, & White, 2007). In clinical context, restoration of blood flow is necessary to salvage the ischemic cardiomyocytes, however, reperfusion and reoxygenation to the tissue are usually associated with exacerbation of the injury and significant inflammatory response, termed "reperfusion injury" (Eltzschig & Eckle, 2011). Several mechanisms are responsible for the death of cardiomyocytes including calcium overload, mitochondrial permeability transition, and cellular fragility; and treatments that interfere with these mechanisms can reduce the infarct size (Ruiz-Meana & Garcia-Dorado, 2009). Furthermore, a group of ligands known as "damage-associated molecular patterns", that is released into the extracellular compartment upon tissue damage, causes recruitment and activation of cells of both innate and adaptive immune system and activation of the compliment system which contribute further to damage of the tissue (Eltzschig & Eckle, 2011).

Myocardial infarction causes changes in cardiac architecture and corresponding deterioration of cardiac hemodynamic functions. Cardiac remodeling after MI is characterized by progressive left ventricular dilation, rearrangement of myocardial wall structure, hypertrophic myocytes, and eccentric hypertrophy(Bolognese & Cerisano, 1999) which occur alongside functional changes which include increased left ventricular end-diastolic pressure, decreased left ventricular rate of pressure development (dP/dt), and decreased systolic pressure among other findings (Anversa, Olivetti, & Capasso, 1991).

1.2 Stem Cells in Cardiac Regenerative Therapy

During the past decade, the concept that the heart is a terminally differentiated organ has been challenged. Several studies have shown that the heart contains a population of self-renewing progenitor cells that can differentiate into and replenish cardiomyocytes both in physiologic and pathologic conditions (Beltrami, et al., 2003; Hidesama, et al., 2003; Laugwitz, et al., 2005; Martin, et al., 2004). These findings provide a rationale for the use of stem cell replacement therapy in myocardial ischemia and infarction.

Several sources of cells have been identified and studied for use in cell-based cardiac therapy including adult stem cells (e. g. bone marrow-derived stem cells, mesenchymal stem cells, skeletal muscle cells) and embryonic stem cells (Christoforou & Gearhart, 2007). Previous studies have shown that bone marrow-derived stem cell administration or mobilization following myocardial infarction can improve cardiac function (Glimm, Oh, & Eaves, 2000; Muller-Borer, et al., 2004; Wobus, et al., 1997). Moreover, a recent systematic review of clinical trials examining the effectiveness of adult bone marrow-derived stem cells in treatment of acute MI showed that stem cell treatment significantly improves global heart function although it did not significantly affect the incidence of mortality or morbidity (Clifford, et al., 2012). They also observed a correlation between stem cells dose and their effect of preserving ejection fraction. Our laboratory and several others have also demonstrated improved function following administration of stem cells both in animal models (Boomsma, Swaminathan, & Geenen, Intravenously Injected

Mesenchymal Stem Cells Home to Viable Myocardium after Coronary Occlusion and Preserve Systolic Function without Altering Infarct Size., 2007) and in transplanted human hearts (Angelini, et al., 2007; Quaini, et al., 2002; Laflamme, Myerson, Saffitz, & Murry, 2002; Muller, et al., 2002).

Mesenchymal stromal cells (MSC) are non-hematopoietic stromal cells isolated from bone marrow and other connective tissues which possess the potential to differentiate into cells of several lineages including osteocytes, chondrocytes, adipocytes, fibroblasts, epithelial cells, myocytes, and neurons (Fong, Chan, & Goodman, 2011). The International Society for Cellular Therapy proposed that MSC should meet three criteria: First, MSC must be plastic adherent under standard cell culture conditions; Second, MSC must express CD105, CD73, and CD90; and lack the expressions of CD45, CD34, CD14 or CD11b, CD79α or CD19, and HLA class II; Third, MSC must be able to differentiate to osteocytes, adipocytes, and chondroblasts under standard *in vitro* differentiation conditions (Dominici, et al., 2006). Although with the criteria present, MSC still contain a considerable heterogeneous population and their heterogeneity is even more pronounced when comparing studies from different investigators (Clifford, et al., 2012).

Stem cells exert their effects through different proposed mechanisms including transdifferentiation of stem cells into cardiomyocytes, fusion of stem cells to existing cardiomyocytes, and secretion of paracrine factors(Gnecchi, Danieli, & Cervio, 2012; Cashman, Gouon-Evans, & Costa, 2012) although which of these mechanisms is more

important is yet to be established. Regardless of whether MSCs differentiate upon mobilization and engraftment or produce a paracrine effect within the target organ following an inflammatory event, it is well documented that these cells produce functional benefits to the ischemic heart (Hill, et al., 2003; Li, et al., 2007; Uemura, Xu, Ahmad, & Ashraf, 2006; Wu, et al., 2006; Xu, Uemura, Dai, Wang, Pasha, & Ashraf, 2007). A recent systematic review of clinical trials also affirms that stem cell treatment improves heart function and their beneficial effect positively correlates with the dose infused (Clifford, et al., 2012).

Stem cells have classically been defined by their self-renewal capacity and multipotency (Williams & Hare, 2011). Unenriched bone marrow-derived mesenchymal stromal cells (BM-MSCs) from whole bone marrow harvests subjected to multiple passages do not exhibit hallmarks of excitable tissue and fail to generate action potentials or express functional calcium channels. In contrast, our laboratory and others have demonstrated that BM-MSC could be induced to transdifferentiate into myogenic cells displaying cardiac phenotypes (Grajales, García, Banach, & Geenen, 2010; Asumda & Chase, 2012; Ramesh, Bishi, Rallapalli, Arumugam, Cherian, & Guhathakurta, 2012; Mohanty, Bose, Jain, Bhargava, & Airan, 2011). We have recently demonstrated (Grajales, García, Banach, & Geenen, 2010) that delayed enrichment of murine BM-MSCs for specific stem cell markers combined with cell culture conditions to promote differentiation results in electrically active cells exhibiting calcium transients.

Induction of MSC transdifferentiation to cardiomyocytes can be achieved by several means. Majority of established protocols use 5-azacytidine as a cardiogenic inducer but recent works have shown different conditions that can be use to achieve similar result such as low serum media (Grajales, García, Banach, & Geenen, 2010), conditioned media from ischemic myocardium (Ramesh, Bishi, Rallapalli, Arumugam, Cherian, & Guhathakurta, 2012), transforming growth factor beta (TGF-β) (Mohanty, Bose, Jain, Bhargava, & Airan, 2011) and coculture with cardiomyocytes (Wang, Xu, Jiang, & Ma, 2006; Koninckx, et al., 2009). Differentiated MSC have been shown to express cardiac specific markers such as cardiac troponin I (cTnI), cardiac troponin T (cTnT), alpha sarcomeric actinin (αSMA), myosin heavy chain, desmin, Nkx2.5, and GATA-4 although the results vary between investigators. Several investigators also observed cardiomyocyte-associated features such as sarcomeric organization, contraction and spontaneous intracellular calcium transients (Grajales, García, Banach, & Geenen, 2010; Ramesh, Bishi, Rallapalli, Arumugam, Cherian, & Guhathakurta, 2012) while others observed expression of cardiac markers but not cardiac phenotypes (Rose, et al., 2008; Siegel, et al., 2012). Nevertheless, this cell phenotype may be important to overall functional integration *in vivo*.

Paracrine factors have been proposed as one of MSC mechanisms of action since the disparity between substantial functional improvement and low frequency of MSC engraftment and differentiation (Williams & Hare, 2011). The secreted factors have a wide array of effects including suppression of the immune system, induction of angiogenesis,

stimulation of stem cell differentiation, and inhibition of fibrosis and apoptosis. A recent work from our laboratory demonstrated increased levels of vascular endothelial growth factor (VEGF), monocyte chemoattractant protein-1 (MCP-1), macrophage inflammatory protein-1 alpha (MIP-1α), macrophage inflammatory protein-1 beta (MIP-1β), and monokine induced by interferon gamma (MIG)(Boomsma & Geenen, Mesenchymal Stem Cells Secrete Multiple Cytokines That Promote Angiogenesis and Have Contrasting Effects on Chemotaxis and Apoptosis, 2012). This study also showed that conditioned media from MSC culture was able to induced angiogenesis in canine vascular endothelial cells and reduced apoptosis in hypoxic H9c2 cells. Apart from this study, other factors has been identified over recent years including fibroblast growth factors (FGF), platelet-derived growth factor (PDGF), TGF-β, matrix metalloproteinases, plasminogen activator, tumor necrosis factor alpha, granulocyte colony stimulating factor (G-CSF), insulin-like growth factor-1 (IGF-1), macrophage colony stimulating factor (M-CSF), stromal cell-derived factor, hepatocyte growth factor (HGF), inducible nitric oxide synthase (iNOS), interleukin-6 (IL-6), and prostaglandin E2 (PGE2) (Williams & Hare, 2011).

In this project, we hypothesized that improving number of stem cells in the heart after myocardial ischemia could lead to better preservation of cardiac function. This could be achieve by either increase homing of stem cells to the target region or improve their retention in the affected site.

1.3 Stem Cell Migration and Homing

As previously stated, the number of stem cells given in stem cell therapy significantly correlates with functional improvement. Since effectiveness of stem cell therapy relies on number of cells that home and engraft in the target tissue, understanding of factors affecting homing to the target tissue and survival within target tissue environment could contribute to overall effectiveness of stem cell therapy.

Migration of MSC has been shown in response to injury of several organs and occurs through multi-step process (Fong, Chan, & Goodman, 2011). When the injury happens, signals from the injured organ cause a release of MSC from their niche into the circulation, a step usually refer to as mobilization. MSC, mobilized or injected, then migrate to and engraft in the target tissue where they exert functional effects, a process called homing. Several studies have demonstrated that MSC selectively home to the injured organ regardless of tissue (Yagi, et al., 2010). This has also been shown in a work from our laboratory where murine BM-MSC injected intravascularly significantly homed better to the heart of animals with MI (Boomsma, Swaminathan, & Geenen, Intravenously Injected Mesenchymal Stem Cells Home to Viable Myocardium after Coronary Occlusion and Preserve Systolic Function without Altering Infarct Size., 2007). Homing of MSC is poorly understood but the rather well described leukocyte and hematopoietic stem cell (HSC) homing processes are usually used as references to describe and investigate MSC homing

(Fong, Chan, & Goodman, 2011; Yagi, et al., 2010). Homing is multi-step process which constitutes rolling, integrin activation, firm adhesion, and extravasation.

Stem and progenitor cell therapy preserves cardiac function and improves coronary blood flow following ischemia. Nevertheless, a significant loss of progenitor cells from the myocardium occurs within hours after transplantation and likely diminishes the long-term benefits of cardiac regenerative therapy (Chedrawy, Wang, Nguyen, Shum-Tim, & Chiu, 2002; Pillekamp F. , et al., 2009; Rota, et al., 2007; Xue, et al., 2005).

1.4 CXC-Chemokine Receptor 4 and Stromal Cell-Derived Factor-1

Chemokines are small (8–10 kDa) secreted proteins that are important regulators of stem cell mobilization, trafficking and homing (Fong, Chan, & Goodman, 2011). They can be categorized, based on whether their conserved cysteine residues are separated by an amino acid, into 2 main subfamilies: CXC and CC chemokines (Burger & Kipps, 2006). Chemokine receptors are seven transmembrane domain, G protein-coupled receptors (GPCRs) which coupled to pertussis toxin sensitive inhibitory regulative G-proteins (G_i), expressed on surface of many different cell types and named according to their preference for certain chemokines: CXCR1 through CXCR5, CCR1 through CCR11, XCR1, and CX3CR1(Busillo & Benovic, 2007; Burger & Kipps, 2006). Honczarenko and colleagues (Honczarenko, Le, Swierkowski, Ghiran, Glodek, & Silberstein, 2006) identified expression

of a unique set of six chemokines receptors in human BM-MSC (CCR1, CCR7, CCR9, CXCR4, CXCR5, and CXCR6) while another group (Sordi, et al., 2005) observed different but overlapping set of chemokine receptors (CCR1, CCR7, CXCR4, CXCR6, and CX3CR1).

CXC chemokine receptor 4 (CXCR4), and its ligand, stromal cell-derived factor-1 (SDF-1, CXCL12), has been shown to be essential for migration of and engraftment into bone marrow by human severe combined immunodeficient repopulating stem cells (Peled, et al., 1999; Wen, Zhang, Huang, & Wang, 2012). CXCR4, also known as CD184 and fusin, is a 39.7 kDa seven-transmembrane GPCR with structure similar to rhodopsin. It was originally identified as an orphan receptor called leukocyte-derived seven-transmembrane domain receptor (LESTR)(Alkhatib, 2009) but gained more attention after the discovery of its natural ligand, SDF-1, and its function as a coreceptor for fusion and entry of T-tropic human immunodeficiency virus into $CD4^+$ T cells (Feng, Broder, Kennedy, & Berger, 1996; Alkhatib, 2009). *Cxcr4* gene is expressed in 2 isoforms: The main isoform and primary receptor of SDF-1, CXCR4, which comprises 352 amino acids and the longer, less abundant CXCR4-LO isoform. CXCR4's N-terminus and three extracellular loop domains constitute ligand binding complex while its intracellular C-terminus and three intracytoplasmic loops associate with and activate G_i family of G proteins (Sharma, Afrin, Satija, Tripathi, & Gangenahalli, 2011). CXCR4 transcription is positively controlled by nuclear respiratory factor-1 (NRF-1) and possibly SP-1, and negatively by Ying Yang 1 (YY1). Furthermore, CXCR4 transcription can be upregulated by several molecules including calcium, cyclic AMP,

several ILs, TGF-1β, and growth factors and downregulated by inflammatory cytokines such as tumor necrosis factor-alpha (TNF-α), interferon-gamma (IFN-γ), and IL-1β (Busillo & Benovic, 2007). Additionally, CXCR4 can undergo posttranslational modification by N-linked glycosylation and tyrosine sulfation, both of which alter the binding of SDF to the receptor.

Activation of CXCR4 by SDF-1 binding causes conformational change in the receptor and phosphorylation of serine and threonine residues within the third intracytoplasmic loop and C-terminus, enabling association with and activation of intracellular heterotrimeric G protein (Alkhatib, 2009). Activated heterotrimeric G protein dissociates into G_i and Gβγ subunits. Then the liberated G_i is able to inhibit adenylyl cyclase and activate Src family of tyrosine kinases while Gβγ subunit activates phospholipase C-beta (PLC-β) and phosphoinositide-3 kinase (PI3K) (Busillo & Benovic, 2007). Majority of signaling pathways and biological outcomes of CXCR4 activation are G-protein dependent while the G-protein-independent signaling involves activation of JAK/STAT pathway. Signaling through CXCR4, similar to other GPCRs, can be primarily regulated by three processes: desensitization, internalization, and degradation. Desensitization is achieved through phosphorylation of serine or threonine residues of the third intracytoplasmic loop or C-terminus by G protein-coupled receptor kinase (GRK) following receptor activation, and successive binding of arrestin-2 and/or arrestin-3 which uncouple the receptor from G protein activation (Busillo & Benovic, 2007). Binding of arrestin also often targets the

receptor and results in endocytosis of the receptor complex, termed internalization. The internalized receptor will be subsequently either recycled to plasma membrane, or sorted to lysosomal for degradation. Internalization of CXCR4 requires intact C-terminus as evidenced in WHIM (warts, hypogammaglobulinemia, infections, and myelokathexis) syndrome where frameshift mutation resulted in truncation of the receptor's C-terminal tail and consequent constitutively active receptor (Busillo & Benovic, 2007). Recent evidence indicated additional way of modulation in which products released during inflammatory responses or platelet activation can "prime" CXCR4 for SDF-1 activation, the ensuing sensitization of CXCR4 is dependent on incorporation of the receptor into membrane lipid rafts (Busillo & Benovic, 2007; Ratajczak, et al., 2012).

SDF-1 was initially isolated from murine bone marrow stromal cells and identified as pre-B-cell growth stimulating factor (PBSF) (Nagasawa, et al., 1996). The predominant form of SDF-1 is the 89 amino acids SDF-1α. Other five splice variants of SDF-1 have been identified, with varying tissue distribution, but their significances are still unknown(Busillo & Benovic, 2007). SDF-1 is a highly conserved protein with 99% homology between mouse and human, allowing cross-reaction between species(Alkhatib, 2009; Burger & Kipps, 2006). SDF-1 is constitutively secreted by several cell types including bone marrow stromal cells and putatively sequesters MSC inside the bone marrow in physiologic condition and has been implicated in migration, proliferation, differentiation, and survival of several cell types (Fong, Chan, & Goodman, 2011; Lapidot & Kollet, 2002). Unlike most

chemokines and chemokine receptors, SDF-1 and CXCR4 have been originally demonstrated to be binding exclusively to each other as indicated by almost identical phenotypes observed in mice with either *Cxcr4* or *Cxcl12* gene knocked out: embryonic lethality, abnormal neuronal and cardiovascular development, and deficient B-lymphopoiesis and myelopoieses (Alkhatib, 2009). Although SDF-1 has been showed recently to bind to another GPCR, CXCR7, the effect of SDF-1 in this context is yet to be characterized due to more restricted surface expression of the receptor (Cencioni, Cencioni, Capogrossi, & Napolitano, 2012).

SDF-1 and CXCR4 together play an important role in hematopoiesis, development, and organization of the immune system (Burger & Kipps, 2006). SDF-1 can induce migration of human MSC in *in vitro* migration assay and the effect could be blocked by a blocking antibody against CXCR4(Sordi, et al., 2005). Moreover, hypoxia-inducible factor-1 (HIF-1) which is a central mediator of tissue hypoxia induces SDF-1 expression proportionally to reduced oxygen tension (Burger & Kipps, 2006). SDF-1 has been shown as one of chemoattractants with increased expression in infarcted myocardium which peaked at around 48 hours after MI (Kucia, et al., 2004). This data and our work showing more of injected MSCs home to the heart affected by MI (Boomsma, Swaminathan, & Geenen, Intravenously Injected Mesenchymal Stem Cells Home to Viable Myocardium after Coronary Occlusion and Preserve Systolic Function without Altering Infarct Size., 2007) suggests that CXCR4–SDF-1 signaling could be essential for homing of MSC to target tissue.

In the first part of this study, we explored the possibility of improving migration and homing of MSC to the heart by increasing the expression of CXCR4 in MSCs by adenoviral transduction.

1.5 Gap Junction Intercellular Communication

The rapid loss of stem cells after transplantation could be a bystander effect which refers to the death of otherwise healthy cells induced by exposure to dying cells. A bystander effect has been described and studied extensively in radiation-induced injury and has been associated with gap junction intercellular communication. Communication between cells is important for maintenance and function of multicellular organisms. Gap junction is a type of specialized plasma membrane regions composes of several intercellular channels and mediates communication between neighboring cells via exchange of ions, second messengers and small metabolites allowing coupling between them. In the heart, gap junction intercellular communication capacitates functional syncytium of cardiomyocytes. Gap junction channel is a highly specialized membrane structure consisting of two apposing hemi-channels called connexons. Each connexon comprises six protein subunits, called connexins in chordate animals, surrounding a central pore. Connexins are ubiquitous and fundamental proteins involved in cell–cell coupling and intercellular communication via formation of gap junctions. Channels formed by the

connexins play a seminal role in organ development, cell growth, cell differentiation, and the maintenance of cell phenotypes within specific organs and system niches (Dbouk, Mroue, El-Sabban, & Talhouk, 2009; Kunze, et al., 2009; Leung, Unsicker, & Reuss, 2002; Pearson, Luneborg, Becker, & Mobbs, 2005; Reaume, et al., 1995; Rozental, et al., 1998). There are 21 connexin isoforms in human with diverse properties, regulations, and distribution (Maeda & Tsukihara, 2011). Gap junction channels could be formed by different type of connexons (heterotypic) or different composition of connexin isoforms in a connexon (heteromeric) which granted them divergent properties and functions. Recent studies demonstrate increasingly diverse roles for gap junctions and describe them as intercellular signaling complexes that alter cell functions and produce bystander effects in coupled cells (Dbouk, Mroue, El-Sabban, & Talhouk, 2009; Lin, et al., 1998; Peixoto, Ryu, Pruzansky, Kuriakose, Gilmore, & Kinnally, 2009; Ramachandran, Xie, John, Subramaniam, & Lal, 2007). Role of gap junction channels in propagation of cell death has been indicated in both physiological and pathological conditions. For example, in work by Cusato *et al.* it was demonstrated that gap junctions transmit apoptotic signals in developing retina (Cusato, et al., Gap Junctions Mediate Bystander Cell Death in Developing Retina, 2003). Maass *et al* has implicated the involvement of gap junction communication in infarct expansion and showed that preventing gap junction from closing resulted in increased infarct size in their model (Maass, Chase, Lin, & Delmar, 2009). Furthermore, Qiao *et al.* examined the changes in number of stem cells given intramyocardially and found that both

positron emission tomography scanning and reverse transcriptase polymerase chain reaction (RT-PCR) measurements of cell numbers showed a rapid decrease of transplanted cells within the first 24 hours of their administration which corresponded with an increase in percentage of apoptotic cells measured by terminal deoxynucleotidyl transferase dUTP nick end labeling (TUNEL) staining (Qiao, et al., 2009). The mechanism by which this occurs has not been elucidated but we speculated that it involves at least in part the coupling of BM-MSCs to cells in target organ and transmission of cellular metabolites, molecules and ions between target and engrafting cells.

The coupling of MSCs to cardiomyocytes has been shown by a dye transfer experiment in work by Chang *et al* (Chang, et al., 2006) and confirmed by data from our laboratory. We cocultured unlabeled MSCs to HL-1 myocytes double-labeled with CFMDA and Calcein Red/Orange for four hours. After the coculture, the cells were lifted and analyzed by flow cytometry. The increase in Calcein dye in MSCs which could be attenuated significantly by oleamide, a gap junction blocker, demonstrated that gap junction-mediated exchange of molecules between MSCs and cardiomyocytes actually happens and as early as 4 hours after coculture (Figure 1). To rule out the possibility of leakage of dye from HL-1 which can be taken into MSC and result in a false negative, we did the coculture experiment where the cells were in the same culture media but physically separated by porous membrane which prevent physical interaction between two cell populations and detected negligible amount of Calcein-positive MSCs in this control group.

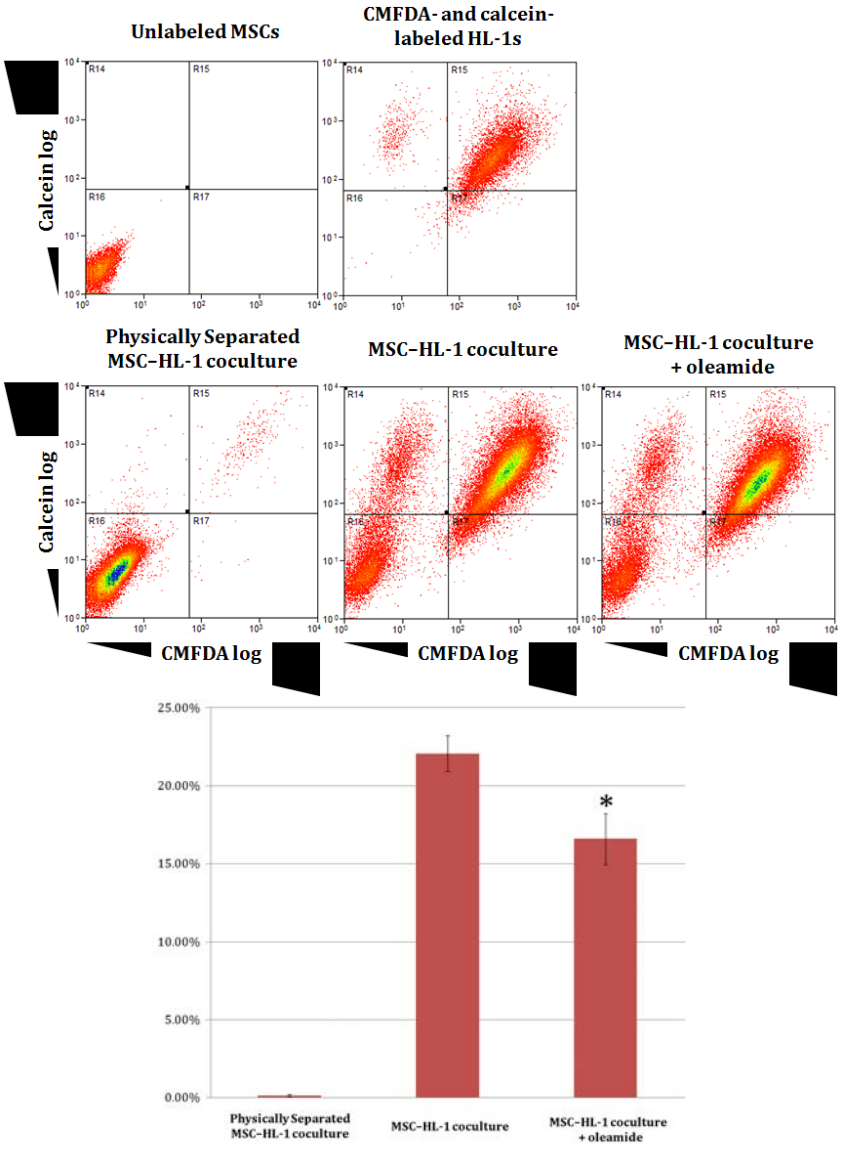

Figure 1: Dye-transfer experiments between MSC and HL-1. HL-1s loaded with cell-impermeant CMFDA and gap junction-permeant calcein dyes were cocultured with unlabeled MSCs for 4 hours with or without gap junction blocker oleamide. Top: representative data from each experimental group. Bottom: Summary of data comparing percentage of MSC that is positive for calcein. n = 3, 6, and 3, respectively. *: statistically significant when compared to coculture without oleamide, $p<0.05$.

Several studies also report a role for connexins in regulating bone marrow cell proliferation and differentiation (Villars, et al., 2002; Rose, et al., 2008; Durig, et al., 2000). These studies are also clinically relevant because regardless of the cell type used in regenerative therapy (e.g. embryonic stem cell, induced-pluripotent stem cell, BM-MSC), understanding the mechanism(s) behind cell coupling and integration is key to enhancing the potential benefits of cardiac regenerative therapy.

The failure to decipher the mechanisms responsible for cell–cell coupling is not unique to BM-MSCs. There has been much attention placed on whether these stem cells and others (e.g. embryonic and induced-pluripotent stem cells) can differentiate upon transplantation while mechanisms responsible for coupling and integration have not been elucidated. The ability of the transplanted cell to couple and integrate *in vivo* is also dependent on the environment within the target tissue, the method of delivery, and characteristics of the cell that might enhance coupling. This is a critical barrier to the field because without understanding the mechanisms that affect cell integration, regenerative therapy employing embryonic, induced-pluripotent, or somatic stem cells will be transient at best and potentially arrhythmogenic. Furthermore, the cardiac environment into which these cells "home" or are transplanted *in vivo* undergoes inflammation, ischemia/hypoxia, and deposition of scar tissue. Thus our aim is to determine the effect of these factors on coupling and communication of the cells under ischemic conditions within the myocardium.

Until recently, the primary role of connexins in cell–cell coupling was thought to be the formation of gap junctions and the exchange of ions through these intercellular channels. But the concept of the gap junction has changed considerably to where connexins and their junctional components are now thought to be complex signaling sites and control a number of other cellular functions. Electrical integration is an essential component in smooth propagation of the action potential and in regenerative medicine a great deal of attention has been paid to promoting gap junction formation as a means to integrate newly administered stem cells into the existing myocardium. In contrasts, very little is known about the detrimental effects of early cell–cell coupling on stem cell retention within the ischemic myocardium despite evidence that gap junctions mediate a bystander effect.

Overall hypothesis of this study is that gap junction channels are at least partially responsible for the propagation of cell death from hypoxic cardiomyocytes to the stem cells and caused the loss observed shortly after their transplantation. We examined roles of gap junction channels in this context by utilizing both *in vitro* and *in vivo* experimental models to elucidate our questions.

2. Specific Aims

The objective of this thesis project was to examine the factors affecting homing and survival of newly transplanted MSCs in the ischemic myocardium. The first part of the project explored the potential contribution of CXCR4 to regulating migration and retention of MSCs. The second part addressed the role of gap junction and cell–cell coupling in survival and retention of MSCs *in vitro*. And in the last series of experiments, we determined the effect of inhibiting cell–cell coupling on the ability of transplanted MSCs to attenuate cardiac dysfunction following ischemia. To achieve these goals, the following specific aims, hypotheses and experimental approaches were established:

2.1 Specific Aim #1: To determine the involvement of CXCR4 in migration and retention of BM-MSCs.

Since CXCR4 has been shown to be involved in chemotaxis of various cell types, we proposed that by increasing MSC expression of this receptor we would be able to enhance migration and consequently retention of MSC both *in vitro* and *in vivo*. Due to the low level of CXCR4 expression in wild-type BM-MSCs, we intended to overexpress the protein by adenoviral vectors. The adenoviral vector expressing CXCR4 was created using a murine *Cxcr4* gene cloned from mouse spleen. BM-MSCs were transduced with the virus and the expression of CXCR4 was confirmed by immunofluorescence, immunoblot, and flow cytometry analysis. BM-MSCs overexpressing CXCR4 were then used in an *in vitro*

migration assay to determine their chemotactic response and in an intact mouse model of ischemia–reperfusion injury to examine their retention *in vivo*.

2.2 Specific Aim #2: To determine if gap junction communication is important to the survival of BM-MSCs exposed to hypoxic cardiomyocytes in coculture.

We hypothesized that attenuating the cell–cell coupling between hypoxic HL-1s and BM-MSCs reduces stem cell death. To investigate whether hypoxic cardiomyocytes could induce death and apoptosis of BM-MSCs, we used an *in vitro* coculture model. HL-1 cardiomyocytes were exposed to hypoxic conditions followed by coculture with BM-MSCs. The percentage of BM-MSCs that became apoptotic and died was determined by flow cytometry analysis. For this specific aim, we used carbenoxolone, a gap junction uncoupler which does not affect ionic currents (de Groot, et al., 2003).

2.3 Specific Aim #3: To determine if if gap junction inhibition with cell therapy affects early remodeling of the ischemic myocardium.

In this aim, we specifically addressed the role of gap junction-mediated intercellular communication between ischemic cardiomyocytes and transplanted stem cells. We hypothesized that disrupting gap junction formation in BM-MSCs will result in increased stem cell retention and reduced infarct size following ischemia–reperfusion. These studies

used a mouse model of ischemia–reperfusion and flow cytometry analysis to determine the number of BM-MSCs in whole heart digests following transplantation.

2.4 Specific Aim #4: To determine if pretreatment of BM-MSCs with a gap junction inhibitor can alter global cardiac function following ischemia–reperfusion and cell therapy.

The ultimate goal of this study was to understand how transplanted stem cells integrate during acute myocardial ischemia and whether transient cell–cell uncoupling affects cardiac function in the early phase of ischemia. Thus, we proposed to assess the impact of blocking gap junctions on recovery/preservation of cardiac function in our ischemia–reperfusion model. We hypothesized that BM-MSC cell therapy during cardiac reperfusion will lead to early recovery from ischemic injury and by inhibiting gap junctions in BM-MSCs prior to injection we will be able to enhance functional recovery from ischemia–reperfusion injury. In this aim, we examined changes in hemodynamic function 24 hours after the ischemic injury.

II. MATERIALS AND METHODS

1. Materials

Chemicals were obtained from Fisher Scientific, Sigma, or Invitrogen, unless otherwise noted.

2. Animals

Mice were housed in the AAALAC-accredited Biological Resources Laboratory at UIC and maintained in accordance with the Guide for the Care and Use of Laboratory Animals (National Research Council, 1996). Experimental protocols were approved by the Institutional Animal Care and Use Committee at UIC.

3. Bone Marrow-Derived Mesenchymal Stem Cell Isolation, Characterization and Culture

BM-MSCs were isolated from C57BL/6 mice (Jackson Laboratory, Maine) as previously described (Boomsma, Swaminathan, & Geenen, Intravenously Injected Mesenchymal Stem Cells Home to Viable Myocardium after Coronary Occlusion and Preserve Systolic Function without Altering Infarct Size., 2007). Tibia and femur were stripped of muscle and placed in ice-cold phosphate buffered saline (PBS) + 2% fetal

bovine serum (FBS). The epiphyseal ends were removed and the bones were centrifuged at 4,000×*g* for 1 minute in a microfuge tube containing the cut end of a 1 ml pipette tip inside its other half (see Figure 2, next page). The tips provided support for the bones during centrifugation and allowed the marrow to collect at the bottom of the tube. The bone marrow cells were suspended in ice-cold PBS + 2% FBS, passed through a 70-μm filter and counted with a hemocytometer.

Filtered bone marrow cells were suspended in PBS + 2% FBS + 0.1 g/L phenol red and enriched for lineage negative (Lin^-) cells using SpinSep system (StemCell Technologies, Canada). The cells were incubated with Murine Progenitor Enrichment Cocktail (anti-CD45, anti-CD45R, anti-CD11b, anti-Gr-1, anti-TER119, and anti-7/4; StemCell Technologies) on ice for 30 minutes, washed, and incubated with dense particles on ice for 20 minutes. The cells were layered on density medium, centrifuged at 1,200×*g* for 10 minutes, and the layer of cells at the density medium/PBS interface was collected, washed, and counted.

Enriched bone marrow cells were seed on tissue culture-treated plates at a density of 0.1×10^6 cells/cm^2 in murine MesenCult media (StemCell Technologies) with 100 U/ml penicillin, 100 μg/ml streptomycin, and 0.25 μg/ml amphotericin B added. The media were changed after 48 hours and adherent cells were maintained in culture with twice weekly media changes. After 4 weeks, the confluent cells were detached with trypsin and split 3:1. Lin^- MSCs were characterized for surface antigens using flow cytometry. Antibodies were obtained from BD Pharmingen unless otherwise noted. Cultured cells were detached with

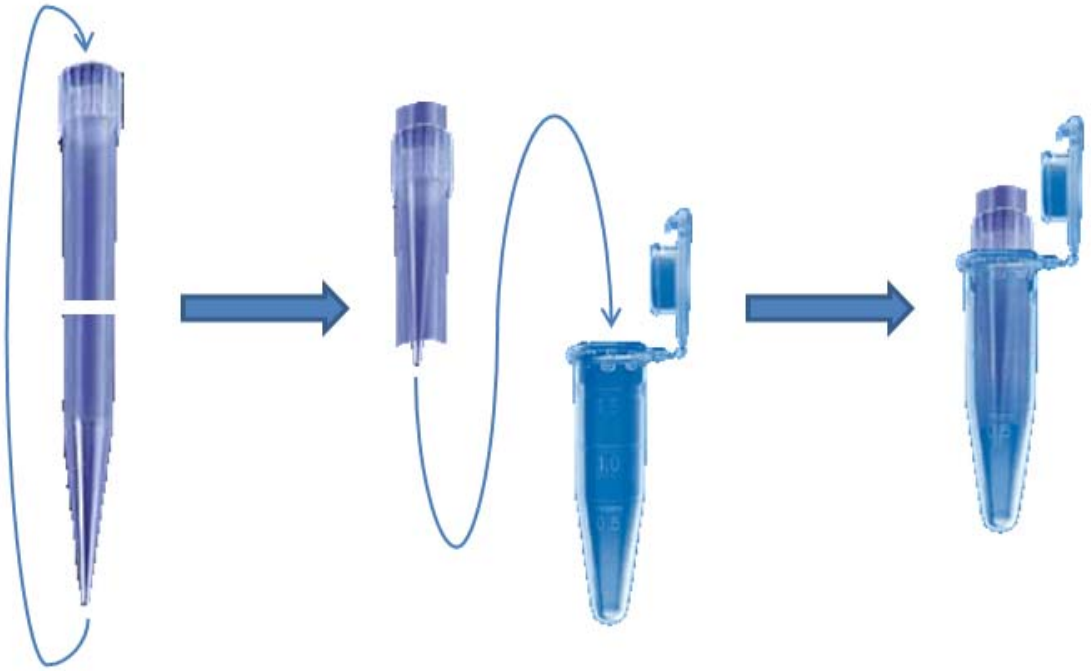

Figure 2: Modified microfuge tube for bone marrow cell isolation. One–ml pipette tip is cut in half, the tip is inserted into the other end and then they are fit on top of a microfuge tube and act as a cradle to hold the bone in place.

trypsin and incubated with 1 µl mouse Fc block (1:50 dilution; clone 2.4G2, rat anti-mouse CD16/CD32; Sigma, Missouri) for 5 minutes on ice. Cells were then incubated with 1 µl fluorescent-conjugated antibodies (1:50 dilution) for 1 hour on ice, washed, and analyzed.

The following mouse monoclonal antibodies were used: anti-CD45-Cy5 (clone 30-F11), anti-Sca1-PE (clone E13-161.7), anti-Sca1-Cy5 (clone D7; eBioscience, California), anti-CD34-PE (clone RAM34), anti-CD90.1-PE (clone HIS51), anti-CD117(cKit)-PE (clone 2B8), anti-CD105-biotin (clone MJ7/18; eBioscience). Those treated with biotinylated antibodies were washed and incubated for 20 minutes at room temperature with 1 µl streptavidin-PE or streptavidin-Cy5. Control samples were treated with immunoglobulin of the appropriate isotype. Cells were analyzed in a FACSCalibur flow cytometer or in a Beckman Coulter FC500 equipped with, respectively, one and two lasers for multiparametric and multicolor analysis including a 488-nm argon laser for measurement of forward light scatter, orthogonal scatter, and three to five colors.

4. Cloning of Murine CXCR4 cDNA from Mouse Spleen

Mouse total RNA from spleen was prepared using Trizol reagent (Invitrogen) according to manufacturer's instruction. Briefly, spleen was obtained from a wild type C57BL/6 mouse and weighed. A 100 mg portion of the spleen was homogenized in 1 ml of Trizol and incubated for 5 minutes at room temperature. Then 0.2 ml of chloroform was

added to the sample and mixed by shaking vigorously for 15 seconds and let the sample incubate at room temperature for 2 to 3 minutes. The sample was then centrifuged at 12,000×*g* for 15 minutes at 4 °C. After the centrifugation, upper aqueous phase was transferred into a fresh tube, mixed with 0.5 ml of isopropanol, and centrifuged at 12,000×*g* for 10 minutes at 4 °C. The supernatant was removed; RNA pellet was washed with 1 ml of 75% ethanol, mixed by vortexing and centrifuged at 7,500×*g* for 5 minutes at 4 °C. After removing the supernatant, the RNA pellet was briefly dried for 5 minutes and dissolved by adding 50 µl of RNAse-free water.

RT-PCR was performed using the extracted RNA and M-MLV reverse transcriptase (Invitrogen) and Oligo d(T)16 (Invitrogen). The first strand cDNA then was amplified by regular PCR using primers designed specifically for cloning into subsequent vector based on manufacturer's specification and GenBank's published CXCR4 mRNA sequence (Accession number: NM_009911): forward primer 5'–GTA GAG CGA GTG TTG CCA TGG AAC CGA TCA GT–3'; reverse primer 5'–GCG GAT CTG CAT AAG TGT TAG CTG–3'. The PCR product was fused with internal ribosome entry site (IRES) and enhanced green fluorescent protein (eGFP) gene taken from pIRES-AcGFP1 vector (Clontech, California) using PCR (forward primer 5'–CAG CTA ACA CTT ATG CAG ATC CGC–3'; reverse primer 5'–GGC CGC TCA CTT GTA CAG C–3'). The resulting CXCR4-IRES-eGFP gene or IRES-eGFP alone was further sequentially cloned into pENTR/D-TOPO, pDONR221, and pAd/CMV/V5-DEST (all from Invitrogen). The plasmids were sequenced by Research Resources Center

DNA Services Facility to verify integrity of the cloned gene. The plasmids were transfected into 293A cells (Invitrogen) to produce viral vectors containing CXCR4-IRES-GFP (AdCXCR4) or IRES-GFP (AdGFP) according to manufacturer's protocol.

5. Adenoviral Overexpression of CXCR4 in Mesenchymal Stromal Cells

BM-MSCs (10^5 cells) were plated in a 100-mm tissue culture dish in MesenCult media with 100 U/ml penicillin, 100 µg/ml streptomycin, and 0.25 µg/ml amphotericin B. AdCXCR4 or AdGFP was added to the culture at the time of plating at multiplicity of infection (MOI) of 2000 and 15, respectively. After 48 hours, the cells were lifted with trypsin and used for further experiment.

6. Flow Cytometry Analysis and Sorting

Cells were harvested by trypsinization for 5 minutes at 37 °C, washed with flow cytometry buffer (PBS + 0.25% bovine serum albumin + 2 m*M* EDTA), and then collected by centrifugation at 1,000×*g* for 10 minutes at room temperature, and resuspended at a concentration of 6×10^3 cells/50 µl. The cells were incubated with mouse Fc block (1:50) for 5 minutes on ice and then with antibodies for 1 hour on ice. The antibodies used included anti-Sca1-APC (1:50, Clone: D7; eBioscience), anti-CXCR4-PE (1:50, Clone: 2B11;

eBioscience), SYTOX-Red (Invitrogen), and anti-Annexin V-Pacific Blue (Invitrogen). Cells were washed twice with flow cytometry buffer, resuspend in 100 µl of flow cytometry buffer and transferred to 12×75 round bottom tubes with 35-µm cell strainer cap (BD Biosciences, California) by passing through the strainer. The cells were kept on ice until ready to be examined by either Cyan ADP (Beckman Coulter) or LSRFortessa (BD Biosciences) in the Flow Cytometry Laboratory of UIC's Research Resources Center. The data from the experiments were analyzed by either Summit software (version 4.3, Beckman Coulter) or FACSDiva software (version 6.0, BD Biosciences)

For cell sorting, the cells was prepared as described above but resuspended in flow cytometry buffer at a concentration of 2×10^7 cells/ml. The cells were then sorted by MoFlo High Speed Sorter (Dako-Cytomation) in Flow Cytometry Service center of UIC's Research Resources Center. The sorted cells were plated or frozen for later use.

7. Cell Migration Assay

AdCXCR4- or AdGFP-transduced BM-MSCs (10^4 cells) in 300 µl of MesenCult were plated over the membrane in the upper chamber of FluoroBlok cell culture insert (3 µm pore Ø, BD Biosciences) in a 24-well cell culture plate, with 700 µl of MesenCult added to the well below each chamber. The cells were allowed to attach for 3 hours then recombinant human SDF-1α (R&D Systems, Minnesota) was added to the wells below the

insert to obtain final concentration of 250 ng/ml. Other groups of cells were pretreated with AMD3100 (250 ng/ml; Sigma) 30 minutes before SDF-1 treatment. After 6 hours of incubation, the migrated cells were stained with DAPI and observed under a fluorescent microscope where only migrated cells were visualized due to the opacity of the FluoroBlok membrane. Images of each membrane were acquired at 10× magnification on an IX81 inverted microscope (Olympus, Pennsylvania) utilizing an EXi Blue Fluorescence Microscopy Camera (QImaging, Canada) and Metamorph software (Molecular Devices, California). All the images from each membrane were merged together to form a composite image of the membrane using Adobe Photoshop CS5 software (Adobe, California), converted into bitmap format and the number of cells were counted by Image J software (NIH).

8. Polyacrylamide Gel Electrophoresis and Immunoblotting

The mouse at 24 hours after coronary ligation was anesthetized with 3% isoflurane and 100% O_2 in an induction chamber. After the mouse was fully anesthetized, cervical dislocation was performed. The chest was open and the heart was removed. The heart was perfused with PBS to remove excess blood, placed in a prechilled acrylic heart matrix with 1.0 mm transverse section slices interval and cooled in -20 °C freezer for 20 minutes. The heart was then cut transversely at 3 and 6 mm from the apex and each third (apex, mid, and

base, respectively) was stored in a cryogenic tube, weighed, snap frozen in liquid nitrogen, and stored in at -80 °C until ready to be analyzed.

Apexes of the hearts were used for western blot analyses. Tissue lysates were prepared using RIPA lysis buffer system (Santa Cruz Biotechnology, California) according to manufacturer's protocol. Briefly, RIPA buffer was added to each sample according to the tissue weight (3 ml buffer per gram of tissue). The tissue was homogenized and incubated for 2 hours at 4 °C with constant agitation. The samples were centrifuged at 12,000×g for 20 minutes at 4 °C and the supernatant were collected for gel electrophoresis.

The samples were mixed 1:1 with Laemmli sample buffer (Bio-Rad, California) and loaded equally into 4–20% Mini-Protean TGX gels (Bio-Rad), with Precision Plus Protein Kaleidoscope Standard (Bio-Rad) as molecular weight marker in at least one well. The gels were run at 100 V at room temperature for 60–90 minutes and the proteins were transferred to PVDF membrane (Bio-Rad) at 100V for one hour at room temperature. The membranes were incubated for 1 hour with 5% non-fat milk in tris-buffered saline with 0.1% tween-20 to block non-specific binding. The membranes were then incubated with primary antibody in tris-buffered saline with 0.1% tween-20 overnight at 4 °C. Primary antibodies used were rabbit polyclonal anti-CXCR4 and mouse monoclonal anti-GFP (both were used at 1:500 dilution and from Santa Cruz Biotechnology). The membranes were washed three times for 10 minutes each in tris-buffered saline with 0.1% tween-20, followed by incubation with horseradish peroxide-conjugated secondary antibody

(1:10,000; Promega, Wisconsin) for 1 hour at room temperature. Membranes were washed 5 times, 10 minutes each with tris-buffered saline with 0.1% tween-20, incubated with ECL Plus western blot detection reagent (GE Healthcare, New Jersey) for 5 minutes, placed in the cassette and exposed to x-ray films. The films were developed and images of the films were taken and analyzed using ChemiDoc XRS system (Bio-Rad) and Quality One software (Bio-Rad).

9. Immunofluorescent Staining

BM-MSCs plated on 22-mm circular cover slips for immunofluorescent staining. Cells were washed briefly with ice-cold PBS, and fixed with 2% paraformaldehyde (Electron Microscopy Sciences, Pennsylvania) for 20 minutes at room temperature. Then the cells were blocked with 5% horse serum in PBS with 0.1% tween-20 for 45 minutes at room temperature. Anti-CXCR4 antibody or isotype control (Both 1:100; Santa Cruz Biotechnology) in PBS were incubated with the samples at 4 °C overnight. The samples were washed twice with PBS then incubated with Alexa Fluor 488-conjugated goat anti-rabbit antibody (Jackson ImmunoResearch Laboratory, Pennsylvania) for 1 hour at room temperature. The cover slips were washed twice with PBS then mounted onto glass microscopic slides using mounting medium with DAPI (Vector Laboratories, California) and examined with IX81 inverted microscope (Olympus, Pennsylvania). The images of cells

were acquired by using EXi Blue Fluorescence Microscopy Camera (QImaging, Canada) and Metamorph software (Molecular Devices, California).

10. HL-1 and BM-MSC Coculture Experiments

HL-1 murine atrial myocytes were seeded at 1×10^5 cells/well in a 6-well plate and placed in either DMEM with glucose under normoxic conditions or in DMEM with 2-deoxy-glucose and pH 6.2 in a sealed chamber (ischemia; 1% O_2, 5% CO_2, balance N_2) for 4 hours. At the end of 4 hours, 2×10^4 Lin^- murine BM-MSCs were seeded on the HL-1 cell monolayer and the cocultures were returned to the cell incubation chamber. One coculture group continued under normoxic conditions in control DMEM and a second group continued under ischemic conditions. In a third group, the ischemic media was replaced with control DMEM and incubation continued under normoxic conditions (ischemia/reperfusion). The non-selective gap junction inhibitor carbenoxolone (CBX) was added to half of the wells from each of the three groups at a final concentration of 100 μ*M* immediately prior to the coculture. Cells remained in coculture for additional 2 hours after which time they were lifted and labeled with fluorescent probes (anti-Sca-1-APC, SYTOX-Red, and anti-Annexin V-Pacific Blue, described above) for flow cytometry analysis. Samples were gated by their Sca1-APC signal to select only BM-MSC (~80% Sca1 positive vs. 1% in HL-1) for cell death analysis.

11. Coronary Ligation, BM-MSC Injection, and Hemodynamic Measurements

Sorted GFP^+ BM-MSCs were detached from the cell culture plate with trypsin and washed in injection buffer (Ca^{2+}/Mg^{2+} free PBS + 2 m*M* EDTA + 0.25% bovine serum albumin), passed through a 35 μm cell strainer and suspended in a final concentration of 10^5 cells/10 μl. For the other experimental groups for *in vivo* injections, GFP^+ BM-MSCs were treated overnight with CBX (100 μ*M*), or CBX in injection buffer (100 μ*M*), and vehicle alone were used.

Wild type C57BL/6 mice were initially anesthetized with etomidate (10 mg/kg body weight; i.p.) and intubated with an 18-gauge angiocath sleeve. Surgical anesthesia was maintained using 1.5% isoflurane delivered through a vaporizer with 100% oxygen connected in series to a rodent ventilator with the tidal volume set at 0.2 to 0.3 ml/min (based on body weight) and a respiratory rate of 135 per minute. A left thoracotomy was performed to expose the heart and the pericardium was ruptured. The left coronary artery was ligated 3 mm from the ostium with 8-0 prolene suture to produce myocardial ischemia. The mouse was maintained on isoflurane for 90 minutes following the coronary ligation after which, the sutured was removed and the ischemic area was reperfused. Sorted GFP^+ BM-MSCs ($1x10^5$; suspended in 10 μl), CBX-treated BM-MSCs ($1x10^5$), CBX injection buffer, or vehicle alone was injected into the apical myocardium with a 30 gauge microliter syringe (Hamilton, Nevada). Following injection a chest tube was placed in the thoracic cavity and the thoracotomy was closed in three layers (intercostal muscles, pectoral

muscles, and skin) followed by evacuation of the chest cavity and removal of the tube. During the surgery and hemodynamic measurements, an adequate plane of anesthesia was judged by respiration, heart rate and toe pinch reflex. Animals received buprenorphine (0.1 ml of 0.03 mg/ml; s.c.) at the time of surgery and were allowed to recover in a heated cage for 24 hours. Sham–operated mice underwent the same procedure as described above except the left coronary artery was not ligated. All subsequent experiments were performed at 24 hours after ischemia/reperfusion.

Hemodynamic measurements were taken at 24 hours following the coronary ligation as previously described (Goldspink, et al., 2004). Mice was anesthetized and intubated with isoflurane. An incision was made in the lower chest to expose the xiphoid process and a stay suture was placed around the xiphoid to stabilize and lift the chest wall. The diaphragm was then cut and retracted to expose the heart and inferior vena cava. A 1.4 French ultra-miniature pressure–volume catheter (SPR-839; Millar Instruments, Texas) was inserted into the apex of the heart to measure baseline recordings of heart rate, LV systolic/diastolic pressure, the first derivative of pressure (±dP/dt), and pressure–volume loops. The mouse was allowed to stabilize before inferior vena cava occlusion. The inferior vena cava was isolated and occluded while simultaneously measuring pressure–volume loops to determine end-systolic pressure–volume relationships and contractility of the ventricle independent of loading conditions. A series of 10–20 loops were used to estimate the end-systolic pressure–volume relationship (ESPVR) and end-diastolic pressure–volume

relationship (EDPVR). All data were analyzed using the PVAN software package (Millar Instruments).

12. Whole Heart Digests

Enzymatic digestion of the whole heart was done using a method modified from O'Connell *et al*. (O'Connell, Ni, Lin, Han, & Yan, 2003). The mouse was injected i.p. with 0.5 cc heparin (100 IU/ml in PBS) and then anesthetized with 3% isoflurane and 100% O_2 in an induction chamber. After the mouse was fully anesthetized, cervical dislocation was performed. The chest was open and the heart was excised, washed in PBS, and placed in a 60-mm dish containing perfusion buffer (113 m*M* NaCl, 4.7 m*M* KCl, 0.6 m*M* KH_2PO_4, 0.6 m*M* $Na_2H_2PO_4$, 1.2 m*M* $MgSO_4$, 0.032 m*M* phenol red, 12 m*M* $NaHCO_3$, 10 m*M* $KHCO_3$, 10 m*M* HEPES, 30 m*M* Taurine, 10 m*M* 2,3-butanedione monoxime, 5.5 m*M* glucose, pH 7.4) at room temperature. The aorta was cannulated with a 22-gauge animal feeding needle connected to a 3-way stopcock and secured with 6-0 silk suture. The cannula was connected to the end of a perfusion system and the perfusion buffer was started immediately at a rate of 3 ml/min for 4 minutes. After 3 minutes, the buffer was switched to digestion buffer (perfusion buffer + 0.1 mg/ml liberase TM (Roche Applied Science, Indiana) and 0.14 mg/ml trypsin + 12.5 μ*M* $Cacl_2$) for 7–10 minutes. The heart was removed from the cannula and the right and left ventricle were separated and minced in

the same buffer at 37 °C until completely digested. Digestion was terminated by adding an equal volume of stop buffer (perfusion buffer + 10% bovine calf serum + 12.5 μ*M* $CaCl_2$). Cells were centrifuged at 1,000×*g* for 5 minutes and the buffer replaced with flow cytometry buffer for subsequent flow cytometry analysis (see above). Flow cytometry measurements were gated for the MSC population and the number of GFP-positive cells was recorded.

13. Infarct Size Measurement by Tetrazolium Staining

Infarct size and area-at-risk were determined by a method modified from Redel *et al*. (Redel, et al., 2008). Twenty-four hours after ischemia/reperfusion, the mice were anesthetized and the hearts harvested. The aorta was cannulated, as previously described and ice cold PBS (3 ml) was infused into the heart. Following PBS infusion, the coronary artery was ligated with 8-0 prolene suture in the exact location of the previous suture. Evans blue dye (1.0 ml of 0.1 g/ml; Sigma) was injected retrograde into the aorta and perfused the heart excluding the left coronary artery bed. The heart was then removed from the cannula, placed in a prechilled acrylic heart matrix with 1.0 mm transverse section slice intervals (Astor Industries, Pennsylvania) and cooled at -20 °C for 20 minutes. Subsequently the heart was cut into 6–7 one-mm-thick transverse slices. The heart slices were sandwiched between glass cover slips and incubated at 37 °C for 25 minutes in 2%

2,3,5-triphenyltetrazolium chloride (TTC, Sigma) dissolved in 0.1 M Na_2HPO_4/NaH_2PO_4 buffer adjusted to pH 7.4. Heart slices were fixed in 10% buffered formalin at 4 °C overnight and placed between two glass slides for imaging.

The images of slices from each heart were taken at 3.2× magnification with a Stemi 2000C stereomicroscope (Carl Zeiss, Massachusetts) using a Nikon D300s digital camera (Nikon, Japan) and Clearshot 600 Digital Camera Adapter System (Alexis Scientific) (Figure 3). The images then were analyzed using the Mobile Infarct Tool program(Downey) to measure the area of Evans Blue, TTC (red) and unstained (white). Data from all the slices from each heart were combined to provide total area of area-at-risk and infarct. Area-at-risks are reported as percent of area-at-risk to total myocardial area, and infarct sizes are reported as percent of infarcted area to area-at-risk area.

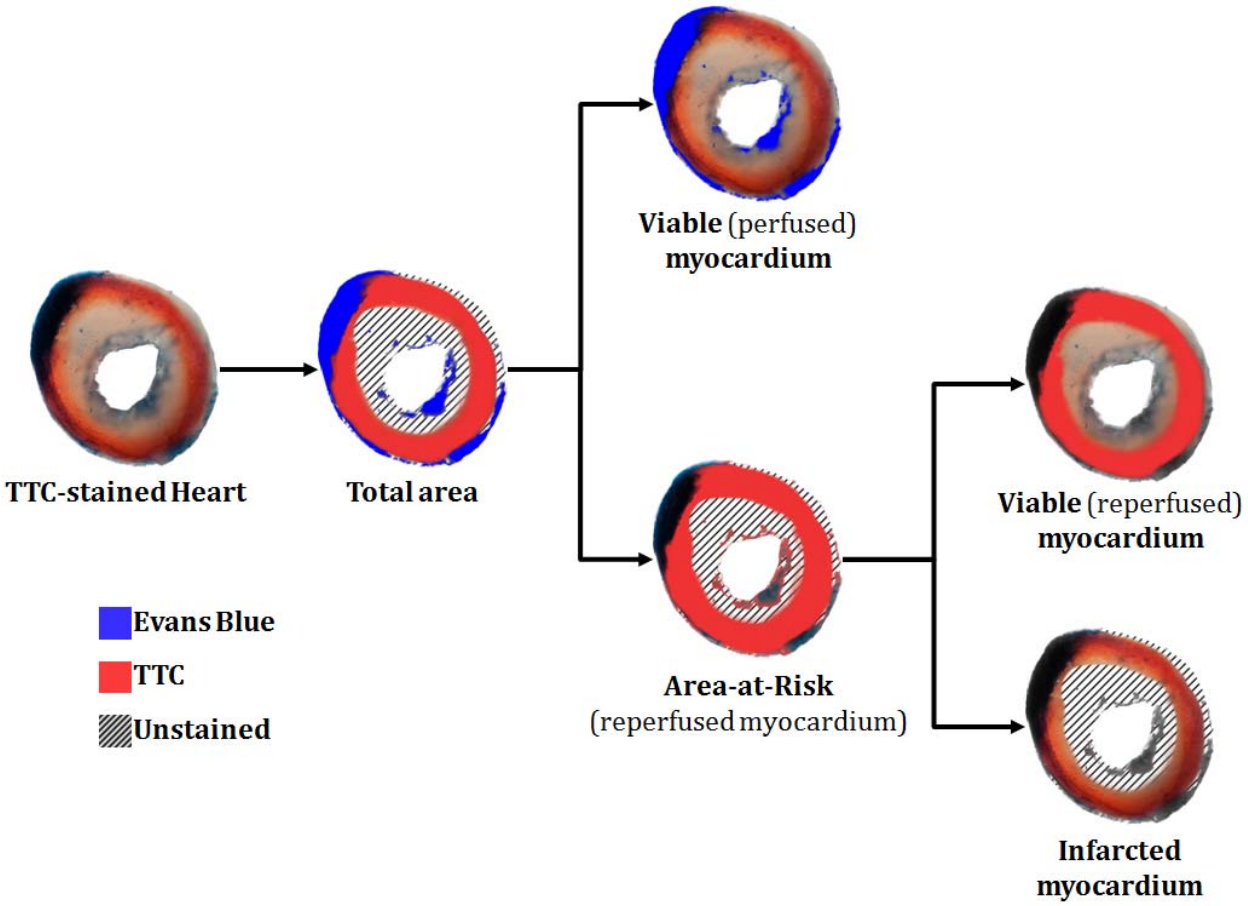

Figure 3: Infarct size measurement by tetrazolium staining. Diagram depicted measurement of myocardial areas by TTC staining. Blue area represents viable perfused myocardium, red area represents reperfused myocardium that is still viable (hibernating), and white (shaded) area represents reperfused but irreversibly infarcted myocardium. Area-at-risk represents reperfused area of the myocardium, which includes both red and white areas.

14. BM-MSC Proliferation Assay

To simulate the time course of cells used for injection, sorted GFP^+ BM-MSCs were culture overnight in either MesenCult or MesenCult with 100 μ*M* CBX. On the next day, the cells were detached with trypsin, and plated in 6- well plate at 1×10^5 cells/well in MesenCult. Number of cells at day 0, 1, and 2 were counted using Cellometer Auto 2000 Cell Counter (Nexcelom Bioscience, Massachusetts) at UIC's Research Resources Center. Experiments in each group were done in triplicates.

15. Statistical Analysis

Data from the experiments were calculated in Microsoft Excel 2007 (Microsoft, Washington). Values are presented as means ± standard error of the mean (S.E.M.) and *n* is the number of experiments. Statistical differences among means were analyzed by an unpaired t-test analysis with the criteria for statistical significance set at $p\leq0.05$.

III. RESULTS

1. Overexpression of CXCR4 in BM-MSC

We successfully cloned mouse CXCR4 cDNA from mouse spleen using RT-PCR, fused it with GFP gene then cloned them into expression plasmids. The plasmids were then used to produce adenoviral vectors expressing CXCR4 and GFP (AdCXCR4) or GFP alone (AdGFP).

Flow cytometry analysis of BM-MSC transduced by either AdGFP or AdCXCR4 at 48 hours after transduction indicated increase expression of GFP and/or in both groups. In AdGFP transduced MSC, 86.10% of the cells expressed GFP while in AdCXCR4 a slightly lower (68.66%) GFP expression was observed (Figure 4, upper panel). We could observed and increase in CXCR4 expression in AdCXCR4 group (15.82% vs. 0.61% AdGFP control). The increase in CXCR4 expression was also observed by western blot which showed a dose-dependent level of CXCR4 protein in AdCXCR4 transduced BM-MSC (Figure 5) and could be detected by immunofluorescent staining (Figure 6).

Figure 4: Flow cytometry analysis of BM-MSC transduced by AdGFP or AdCXCR4. Top: 2D plot showing flow cytometry analysis of BM-MSC tranduced by AdGFP (left) and AdCXCR4 (right). x-axis represents intensity of GFP fluorescent signals. y-axis represents intensity of APC fluorescent (CXCR4) signals. GFP-positive events are in R4 and R6 quadrants (green shaded) and GFP-and-CXCR4 double positive events are in R4. BM-MSC transduced with either viral vectors have increased GFP expression (AdGFP 86.10%, AdCXCR4 68.66%) and those transduced with CXCR4 have increased CXCR4 expression (AdCXCR4 15.82% vs. AdGFP 0.61%). Bottom: Histogram showing number of cells with APC fluorescent signals. x-axis represents APC fluorescent intensity. y-axis represents number of cells. AdCXCR4 transduction increased expression of CXCR4 (16.92% positive events) in BM-MSC, unlike other groups (AdGFP transduction, untreated cells, and isotype control).

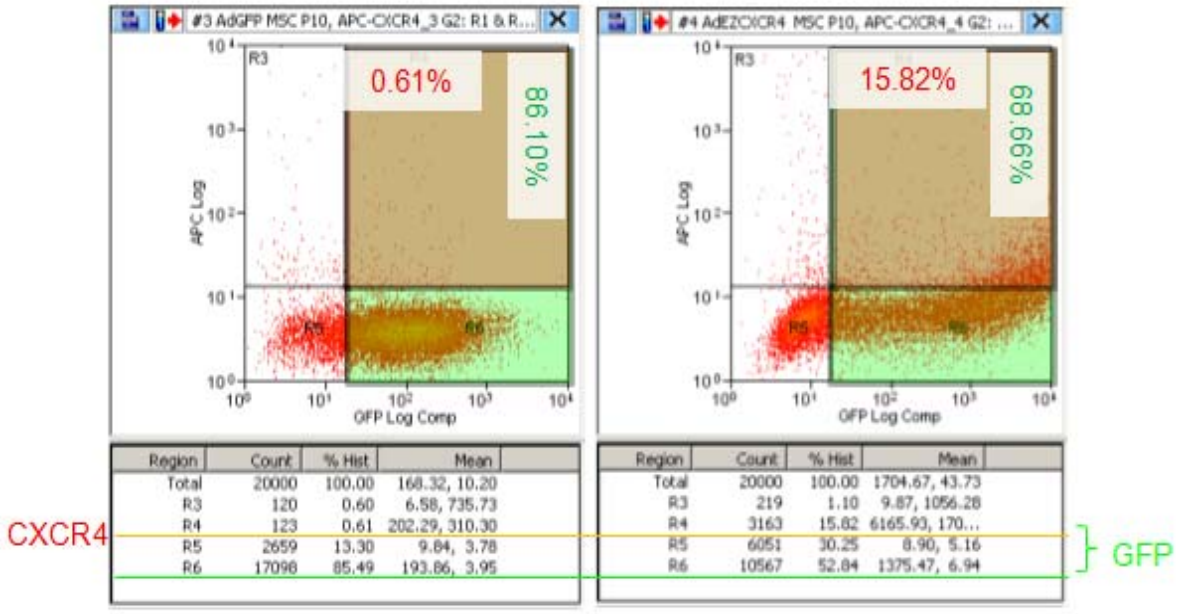

Region	Count	% Hist	Mean
Total	20000	100.00	168.32, 10.20
R3	120	0.60	6.58, 735.73
R4	123	0.61	202.29, 310.30
R5	2659	13.30	9.84, 3.78
R6	17098	85.49	193.86, 3.95

Region	Count	% Hist	Mean
Total	20000	100.00	1704.67, 43.73
R3	219	1.10	9.87, 1056.28
R4	3163	15.82	6165.93, 170...
R5	6051	30.25	8.90, 5.16
R6	10567	52.84	1375.47, 6.94

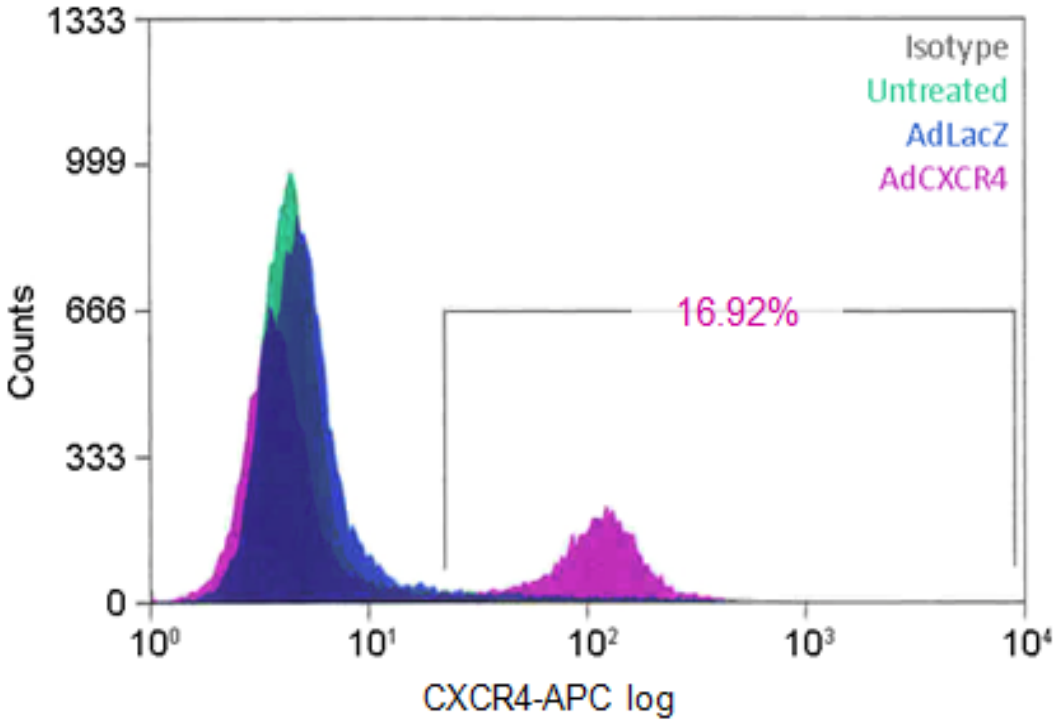

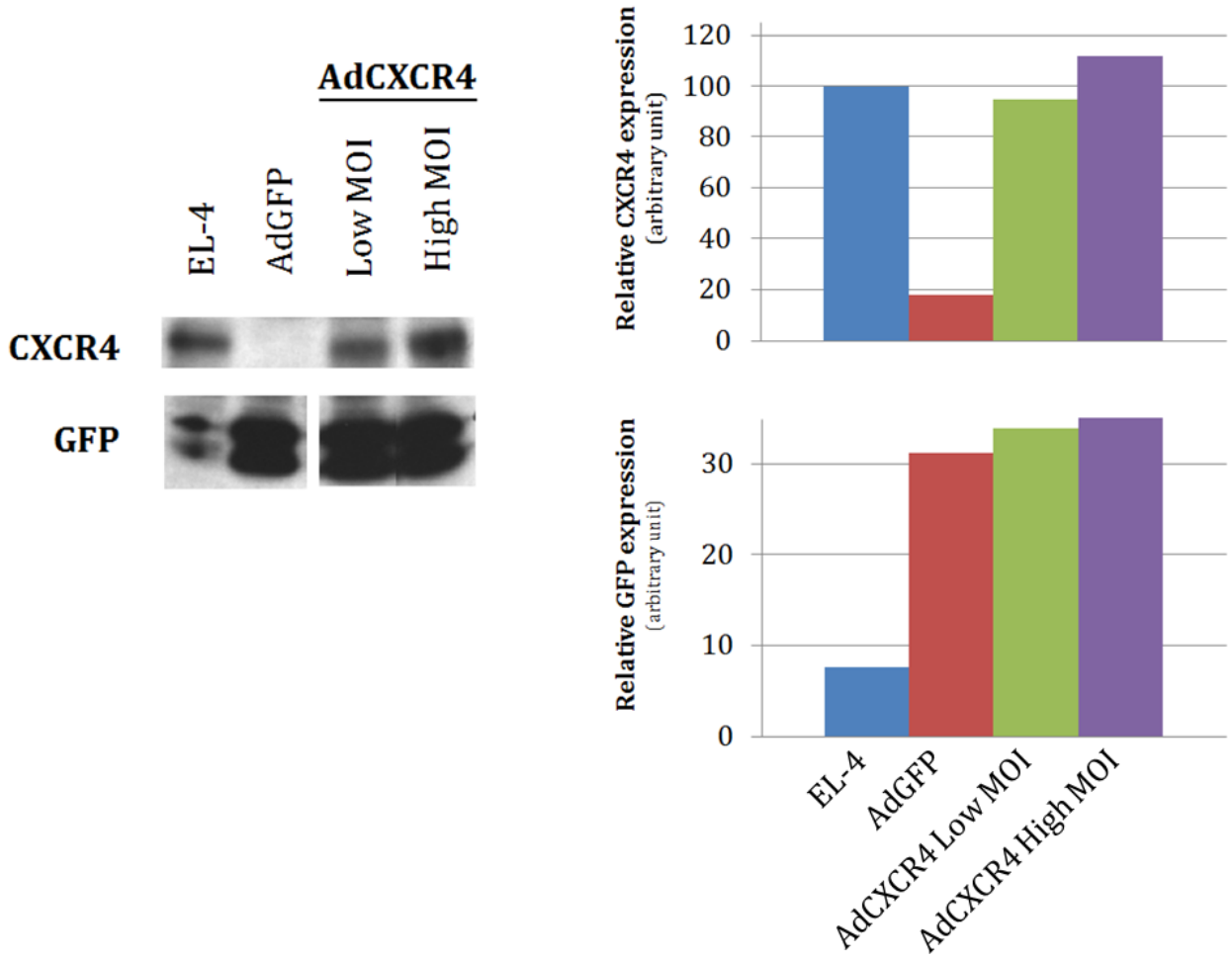

Figure 5: CXCR4 protein level in AdCXCR4-transduced cells. Left: western blot data showing CXCR4 protein expression. EL-4 (mouse lymphoma cell) lysate was used as a positive control. Cell lysate from AdCXCR4 demonstrated increased CXCR4 expression which correlated with the amount of virus used to infect. Right: Aggregated data of CXCR4 (top) and GFP (bottom) expression. Data shown as means (n=2) (MOI: multiplicity of infection. Low: 10 MOI, High: 20 MOI).

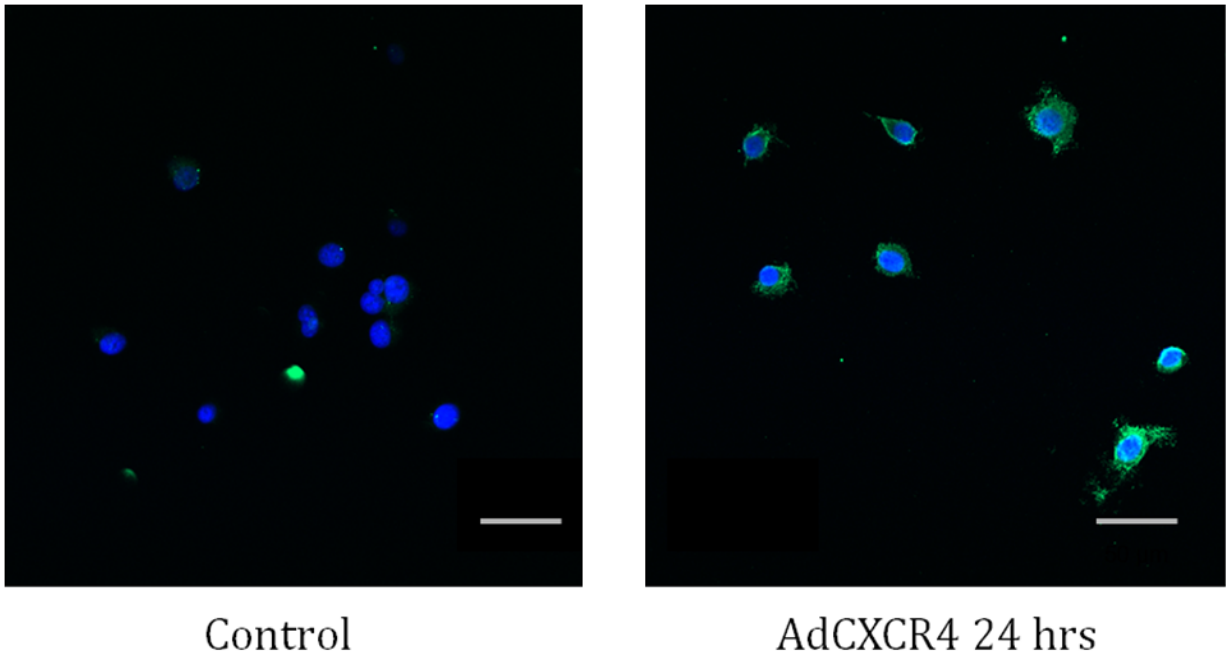

Figure 6: CXCR4 expression in BM-MSC by immunofluorescent staining. Representative immunofluorescent staining of BM-MSC at 24 hours after AdCXCR4 transduction. Blue: DAPI, Green: CXCR4. Scale bar = 20 μm.

2. Effect of Hypoxia on CXCR4 Expression in BM-MSC

To examine the effect of low oxygen tension on CXCR4 expression, we cultured BM-MSC under either normoxic (21% O_2, 5% CO_2) or hypoxic (1% O_2, 5% CO_2) for 24 hours. The cells were then lifted and their lysates were prepared for gel electrophoresis and western blot analysis. We found that reduced oxygen tension decreased protein expression of CXCR4 in BM-MSC (Figure 7).

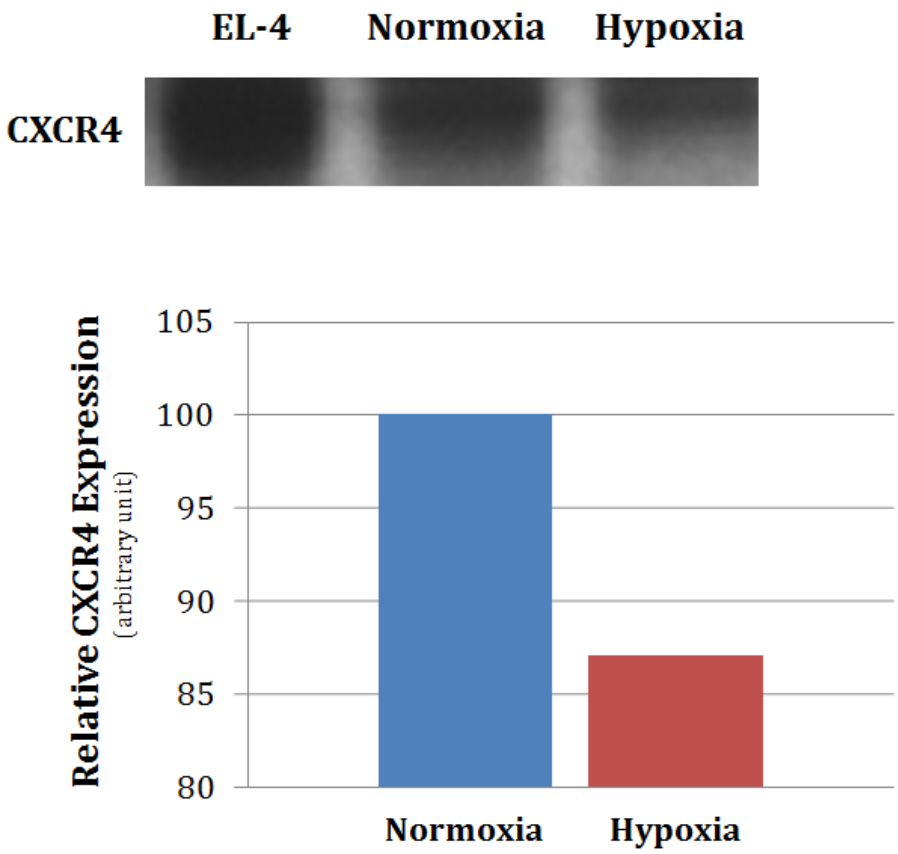

Figure 7: Hypoxia reduced CXCR4 protein expression in BM-MSC. Top: Western blot analysis of CXCR4 protein level in BM-MSC after 24 hours culture in normoxic or hypoxic conditions. CXCR4 expression was decreased in BM-MSC cultured in hypoxic condition for 24 hours compared to cells cultured in normoxic condition. EL-4 cell lysate was used as a positive control. Bottom: Quantitation of average data from two experiments.

3. Effect of CXCR4 Expression and Hypoxia on Migration of BM-MSC

As we observed earlier that hypoxia reduced the expression of CXCR4 within BM-MSC, we asked whether increasing CXCR4 expression using adenoviral transduction would be able to overcome that effect and whether migration of BM-MSC is affected. We performed transwell migration assay using AdCXCR4 transduced BM-MSC with AdGFP transduced cells as our control in either normoxic or hypoxic conditions. The migration assay was done with either vehicle, SDF-1 (200 ng/ml), SDF-1 (200 ng/ml) + AMD3100 (100 ng/ml), or AMD3100 (100 ng/ml) alone in the lower chamber. AdGFP transduced BM-MSC showed a treading increase in number of migrated cells when treated with SDF-1 gradient, both in normoxic and hypoxic conditions, and the increase in either conditions could be attenuated by the presence of AMD3100, a competitive inhibitor of CXCR4, although the differences is not statistically significant (Figure 8). AMD3100 alone did not show any statistically significant change in number of migrated cells when compared to controls. Interestingly, all AdCXCR4 transduced BM-MSC had unexpectedly low number of migrated cells and statistically significantly lower than all AdGFP groups. In normoxia, number of migrated cells in control, SDF-1-treated, and SDF-1+AMD3100-treated groups are comparable although SDF-1 and SDF-1+AMD3100 groups displayed a decreasing trend. Number of migrated cells under normoxia in AMD3100 treated group is comparable to control however it is significantly higher than SDF-1 and SDF-1+AMD3100 treated groups.

Figure 8: Overexpression of CXCR4 impaired migration of BM-MSC. Top: Example fluorescent image (left) of migrated cells (Blue: DAPI) and composite image (right) of the whole membrane which combined ~130 single fluorescent images. Bottom: Data from migration assays. (Each group n=3; data shown as means ± S.E.M.; ‡: statistically significant when compared to all AdGFP groups, $p<0.05$; *: statistically significant when compared to AdCXCR4 SDF-1 and SDF-1+AMD3100 under normoxia, $p<0.05$)

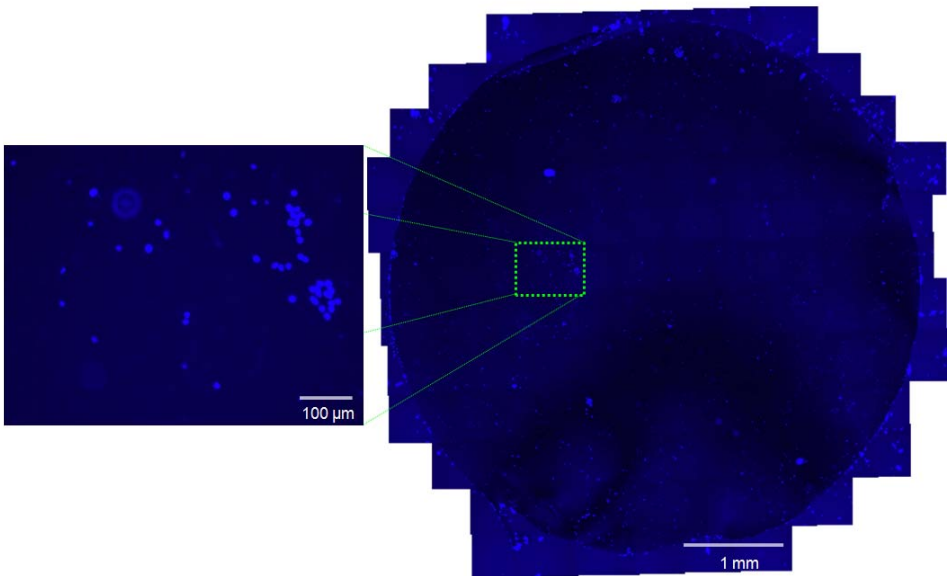
100 µm
1 mm

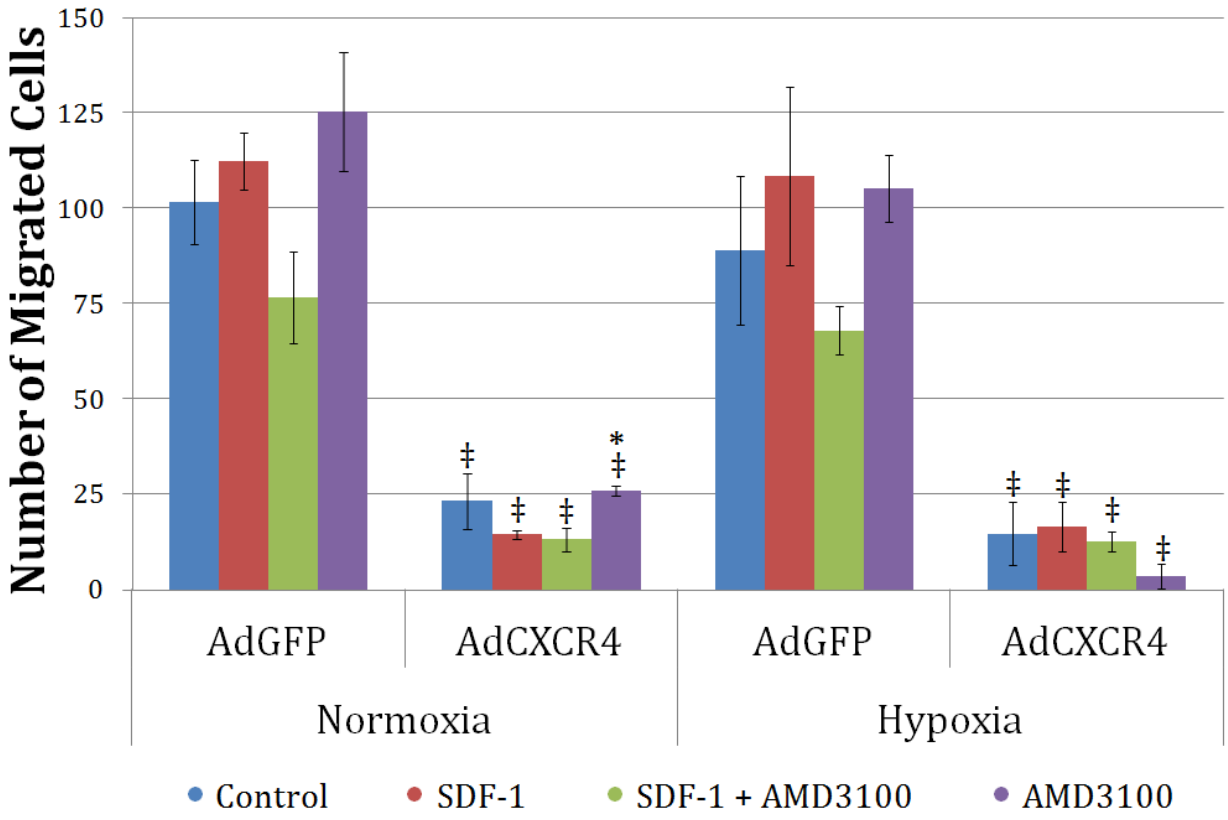
Number of Migrated Cells
150
125
100
75
50
25
0
AdGFP
AdCXCR4
AdGFP
AdCXCR4
Normoxia
Hypoxia
Control
SDF-1
SDF-1 + AMD3100
AMD3100

4. CXCR4-Expressing BM-MSCs Have Enhanced Retention in the Heart after Injury

AdGFP or AdCXCR4 transduced BM-MSC (1×10^5 cells) were injected intramyocardially into the heart of an animal after 90 minutes of ischemia near the apex. After 24 hours, the heart was excised, rinsed, and sectioned transversely into three equal parts. The apical part was homogenized, and the sample was analyzed by gel electrophoresis and immunoblot using antibody against GFP to determine relative amount of BM-MSC that retained in the heart after 24 hours. The amounts of GFP are comparable between sham animals which received either AdGFP or AdCXCR4 transduced cells. Interestingly, although the data were obtained from only two animals, there is about 35% increase in GFP from the animal that received AdCXCR4-transduced BM-MSC and ischemia–reperfusion injury compared to AdGFP ischemia–reperfusion group and both sham controls (Figure 9) suggesting that more of AdCXCR4-transduced BM-MSC retained in the heart after ischemia–reperfusion injury.

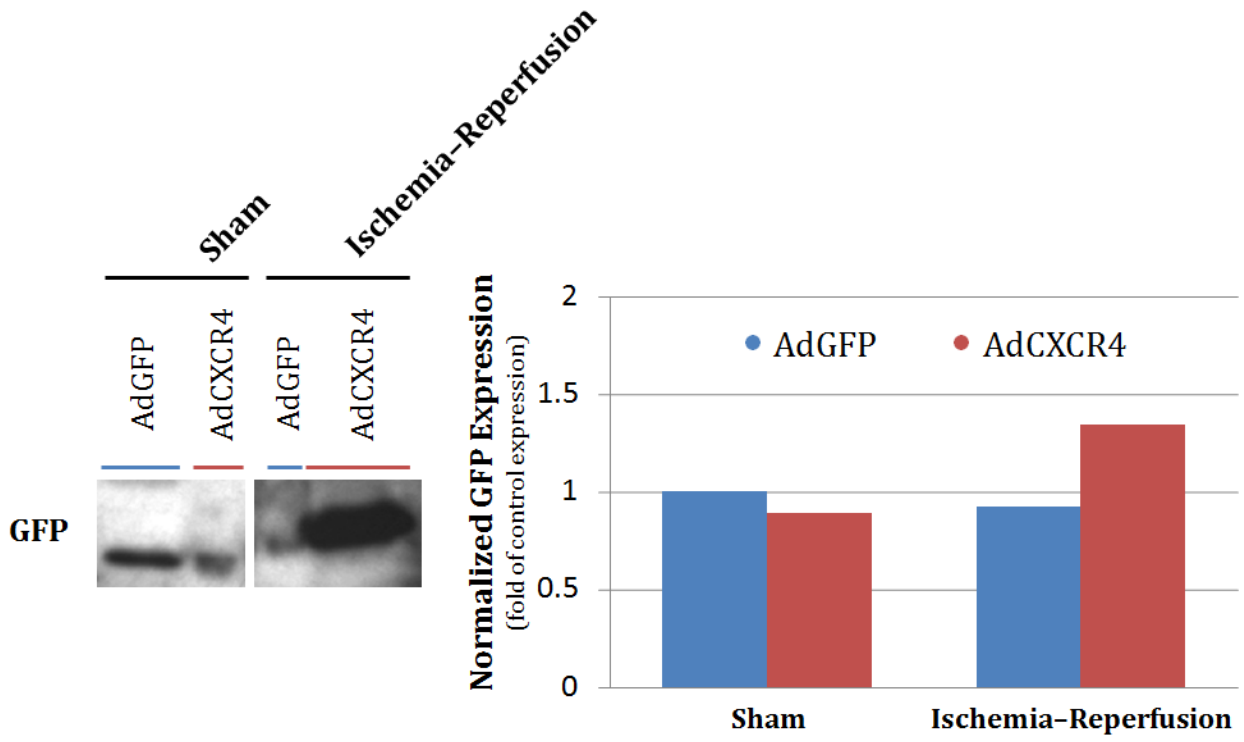

Figure 9: Overexpression of CXCR4 improved retention after ischemia–reperfusion. Left: Representative image of western blot result with antibody against GFP. Right: Relative GFP expression normalized to expression in control AdGFP–sham's lever, each bar represents means from two experiments.

5. Effect of Hypoxic HL-1 on Cocultured BM-MSC

HL-1 monolayers were cultured in normoxic or hypoxic conditions for four hours. At the end of four hours, BM-MSCs were added to the monolayers and cultured together either in the same conditions (Normoxia and Hypoxia, respectively) or switched from hypoxic to normoxic conditions (Hypoxia + Reoxygenation) for additional two hours. Another set of experiments was done in the presence of 100 μ*M* CBX, a non-selective gap junction blocker. After the coculture, the cells were lifted, stained with anti-Sca-1 antibody, SYTOX-Red dead cell stain, and Pacific Blue-conjugated anti-Annexin V, and analyzed by flow cytometry (Figure 10, top panel). Sca-1 was used as a marker to gate for BM-MSC due to the high percentage (~80%) of expression in MSC compared to HL-1 (~1%). There was a very low baseline amount of cells stained positive for SYTOX-Red or Annexin V in BM-MSC from normoxic control cocultures (Figure 10, bottom panel). Coculturing with HL-1 in hypoxic conditions significantly increased the number of dead and late apoptotic BM-MSCs indicated by positive SYTOX-Red staining while Annexin V-positive BM-MSCs showed a slight increase, albeit not statistically significant. Interestingly, BM-MSCs cocultured with hypoxic HL-1 in normoxic condition (hypoxia + reoxygenation) showed a significant increase in the number of early apoptotic cells stained positive for Annexin V. The presence of the non-specific gap junction blocker CBX in the media of the coculture significantly attenuated the increase of SYTOX-Red-positive (dead and late apoptotic cells) and Annexin V-positive BM-MSCs in hypoxia and hypoxia–reoxygenation group, respectively.

Figure 10: Hypoxia and reoxygenation increased cell death and could be prevented by blocking gap junctions. Top: Example of data from flow cytometry analysis of BM-MSCs and HL-1 cells. Sca-1 was used to distinguish HL-1 (Sca-1 negative, left) from BM-MSC (Sca-1 positive, right). Sca-1-positive BM-MSCs were further analyzed for their SYTOX-Red (dead cells) and Annexin V (apoptotic cells) signals (inset). Bottom: Aggregate data from the experiments. Hypoxia and hypoxia–reoxygenation increased number of BM-MSCs stained positive for dead (SYTOX-Red) and apoptotic (Annexin V) markers, respectively. CBX significantly attenuated the increase in number of dead and apoptotic BM-MSCs in the corresponding group. (Data are presented as means ± S.E.M.; n=4–6; † and *: statistically significant when compared to respective normoxia control group, $p<0.05$; ‡ and §: statistically significant when compared to respective control group, $p<0.05$)

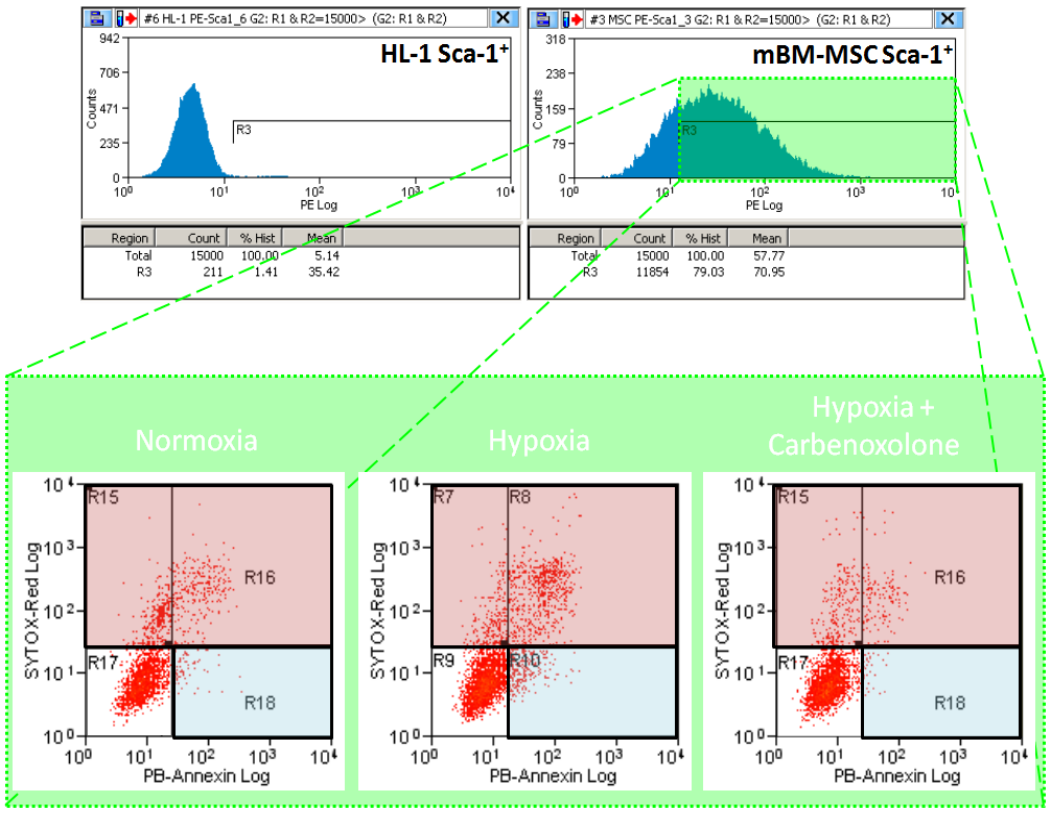
#6 HL-1 PE-Sca1_6 G2: R1 & R2=15000> (G2: R1 & R2)
HL-1 Sca-1+
Counts
PE Log
R3
Region | Count | % Hist | Mean
Total | 15000 | 100.00 | 5.14
R3 | 211 | 1.41 | 35.42
#3 MSC PE-Sca1_3 G2: R1 & R2=15000> (G2: R1 & R2)
mBM-MSC Sca-1+
Region | Count | % Hist | Mean
Total | 15000 | 100.00 | 57.77
R3 | 11854 | 79.03 | 70.95
Normoxia
Hypoxia
Hypoxia + Carbenoxolone
SYTOX-Red Log
PB-Annexin Log
R15
R16
R17
R18
R7
R8
R9
R10

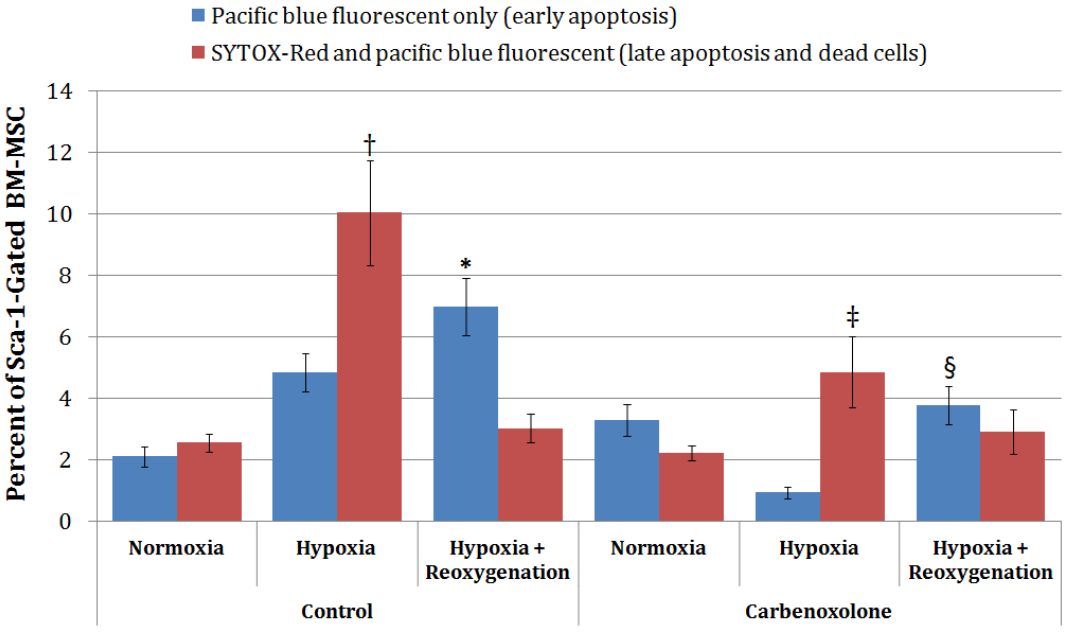
Pacific blue fluorescent only (early apoptosis)
SYTOX-Red and pacific blue fluorescent (late apoptosis and dead cells)
Percent of Sca-1-Gated BM-MSC
Normoxia
Hypoxia
Hypoxia + Reoxygenation
Control
Carbenoxolone
*
‡
§

6. Carbenoxolone Treatment Does Not Affect Proliferation of BM-MSC

Quantification of cell retention following transplantation can also be affected by the proliferative capacity of cells. We conducted *in vitro* studies to determine whether CBX affected proliferative capacity of the transplanted MSCs in culture. Sorted GFP^+ BM-MSCs were treated overnight with 100 μ*M* CBX or vehicle, then plated 1×10^5 cells into 6-well plates and the cell number was counted by an automatic cell counter. The number of cells plated was the same as number of cells we used in our injection studies (1×10^5). After one day of culture, the cells in both groups did not increase from the day of plating (1.02 vs. 1.16 fold original cell number for untreated- and CBX-treated-MSCs, respectively) (Figure 11). On day 2, BM-MSCs in both group showed 4-fold increase in cell number from the day of plating but no statistically significant difference between two groups.

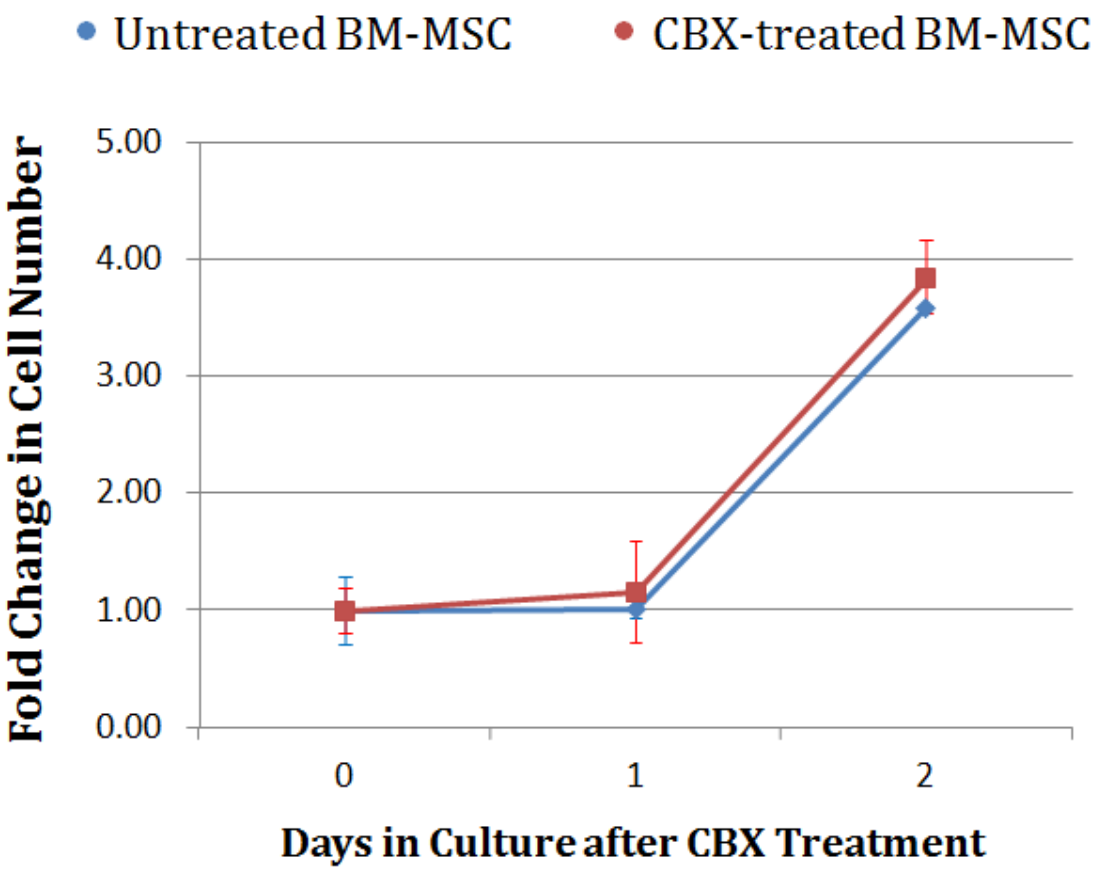

Figure 11: CBX treatment does not affect BM-MSC proliferation. Cells in each group were counted and all data normalized to number of cells at the start of the culture (1×10^5) and presented as means ± S.E.M. (n = 3 per group). No significant difference was observed between groups at any time point (p>0.05).

7. Carbenoxolone-Treated BM-MSC Effect on Cell Retention in the Heart after Ischemia–Reperfusion Injury

To further investigate the effects of CBX on BM-MSC retention in the heart after injury *in vivo*, we used the mouse model of ischemia–reperfusion injury. Mice were anesthetized and subjected to 90 minutes of ischemia followed by injection of 1×10^5 of either GFP^+ MSCs or CBX-treated GFP^+ MSCs in 10 µl injection buffer. The animals were allowed to recover for 24 hours after which their hearts were excised and digested. The whole heart digests were then analyzed for the number of GFP-positive BM-MSCs. The cells were first gated by size to enrich for the MSC population since the cardiomyocytes were larger than MSCs (Figure 12). To determine the ability to quantitatively detect the GFP-positive BM-MSCs, we spiked aliquots of control heart digests with varying numbers of GFP^+ MSCs and demonstrated a correlation between the number of cells added and the number of cells detected (Figure 13). We conclude from our data that flow cytometry accurately detects changes in the number of GFP^+ cells in total heart digests but it consistently underestimates the actual number of GFP^+ cells residing in these digests. These data enable us to more accurately interpret our findings in the subsequent experiments in which GFP^+ cells are injected into the myocardium and suggest that the number of retained transplanted cells is probably higher than that detected by flow cytometry from the whole heart. The average number of GFP^+ cells in heart digests from animals in the CBX-treated MSCs were greater than those in the control MSC group

however the increase was not statistically significant (Figure 14; 15,308.0 ± 11,296.5 vs. 3,619.8 ± 786.5, respectively) due to the large variability in the CBX+MSC group. Additional studies will need to be conducted to achieve a larger sample size and either confirm or refute this conclusion by statistical analysis.

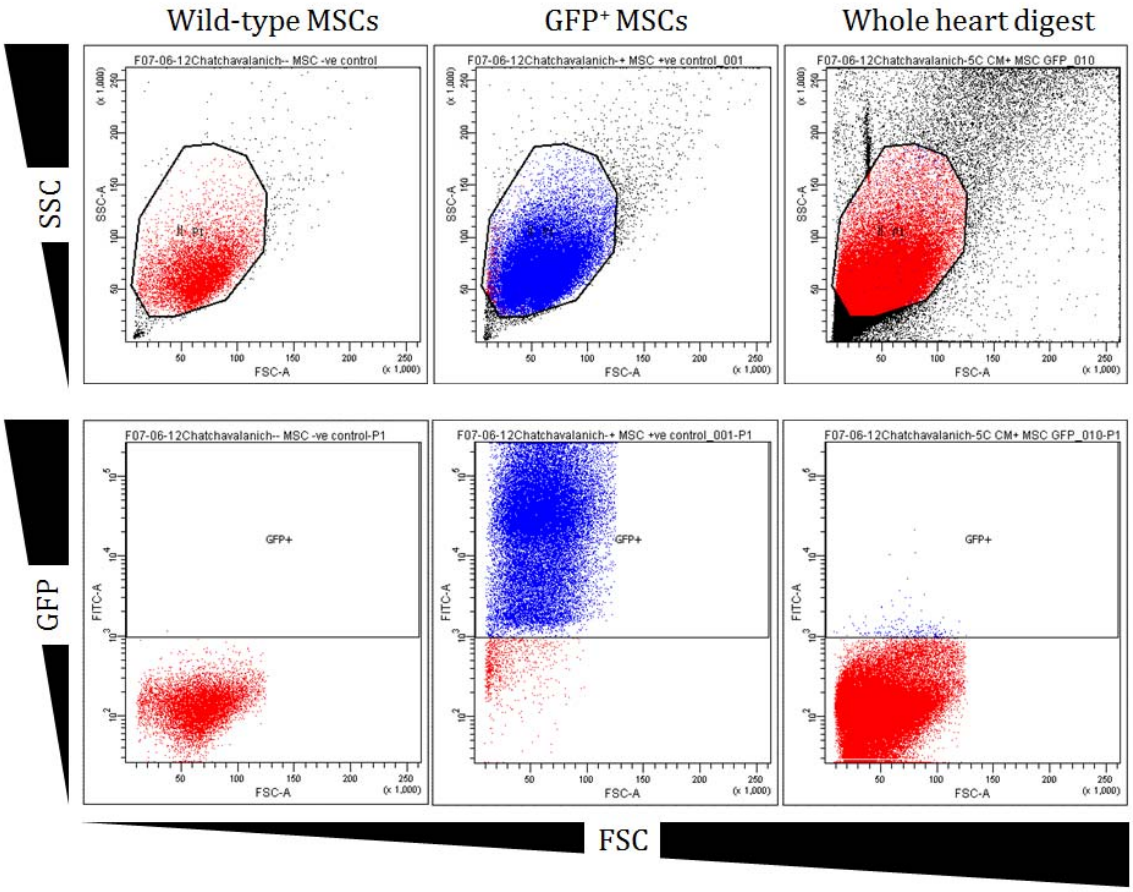

Figure 12: Flow cytometry analysis of whole heart digests. Sample data from wild-type MSCs (left), sorted GFP+ MSCs (middle), and whole heart digest (right) representing cell size (FSC: forward scatter), cell granularity (SSC: side scatter), and GFP signals. The data in the top three panels display all recorded events. The lower panel demonstrated gated event from inside the polygon in each respective upper panel (containing most of the MSCs; colored red), that was further analyzed for GFP-positive cells in MSC population (colored blue).

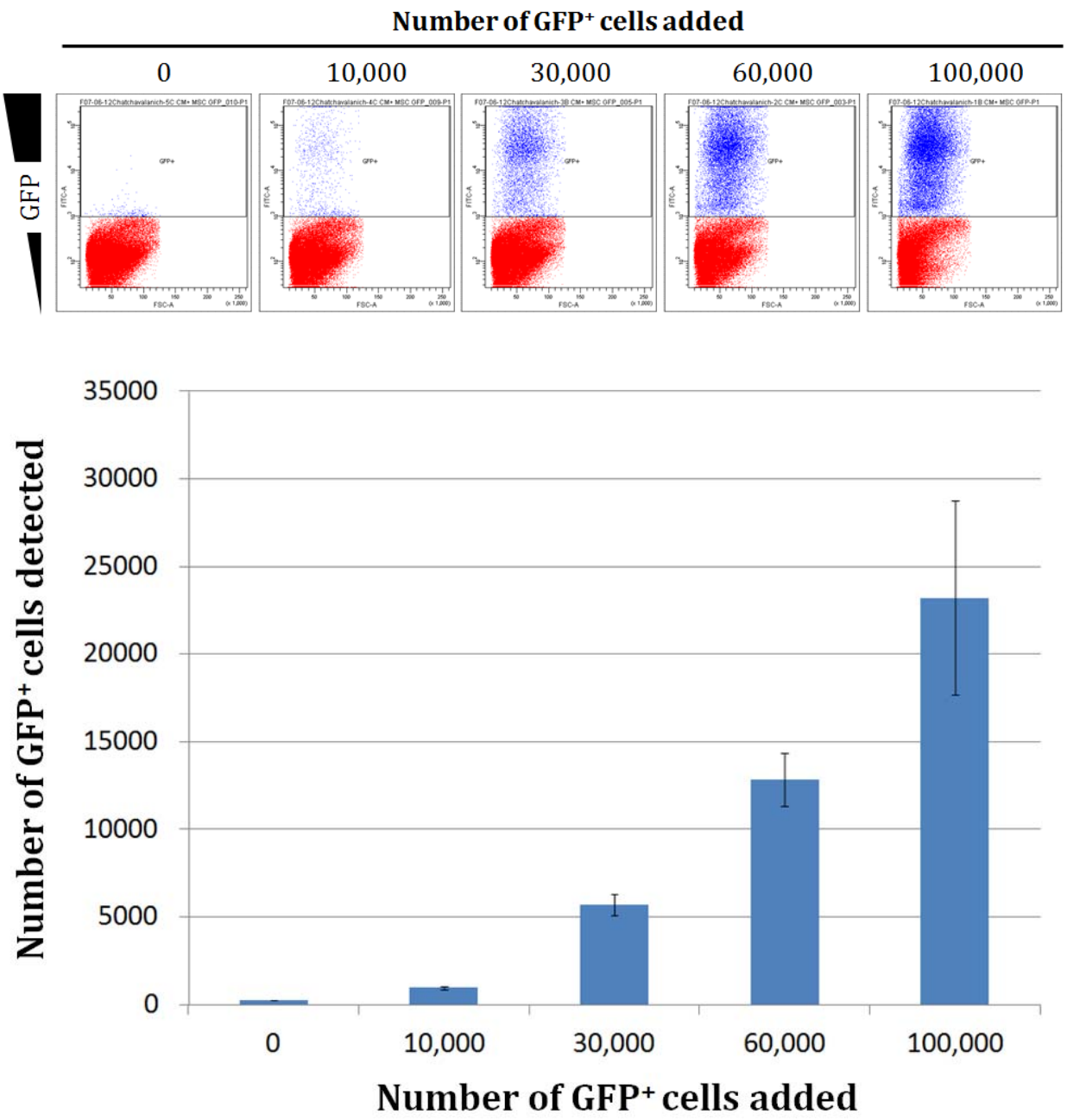

Figure 13: Flow cytometry data from heart digests spiked with GFP⁺ MSCs. Representative data (top) and histograms (bottom) showing number of GFP⁺ cells detected by flow cytometry analysis compared to the number of GFP⁺ MSCs added to an aliquot of heart digest. *n* = 3 except group 0, *n* = 1.

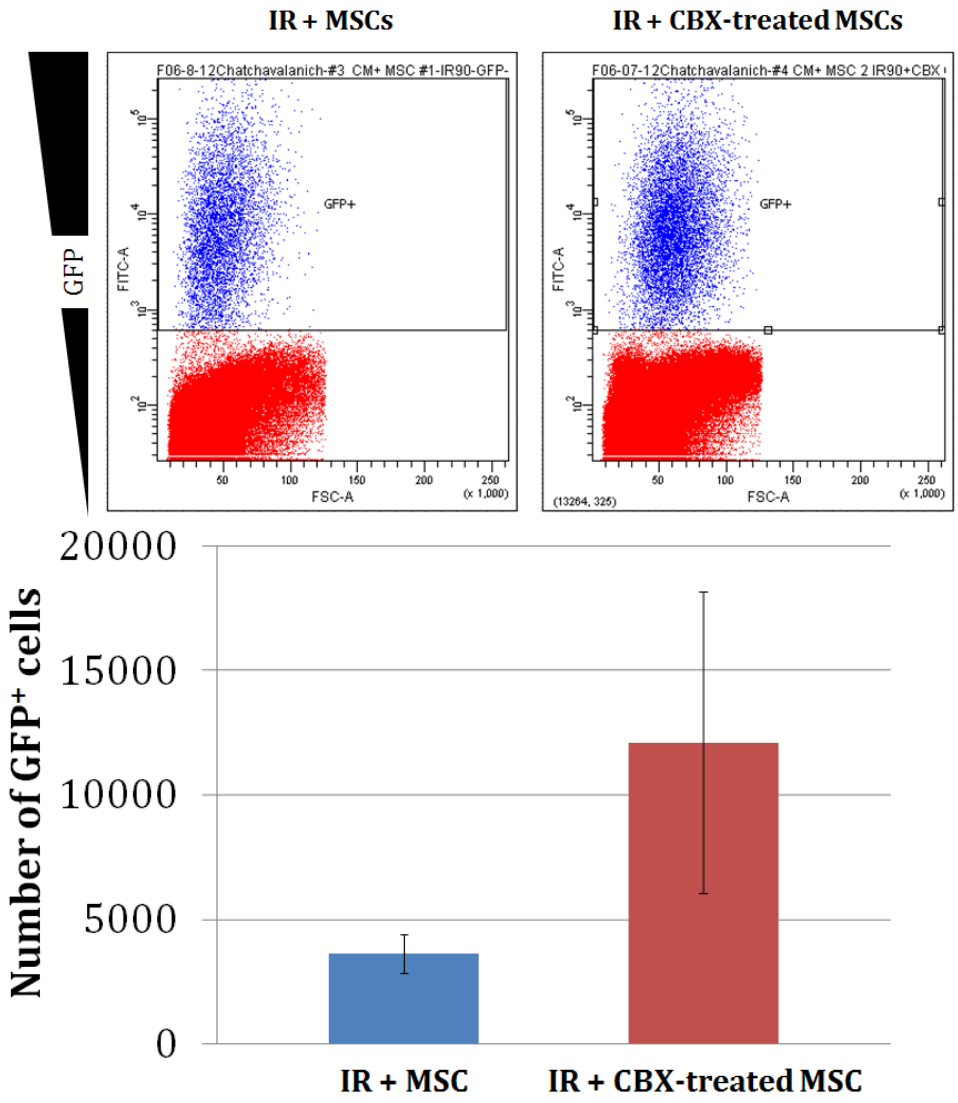

Figure 14: Retention of transplanted MSCs in the heart. Representative data (top) and histograms (bottom) showing number of GFP⁺ cells from whole heart digests detected by flow cytometry analysis. n = 5 and 11, respectively. p>0.05.

8. CBX-Treated BM-MSC Improved Cardiac Function after Ischemia–Reperfusion Injury

Animals suffered from ischemia–reperfusion injury were subjected to hemodynamic study at 24 hours after the surgery. Heart rate, LV pressure, LV volume and pressure–volume loops were recorded during the procedure described in method section. We chose 90 minutes of ischemia due to the observed depressed cardiac function (decreased dP/dt, stroke volume; Figure 15) as opposed to shorter time period which partially recovered after 30 minutes of reperfusion. Data were analyzed in PVAN software to calculate the elastance, ESPVR, and EDPVR (sample data: Figure 16-19). Summary of hemodynamic data is displayed in Figure 20 and TABLE I. Heart rate did not vary among experimental groups except in ischemia–reperfusion (IR) group which is significantly lower than ischemia–reperfusion animal receiving MSCs (IR+MSC). LV pressure was significantly decreased in IR animals compared to Sham+MSC. The decrease in pressure observed in IR group was attenuated by treatment with either untreated MSC (IR+MSC) or CBX-treated MSC (IR+MSC+CBX) groups. Vehicle containing CBX (IR+CBX) failed to emulate the protective effect observed in IR+MSC+CBX. End-systolic elastance (E_{es}) and maximum elastance (E_{max}) were significantly decreased in IR animals compared to Sham+MSC. As expected, MSC treatment improved E_{max} significantly above the levels observed in IR group, albeit not completely back to the Sham+MSC levels. The decreases of E_{es} and E_{max} were abolished when the animals were given CBX-treated MSCs. Similar to earlier observation, CBX alone

did not affect E_{es} and E_{max} in the animals. Consistent with elastances, maximum positive and minimum negative pressure derivatives (±dP/dt) after ischemia–reperfusion reduced significantly when compared to Sham+MSC animals. Treatment with MSCs markedly attenuated the reductions of both values. The pretreatment of MSCs with CBX further improved significantly the pressure derivatives and restored them to levels comparable with those of control animals. On the other hand, CBX alone did not display the same beneficial effects.

In summary, these data recapitulate the beneficial effect of MSC treatment on improving cardiac functions after ischemic injury and illustrated the beneficial effects of CBX treatment of MSCs prior to their administration. These effects however could not be achieve by the treatment with CBX alone hence emphasized the importance of MSCs and their protective effects.

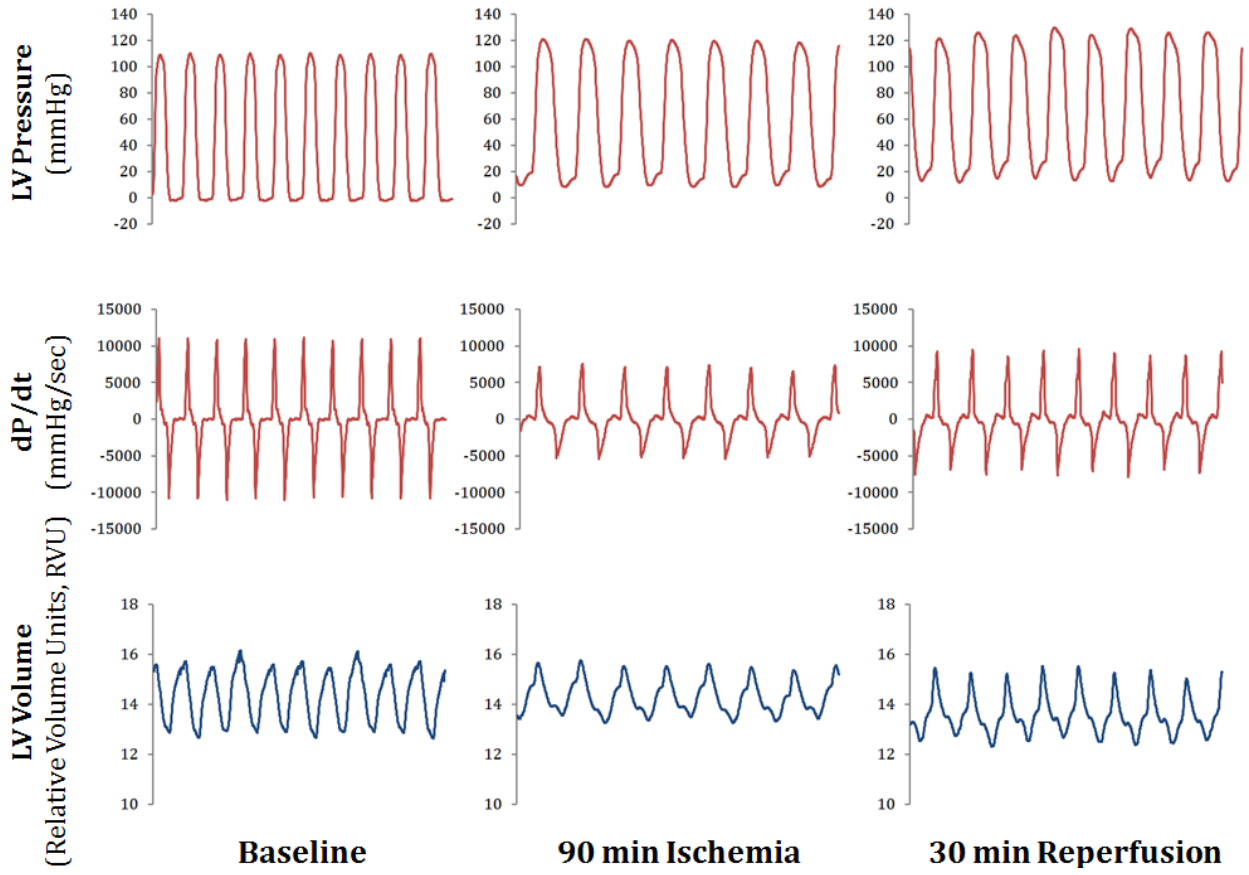

Figure 15: Changes in cardiac function over the course of ischemia–reperfusion. Sample hemodynamic data from one animal undergoing ischemia–reperfusion showing LV pressure (top panels), dP/dt (middle panels), and LV volume (bottom panels) at baseline (left), after 90 minutes of ischemia (center), and after 30 minutes of reperfusion (right). Each panel represents data recorded in 1 second.

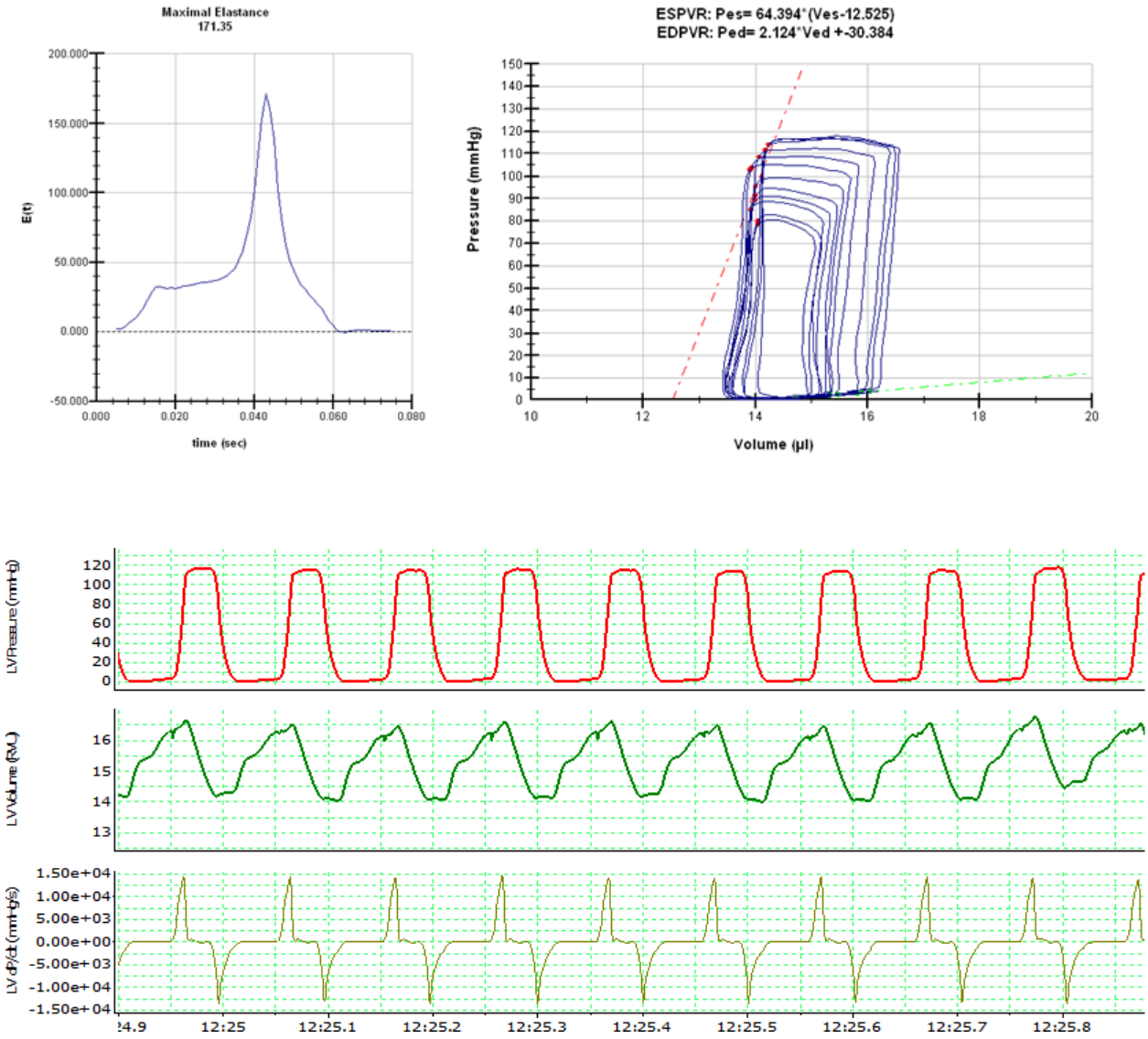

Figure 16: Hemodynamic data from baseline control group. Representative hemodynamic data from control group. Top left: Time course of changes in elastance. Top right: Pressure–volume loops recording (ESPVR: end-systolic pressure–volume relationship; EDPVR: end-diastolic pressure–volume relationship). Bottom: Hemodynamic recordings from a control animal showing recordings of LV pressure, LV volume, and derivative of LV pressure (LV dP/dt). Data from the chart recording in the lower three panels represent 1 second of data collection.

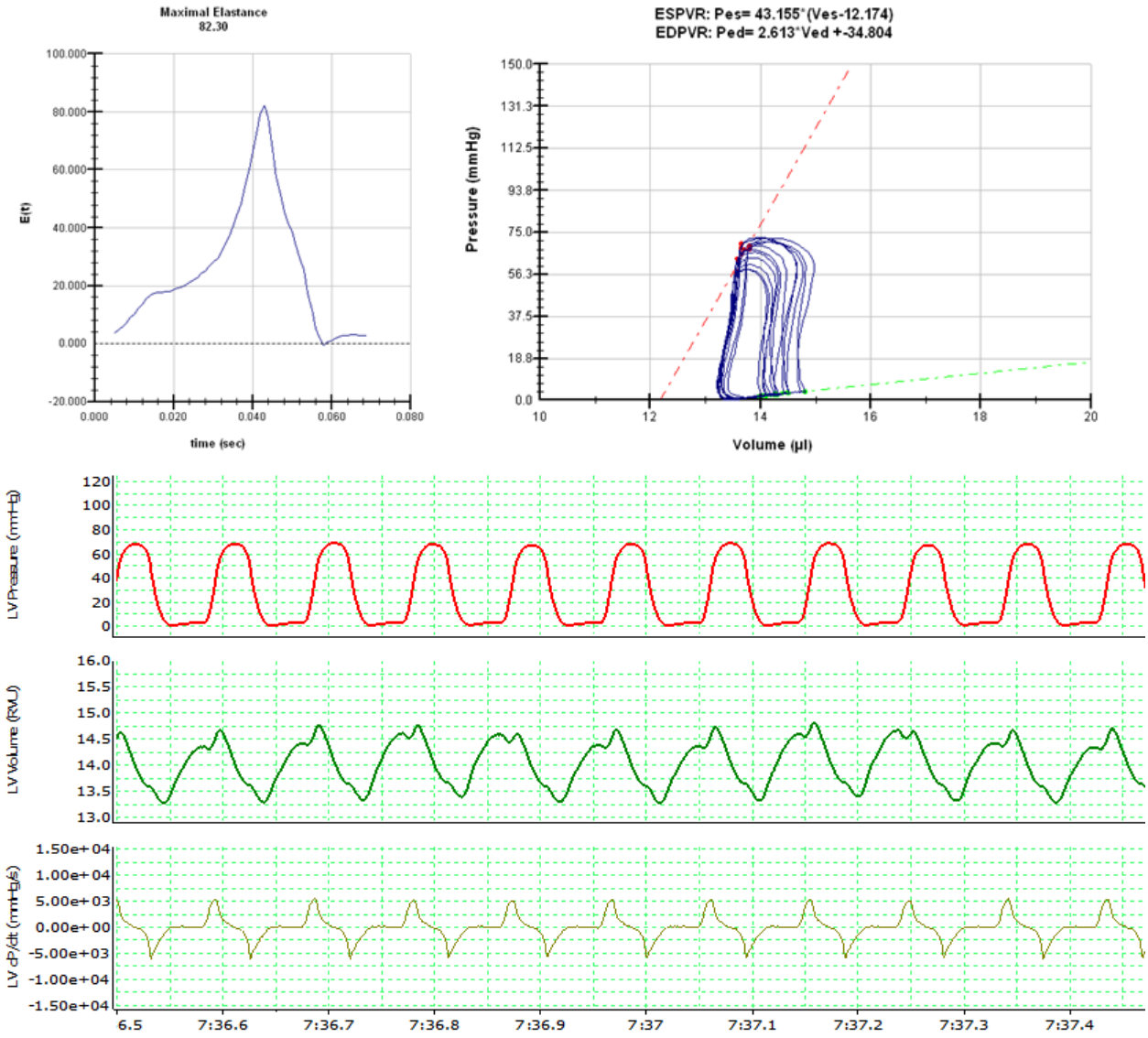

Figure 17: Hemodynamic data from MSC group. Representative hemodynamic data from MSC group. Top left: Time course of changes in elastance. Top right: Pressure–volume loops recording (ESPVR: end-systolic pressure–volume relationship; EDPVR: end-diastolic pressure–volume relationship). Bottom: Hemodynamic recordings from an animal receiving MSC transplantation showing recordings of LV pressure, LV volume, and derivative of LV pressure (LV dP/dt). Data from the chart recording in the lower three panels represent 1 second of data collection.

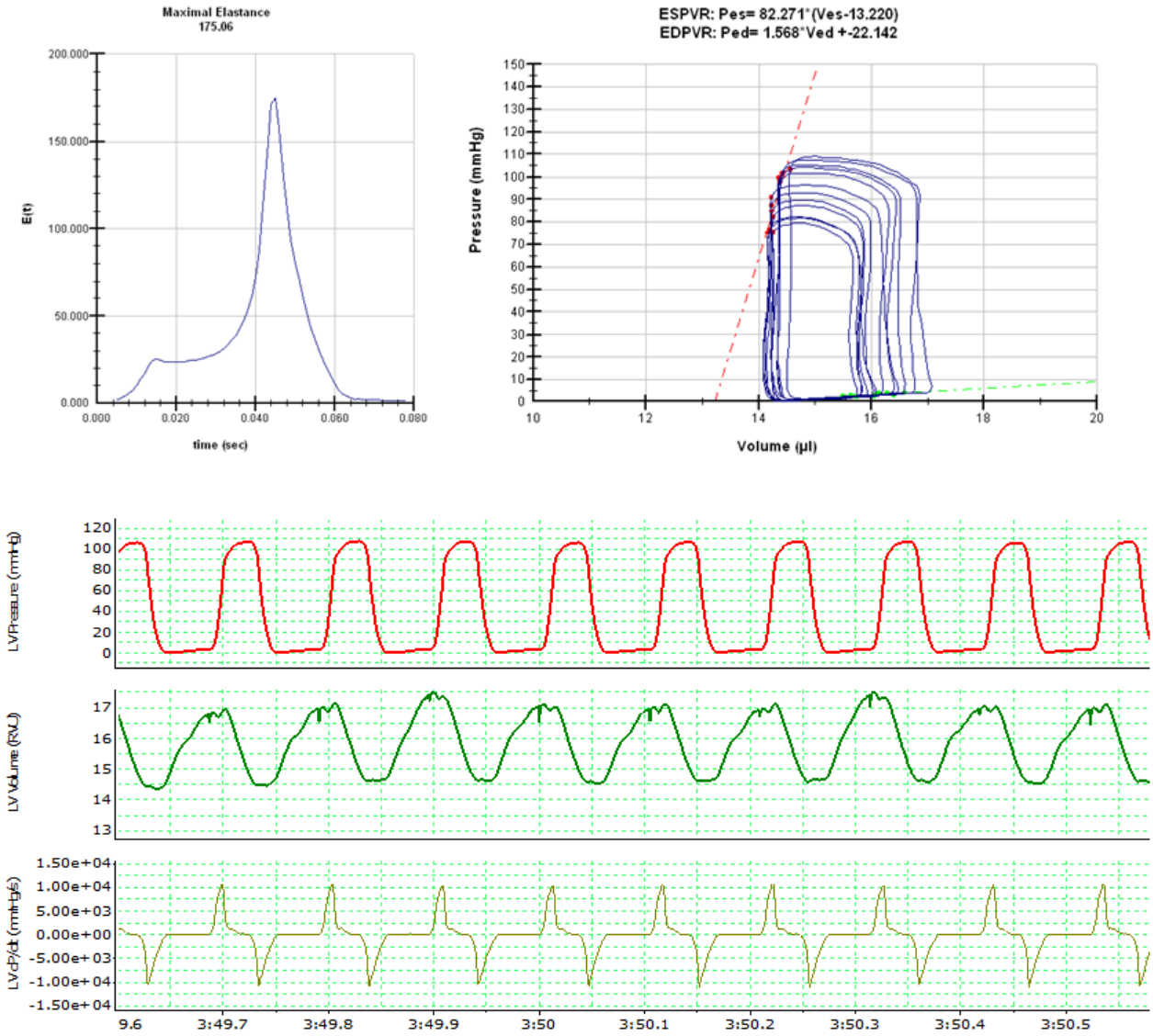

Figure 18: Hemodynamic data from CBX-treated MSC group. Representative hemodynamic data from CBX-treated MSC group. Top left: Time course of changes in elastance. Top right: Pressure–volume loops recording (ESPVR: end-systolic pressure–volume relationship; EDPVR: end-diastolic pressure–volume relationship). Bottom: Hemodynamic recordings from an animal receiving CBX-treated MSC transplantation showing recordings of LV pressure, LV volume, and derivative of LV pressure (LV dP/dt). Data from the chart recording in the lower three panels represent 1 second of data collection.

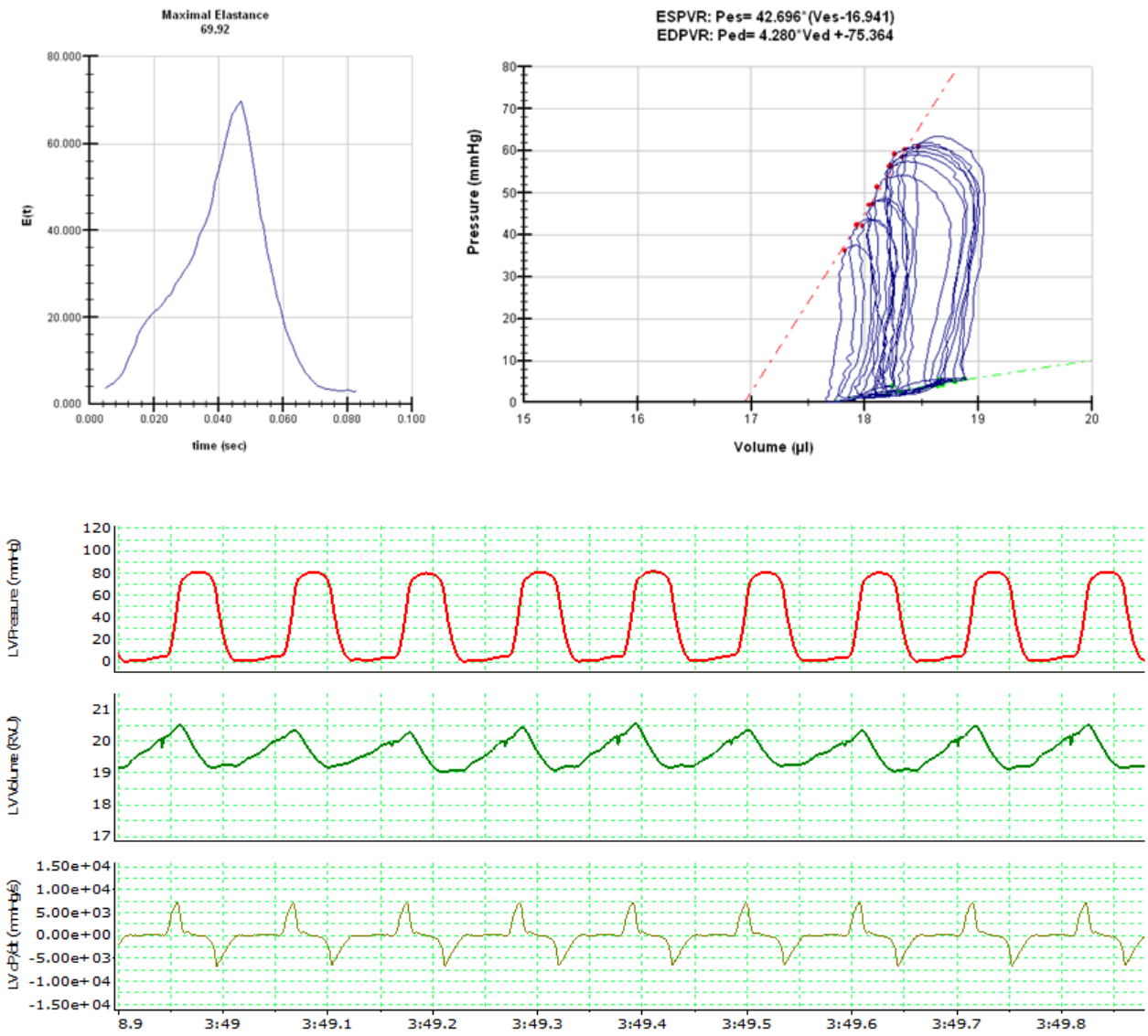

Figure 19: Hemodynamic data from CBX alone group. Representative hemodynamic data from CBX alone group. Top left: Time course of changes in elastance. Top right: Pressure–volume loops recording (ESPVR: end-systolic pressure–volume relationship; EDPVR: end-diastolic pressure–volume relationship). Bottom: Hemodynamic recordings from an animal receiving CBX injection alone showing recordings of LV pressure, LV volume, and derivative of LV pressure (LV dP/dt). Data from the chart recording in the lower three panels represent 1 second of data collection.

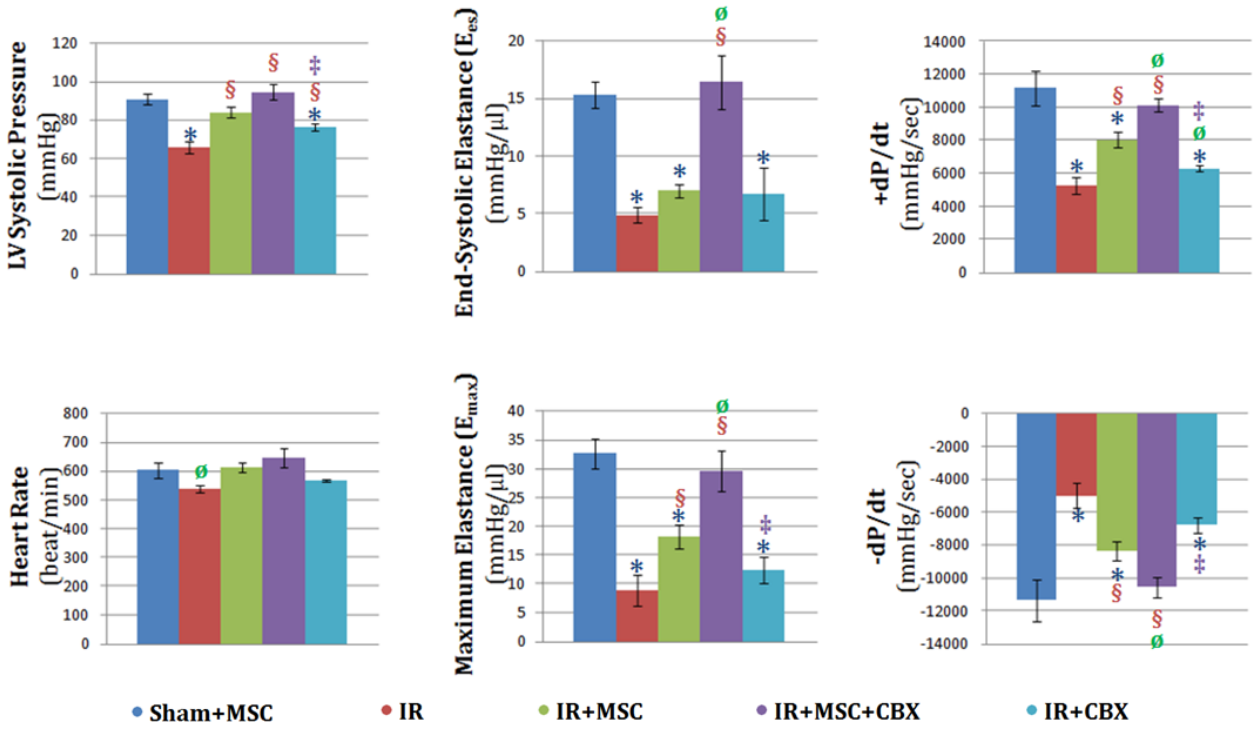

Figure 20: Summary of hemodynamic data. $+dP/dt_{max}$: maximum positive pressure derivative; $-dP/dt_{min}$: minimum negative pressure derivative. Sham+MSC: sham-operated animal receiving MSCs; IR: animal with ischemia–reperfusion without treatment; IR+MSC: animal with ischemia–reperfusion receiving MSCs; IR+MSC+CBX: animal with ischemia–reperfusion receiving CBX-treated MSCs; IR+CBX: animal with ischemia–reperfusion receiving vehicle with CBX. Data are presented as means ± S.E.M.; n=4, 3, 10, 5, and 4, respectively; *: statistically significant when compared to respective Sham+MSC group, $p<0.05$; §: statistically significant when compared to respective IR group, $p<0.05$; Ø: statistically significant when compared to respective IR+MSC group, $p<0.05$; ‡: statistically significant when compared to respective IR+MSC+CBX group, $p<0.05$

TABLE I

HEMODYNAMIC ASSESSMENT OF CARDIAC FUNCTION 24 HOURS AFTER ISCHEMIA–REPERFUSION INJURY

	LVP	HR	E_{es}	E_{max}	$+dP/dt_{max}$	$-dP/dt_{min}$
Sham+MSC [a]	90.9±3.0	604.3±31.5	15.3±1.4	32.7±3.0	11,180.8±1,212.3	-11,341.8±1,432.3
IR [b]	65.9±3.1[*]	539.3±13.3[ø]	4.9±0.7[*]	9.0±2.7[*]	5,254.3±528.8[*]	-4,972.7±783.0[*]
IR+MSC [c]	84.0±2.7[§]	613.5±15.4	7.0±0.6[*]	18.3±2.0[*,§]	8,081.7±438.2[*,§]	-8,331.1±569.3[*,§]
IR+MSC+CBX [d]	94.4±4.0[§]	646.0±34.7	16.4±2.3[ø,§]	29.7±3.4[§,ø]	10,133.4±408.6[§,ø]	-10,538.4±603.4[§,ø]
IR+CBX [e]	76.3±1.7[*,§,‡]	566.5±3.9	6.7±2.2[*,‡]	12.5±2.3[*,‡]	6,304.5±170.9[*,ø,‡]	-6764.0±464.6[*,,‡]

[a]: n=4

[b]: n=3

[c]: n=10

[d]: n=5

[e]: n=4

[*]: statistically significant when compared to respective Sham+MSC group, $p<0.05$.

[§]: statistically significant when compared to respective IR group, $p<0.05$

[ø]: statistically significant when compared to respective IR+MSC group, $p<0.05$.

[‡]: statistically significant when compared to respective IR+MSC+CBX group, $p<0.05$.

9. Treatment with CBX-Treated BM-MSC Does Not Affect Infarct Size at 24 Hours

To determine whether treatment with MSCs or CBX-treated MSCs could effects any detectable change in cardiac remodeling at this early time point, we measured infarct area and area-at-risk, in animals suffered from ischemia–reperfusion injury at 24 hours after the surgery by TTC staining method. The images of heart slices were analyzed to measure area-at-risk and infarct size, as detailed in method section. Both area-at-risk and infarct size were comparable among all experiment groups (TABLE II and Figure 21) with no statistically significant difference.

TABLE II

AREA-AT-RISK AND INFARCT SIZE AT 24 HOURS AFTER ISCHEMIA–REPERFUSION INJURY

	Area-at-risk (% of total area)	Infarct (% of area-at-risk)
Vehicle[a]	41.7	33.9
MSCs[b]	42.6±3.5	29.5±2.5
CBX-treated MSCs[c]	38.2±3.4	36.5±2.9

[a]: n=1

[b]: n=4

[c]: n=6

p>0.05

Figure 21: Treatment with CBX-treated MSCs does not affect Infarct size at 24 hours.
Top: Representative image of heart slices from vehicle, MSCs, and CBX-treated MSCs groups. Bottom: Summary of area-at-risk (left) and infarct (right) size from the experiments. n=1, 4, and 6 for vehicle, MSCs, and CBX-treated MSCs, respectively. p>0.05.

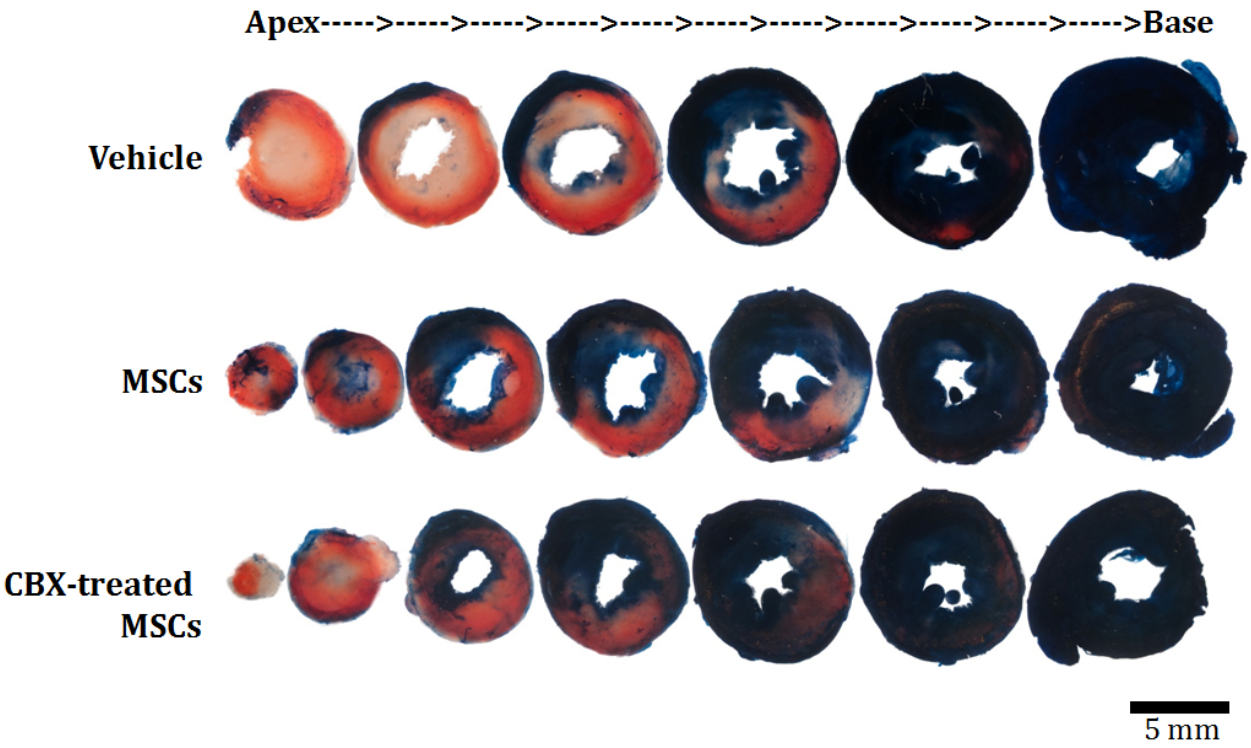
Apex----->----->----->----->----->----->----->----->----->----->Base
Vehicle
MSCs
CBX-treated MSCs
5 mm

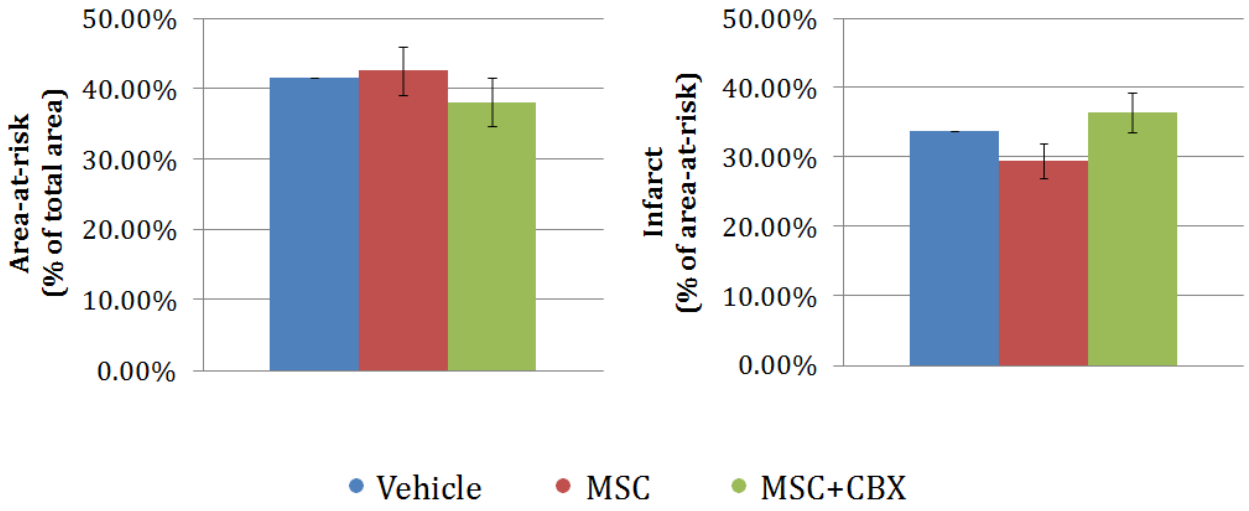
Area-at-risk (% of total area)
50.00%
40.00%
30.00%
20.00%
10.00%
0.00%
Infarct (% of area-at-risk)
50.00%
40.00%
30.00%
20.00%
10.00%
0.00%
Vehicle
MSC
MSC+CBX

IV. DISCUSSION

1. Discussion

The objective of our study was to determine the mechanisms that may be responsible for improved retention of bone marrow-derived mesenchymal stem cells transplanted within ischemic myocardium. To this end, we examined: (1) the ligand-receptor axis SDF-1-CXCR4 involved in stem cell integration, by using an adenoviral construct to overexpress CXCR4 in murine stem cells and (2) pharmacologic inhibition of gap junctions to prevent early cell-cell coupling between ischemic myocytes and transplanted stem cells.

1.1 Effect of SDF-1–CXCR4 on BM-MSC Migration and Retention

Homing of stem/progenitor cells to the target organ is a complex multifactorial process that is not well understood. SDF-1 is the only known potent chemoattractant of hematopoietic stem cells as has been demonstrated in mouse and human (Leri, Anversa, & Frishman, 2007). Along with its receptor, CXCR4, has been suggested to be one of the important regulatory elements in homing and migration of different cell types, both in developing embryo and adult, most notably in cancer and hematopoietic progenitor cells.

In the first part of this study, we tried to elucidate the importance of this receptor–ligand axis in the context of BM-MSC homing and retention in ischemic myocardium. Due to the very low percentage of $CXCR4^+$ cells in BM-MSCs (less than 1%, Figure 2), we decided to use an adenoviral approach to increase the number of $CXCR4^+$ BM-MSCs. BM-MSCs

transduced with an adenoviral vector expressing CXCR4 resulted in 16% of the cells expressing CXCR4 as observed by flow cytometry and greater CXCR4 protein expression as demonstrated by immunoblotting and immunofluorescence. However, AdCXCR4-transduced BM-MSCs did not migrate toward an SDF-1 gradient as expected or previously reported (Wynn, et al., 2004; Cheng, et al., 2008). This might have occurred as a result of overexpressing CXCR4 leading to downregulation of the receptor, possibly through arrestin-mediated internalization and lysosomal degradation. Additionally, Drury *et al*. have demonstrated recently that SDF-1 could present in dimer form and possess opposite effects on cell migration (Drury, et al., 2011). This might also be the reason why AdGFP control BM-MSCs did not show significant migration toward SDF-1 gradients apart from the low baseline percentage of CXCR4-expressing BM-MSCs. Previous studies indicate that hypoxia upregulates SDF-1 and CXCR4 expression in several types of cells, including MSCs, and that the effect is achieved through the PI3K/Akt/HIF-1α pathway (Liu, et al., 2010). Our results were contrary to these findings.

Nevertheless, our *in vivo* experiments in a murine model of myocardial ischemia–reperfusion injury revealed a trend toward an increase in AdCXCR4-induced MSC retention (n=2) while no difference was observed in MSC retention in the AdGFP control group. Our previously published study demonstrated increased homing of wild type BM-MSCs to the heart in mice with chronic MI but not in sham-operated animals (Boomsma, Swaminathan, & Geenen, Intravenously Injected Mesenchymal Stem Cells Home to Viable Myocardium

after Coronary Occlusion and Preserve Systolic Function without Altering Infarct Size., 2007). AdGFP-transduced control BM-MSCs in the present study did not show any difference in retention between sham and ischemia–reperfusion groups which further suggests that the difference we observed in our previous study was a result of differences in BM-MSC homing and not retention. The increase in MSC retention in mice in ischemia–reperfusion receiving AdCXCR4-BM-MSCs group in this study was independent of homing due to the fact that we utilized intramyocardial direct injections to deliver the cells. Even though we observed significantly reduced migration in AdCXCR4-BM-MSCs, these cells displayed enhanced retention in the hearts with ischemia–reperfusion injury and not in sham-operated hearts or in any AdGFP-transduced groups suggesting that the increase in BM-MSCs retention in this case was a result of overexpression of CXCR4 and probably mediated through a different pathway than those that regulate cell migration. Despite these preliminary data we found that cell membrane expression of the CXCR4 in the AdCXCR4-transduced cells (immunofluorescent data) were not consistent with the level of GFP expression in the cell. This could be a result of posttranscriptional regulation of the receptor, possibly by arrestin-dependent internalization and ubiquitin-mediated lysosomal degradation (Busillo & Benovic, 2007). One potential way to circumvent this problem would be to utilize CXCR4 that is constitutively active, either by a mutant form of the receptor (Berchiche, et al., 2007) or one with a truncated C-terminal tail as found in WHIM syndrome

Because of the inconsistent expression of CXCR4 in our transduced cells and because our *in vitro* observations were not in agreement with previously published migration studies using the SDF-1-CXCR4 axis, we focused on the role of cell-cell coupling as a potential mechanism to explain the loss of stem cell retention following transplantation.

1.2 Effect of Hypoxic HL-1 Coculture on BM-MSC Survival

The roles of hypoxia and reoxygenation in causing cell injury have been extensively studied and well established in different cells, including cardiomyocytes. The number of transplanted progenitor cells has been shown to decrease dramatically within hours of administration and the percentage of dead cells peaked at 24 hours after transplantation (Qiao, et al., 2009). Cells that become ischemic could trigger detrimental responses in adjacent cells which have not been affected by the original insult, a phenomenon termed 'bystander effect' which has been extensively described and studied in radiation injury (Sjostedt & Bezak, 2012). Gap junctions have been suggested to play an important role in propagating the signals involved in ionizing radiation-associated bystander effect. Therefore, we proposed that communication through gap junctions could be one of the mechanisms contributing to the loss of transplanted stem cells in ischemic myocardium and impairing their therapeutic efficacy.

We first employed *in vitro* coculture between HL-1 myocytes and BM-MSCs to test our hypothesis. Coculturing with hypoxic HL-1 elicited a significant increase in number of dead and apoptotic BM-MSCs. The difference between ratios of dead to apoptotic cells we observed could be due to the fact that in hypoxia group the HL-1s had been under hypoxia for total of 6 hours, while the insult lasted for only 4 hours in hypoxia+reperfusion group, resulting in more damage to the HL-1s. In hypoxia group, there were more SYTOX-Red-positive dead BM-MSCs than pacific blue-stained Annexin V-positive early apoptotic BM-MSCs while in hypoxia+reoxygenation the majority of dying BM-MSCs was only stained positive for Annexin V indicating that they are early apoptotic. CBX presence in the cocultures dramatically reduced the number of death and apoptotic cells in BM-MSCs cocultured with hypoxic HL-1s. And since CBX non-selectively blocks gap junction channels, this result suggests the important role of gap junction communication in triggering BM-MSCs death and apoptosis.

Role of gap junction channels in propagation of cell death has been implicated in bystander cell damage (Cusato, et al., 2003). The postulated mechanism suggested passage of small molecules which acts as 'bystander signal' between cells through gap junction channels. Due to the constraint in gap junction channel size, the estimated limit is 2 nm in diameter and in the range of 1–10 kDa (Sjostedt & Bezak, 2012; Nikjoo & Khvostunov, 2003). Although this study did not identify the mediator responsible for the death of BM-MSCs, we hypothesize that Ca^{2+} is a very plausible candidate. During ischemia, energy

depletion affects Na^+/K^+ and Ca^{2+} pump and consequently causes increase in cytosolic Ca^{2+} which in turn induces a spectrum of deleterious sequels (Kleinbongard, Baars, & Heusch, 2012). Ca^{2+} accumulates in mitochondria and triggers opening of mitochondrial permeability transition pore which further promotes mitochondrial depolarization and results in the release of cytochrome c from inner membrane of mitochondria to the cytosol. Cytochrome c release sequentially results in oligomerization of Apaf-1, formation of apoptosome, activation of caspase-9, and activation of effector caspases (Muñoz-Pinedo, 2012). Experiments focus on regulating cytosolic Ca^{2+} could further elucidate the importance of Ca^{2+} in death of BM-MSC in this context.

1.3 Effect of CBX on BM-MSC Retention in Heart Suffered from Ischemia–Reperfusion Injury

We demonstrated increased number of BM-MSCs in hearts at 24 hours after ischemia–reperfusion injury in the BM-MSCs that have been pretreated with CBX. Gap junction communication has been implicated in regulation of cell proliferation in several cell types, both in physiological and diseased states (Joshi, Martin, Shaver, Madamanchi, Muller-Borer, & Tulis, 2012; Hei, et al., 2012). In this study, the increase in BM-MSC retention was not a result of increase in BM-MSCs proliferation, as evident by the result from our cell proliferation assay, but presumably a protection from apoptosis bestowed by

pretreatment with CBX. A great deal of attention has been paid to promoting gap junction formation as a means to achieve functional integration of newly administered stem cells into the existing myocardium (Pillekamp F. , et al., 2009; Ramkisoensing, et al., 2012). Results from this study suggest that although gap junction is necessary to integration of transplanted progenitor cells into the host tissue, early coupling through gap junction channels could be pernicious to the cells and ravaging the communication through gap junction could prove beneficial to stem cell survival in the acute phase. Nevertheless, we believe that gap junction intercellular communication is essential in recovery of the organ in the long run and continuous blocking of gap junction could instead be disadvantageous. A study comparing the effect of low- and high-dose Cx43 mimetic peptide in treatment of cerebral ischemia indeed suggested that excessive inhibition of gap junction is associated with adverse outcomes (Davidson, Green, Nicholson, Bennet, & Gunn, 2012).

1.4 Effect of Improved BM-MSC Retention on Cardiac Function

Correlation between numbers of BM-MSCs used in treatment and their functional benefits has been recently substantiated by an updated systematic review of multiple randomized control trials (Clifford, et al., 2012). Although the increased number of MSCs in the ischemic hearts in animals receiving CBX-treated MSCs is not statistically significant, it could be attributed, at least partially, to the improvements in hemodynamic parameters we

observed. One of the modes of action of stem cells is through release of paracrine factors. Our laboratory, for instance, has reported detection of multiple cytokines in conditioned media from MSC which affect MSC migration, angiogenesis, and apoptosis (Boomsma & Geenen, Mesenchymal Stem Cells Secrete Multiple Cytokines That Promote Angiogenesis and Have Contrasting Effects on Chemotaxis and Apoptosis, 2012). Therefore, the increase in number of BM-MSCs equates more paracrine factors released, and accordingly greater effects.

Solely blocking gap junction intercellular communication with inhibitors has been showed to have beneficial effect in recovery of ischemic organ (Davidson, Green, Nicholson, Bennet, & Gunn, 2012). To examine whether the hemodynamic improvements we observed resulted from disrupted gap junction communication among cardiomyocytes *per se*, we performed similar *in vivo* experiments using vehicle containing CBX without BM-MSC. Unlike in the work by Davidson *et al.*, blocking of gap junction alone did not grant the same benefits on hemodynamic evidenced in CBX-treated BM-MSCs. Nevertheless, we could not dismiss the possible benefits of gap junction blocking in cardiomyocytes since we have to take in our consideration that the dose given in this study is several thousand folds lower than that used in their work.

Cardiac remodeling after myocardial infarction typically completes within 4 weeks, although none of the works on time course of ventricular remodeling was done in mice (DeFelice, Frering, & Horan, 1989; Jones, Mata, Yang, French, & Oshinski, 2002; Nahrendorf,

et al., 2003). Aberrations in cardiac functions happen concurrently with coronary occlusion and worsen over time. BM-MSC transplantation has been widely accepted for its benefits in treatment of several conditions, albeit with varying degree of efficacy which could arise from heterogeneity of BM-MSCs used. Although our result indicated that treatment with CBX-treated BM-MSCs could reverse functional abnormalities in the hearts to the levels equivalent to those of control sham-operated animals, it is yet to be determined whether these effects would be persistent through the remodeling process.

1.5 Effect of CBX-Treated MSC Treatment on Infarct Size

We did not observed any statistically significant difference in area-at-risk and infarct size among groups. Nevertheless, the remodeling process, as mentioned previously, is an evolving process which occurs over weeks. Changes at this early period that might be undetectable could eventually develop to become drastically different end points. Infarct scar size has been shown to have a linear relation with ejection fraction and LV volumes (Ørn, et al., 2007). It is reasonable to further examine, at a later time point, the effect of CBX-treated MSCs on infarct size and scar formation.

2. Conclusion

Our study demonstrated a novel mechanism by which cardiomyocytes in injured heart could potentially affect survivability of transplanted stem cells. In this context, early coupling between stem cells and cardiomyocytes is detrimental and interfering with it by disrupting gap junction intercellular communication using gap junction inhibitor is proven to be beneficial. Although we concurs that regulation of stem cell homing and survival is multifactorial, application of this knowledge could prove to be imperative to the success of stem cell replacement therapy under inimical environment.

3. Limitations and Future Direction

Importance of electrical coupling between cardiomyocytes and transplanted cells has been emphasized and often ascribed to gap junction formation. Effort to enhance gap junction conductance has been associated with enhanced integration of transplanted cells (Stagg, et al., 2006) although it might not be desirable in some other context (Fahrenbach, Ai, & Banach, 2008). Nevertheless, the possibility that disruption of gap junction channel communication could be arrhythmogenic needs to be address despite the fact that the dosage we used is almost negligible.

We also still have yet to identify the mediator signaling cell death although we consider Ca^{2+} as a plausible culprit. As shown in other system, cytosolic Ca^{2+} are

responsible for inducing the death of the cells, interfering with their dynamics could further elucidate its role in this process.

Regarding the effect of gap junction communication on MSC retention *in vivo*, even though we could not demonstrated a significant difference between our experimental and control groups we strongly believe that the change we observed is not trivial. The variability we saw in our CBX-treated MSC group could be a result of local change caused by CBX affecting the quality of our sample preparation technique since data from our MSC control samples are notably consistent. Employing alternative techniques to document the number of cells in tissue could prove useful in clarifying this matter.

Another issue that needs to be considered is other effects of CBX which include blocking of pannexon membrane channels and 11β-HSD (11-beta hydroxylsteroid dehydrogenase). Although we believe that the protective effects of CBX we observed are results of their ability to interfere with gap junction communication, we could not rule out the possibility of them being caused by alternative effects of CBX. Our laboratory has recently obtained mice with Cre-inducible Cx43 knock out which could be used to harvest for BM-MSCs to use as an alternative to CBX pretreatment. Additionally, other inhibitors, or even activators, of gap junction could be of use in supporting our current findings.

Lastly, the study in our current project looked at a cross-section of data at a very acute phase where several events concurrently happen at the same time. Any subtle albeit

significant changes in cardiac structure and function could be masked by inflammatory responses in the heart. Ischemic injury-induced cardiac remodeling causes changes in cardiac architecture and function developing several weeks. Further investigations at different time points would further elucidate on whether the observed protective effects would last over the course of changes and whether there is any additional beneficial effects pertaining to CBX-treated MSCs. The result would ascertain the importance of regulating gap junction communication between grafted stem cells and host cardiomyocytes in the critical early period.

CITED LITERATURE

Alkhatib, G. (2009). The Biology of CCR5 and CXCR4. *Curr Opin HIV AIDS , 4* (2), 96-103.

Angelini, A., Castellani, C., Francesco, T., Gambino, A., Caforio, A. P., Feltrin, G., et al. (2007). Continuous Engraftment and Differentiation of Male Recipient Y-Chromosome-Positive Cardiomyocytes in Donor Female Human Heart Transplants. *J Heart Lung Transplant , 26* (11), 1110-1118.

Antman, E. M., Anbe, D. T., Armstrong, P. W., Bates, E. R., Green, L. A., Hand, M., et al. (2004). ACC/AHA Guidelines for the Management of Patients with ST-Elevation Myocardial Infarction: A Report of the American College of Cardiology/American Heart Association Task Force on Practice Guidelines. *Circulation , 110* (9), e82-e292.

Anversa, P., Olivetti, G., & Capasso, J. M. (1991). Cellular Basis of Ventricular Remodeling after Myocardial Infarction. *Am J Cardiol , 68*, 7D-16D.

Asumda, F. Z., & Chase, P. B. (2012). Nuclear Cardiac Troponin and Tropomyosin are Expressed Early in Cardiac Differentiation of Rat Mesenchymal Stem Cells. *Differentiation , 83* (3), 106-115.

Beltrami, A. P., Barlucchi, L., Torella, D., Baker, M., Limana, F., Chimenti, S., et al. (2003). Adult Cardiac Stem Cells are Multipotent and Support Myocardial Regeneration. *Cell , 114* (6), 763-776.

Berchiche, Y. A., Chow, K. Y., Lagane, B., Leduc, M., Paercherancier, Y., Fujii, N., et al. (2007). Direct Assessment of CXCR4 Mutant Conformations Reveals Complex Link between Receptor Structure and Gαi Activation. *J Biol Chem , 282* (8), 5111-5115.

Bolognese, L., & Cerisano, G. (1999). Early Predictors of Left Ventricular Remodeling after Acute Myocardial Infarction. *Am Heart J* , S79-S83.

Boomsma, R. A., & Geenen, D. L. (2012). Mesenchymal Stem Cells Secrete Multiple Cytokines That Promote Angiogenesis and Have Contrasting Effects on Chemotaxis and Apoptosis. *PLoS One , 7* (4), e35685.

Boomsma, R. A., Swaminathan, P. D., & Geenen, D. L. (2007). Intravenously Injected Mesenchymal Stem Cells Home to Viable Myocardium after Coronary Occlusion and Preserve Systolic Function without Altering Infarct Size. *Int J Cardiol , 122* (1), 17-28.

Burger, J. A., & Kipps, T. J. (2006). CXCR4: a Key Receptor in the Crosstalk between Tumor Cells and Their Microenvironment. *Blood , 107* (5), 1761-1767.

Busillo, J. M., & Benovic, J. L. (2007). Regulation of CXCR4 Signaling. *Biochim Biophys Acta , 1768* (4), 952-963.

Cashman, T. J., Gouon-Evans, V., & Costa, K. D. (2012, May 11). Mesenchymal Stem Cells for Cardiac Therapy: Practical Challanges and Potential Mechanisms. *Stem Cell Rev* , xxx-xxx.

Cencioni, Cencioni, C., Capogrossi, M. C., & Napolitano, M. (2012). The SDF-1/CXCR4 Axis in Stem Cell Preconditioning. *Cardiovasc Res , 94* (3), 400-407.

Chang, M. G., Tung, L., Sekar, R. B., Chang, C. Y., Cysyk, J., Dong, P., et al. (2006). Proarrhythmic Potential of Mesenchymal Stem Cell Transplantation Revealed in an In Vitro Coculture Model. *Circulation , 113* (15), 1832-1841.

Chedrawy, E. G., Wang, J. S., Nguyen, D. M., Shum-Tim, D., & Chiu, R. C. (2002). Incorporationand Integration of Implanted Myogenic and Stem Cells into Native Myocardial Fibers: Anatomic Basis for Functional Improvements. *J Thorac Cardiovasc Surg , 124*, 584-590.

Cheng, Z., Ou, L., Zhou, X., Li, F., Jia, X., Zhang, Y., et al. (2008). Targeted Migration of Mesenchymal Stem Cells Modified with CXCR4 Gene to Infarcted Myocardium Improves Cardiac Performance. *Mol Ther , 16* (3), 571-579.

Chiong, M., Wang, Z. V., Pedrozo, Z., Cao, D. J., Troncoso, R., Ibacache, M., et al. (2011). Cardiomyocyte Death: Mechanisms and Translational Implications. *Cell Death Dis , 2* (12), e244.

Christoforou, N., & Gearhart, J. D. (2007). Stem Cells and Their Potential in Cell-Based Cardiac Therapies. *Prog Cardiovasc Dis , 49* (6), 396-413.

Clifford, D. M., Fisher, S. A., Brunskill, S. J., Doree, C., Mathur, A., Watt, S., et al. (2012). Stem Cell Treatment for Acute Myocardial Infarction. *Cochrane Database Syst Rev , 2*, CD006536.

Cusato, K., Bosco, A., Rozental, R., Guimarães, C. A., Reese, B. E., Linden, R., et al. (2003). Gap Junctions Mediate Bystander Cell Death in Developing Retina. *J Neurosci , 23* (16), 6413-6422.

Davidson, J. O., Green, C. R., Nicholson, L. F., Bennet, L., & Gunn, A. J. (2012). Deleterious Effects of High Dose Connexin 43 Mimetic Peptide Infusion After Cerebral Ischaemia in Near-Term Fetal Sheep. *Int J Mol Sci , 13* (5), 6303-6319.

Dbouk, H. A., Mroue, R. M., El-Sabban, M. E., & Talhouk, R. S. (2009). Connexins: A Myriad of Functions Extending beyong Assembly of Gap Junction Channels. *Cell Commun Signal , 7*, 4.

de Groot, J. R., Veenstra, T., Verkerk, A. O., Wilders, R., Smits, J. P., Wilms-Schopman, F. J., et al. (2003). Conduction Slowing by the Gap Junctional Uncoupler Carbenoxolone. *Cardiovasc Res , 60* (2), 288-297.

DeFelice, A., Frering, R., & Horan, P. (1989). Time Course of Hemodynamic Changes in Rats with Healed Severe Myocardial Infarction. *Am J Physiol Heart Circ Physiol , 257* (1 Pt 2), H289-H296.

Dominici, M., Le Blanc, K., Mueller, I., Slaper-Cortenbach, I., Marini, F., Krause, D., et al. (2006). Minimal Criteria for Defining Multipotent Mesenchymal Stromal Cells. The International Society for Cellular Therapy Position Statement. *Cytotherapy , 8* (4), 315-317.

Downey, J. M. (n.d.). *Measuring Infarct Size by the Tetrazolium Method*. Retrieved June 30, 2012, from http://www.usouthal.edu/ishr/help/ttc/

Drury, L. J., Ziarek, J. J., Gravel, S., Veldkamp, C. T., Takekoshi, T., Hwang, S. T., et al. (2011). Monomeric and Dimeric CXCL12 Inhibit Metastatis Through Distinct CXCR4 Interactions and Signaling Pathways. *Proc Natl Acad Sci U S A , 108* (43), 17655-17660.

Durig, J., Rosenthal, C., Halfmeyer, K., Wiemann, M., Novotny, J., Bingmann, D., et al. (2000). Intercellular Communication between Bone Marrow Stromal Cells and CD34+ Haematopoietic Progenitor Cells is Mediated by Connexin 43-Type Gap Junctions. *Br J Haematol , 111*, 416-425.

Eltzschig, H. K., & Eckle, T. (2011). Ischemia and Reperfusion—from Mechanism to Translation. *Nat Med , 17* (11), 1391-1401.

Fahrenbach, J. P., Ai, X., & Banach, K. (2008). Decreased Intercellular Coupling Improves the Function of Cardiac Pacemakers Derived from Mouse Embryonic Stem Cells. *J Mol Cell Cardiol , 45* (5), 642-649.

Feng, Y., Broder, C. C., Kennedy, P. E., & Berger, E. A. (1996). HIV-1 Entry Cofactor: Functional cDNA Cloning of a Sever-Transmembrane, G Protein-Coupled Receptor. *Science , 272* (5263), 872-877.

Fong, E. L., Chan, C. K., & Goodman, S. B. (2011). Stem Cell Homing in Musculoskeletal Injury. *Biomaterials , 32* (2), 395-409.

Formigli, L., Perna, A.-M., Meacci, E., Cinci, L., Margheri, M., Nistri, S., et al. (2007). Paracrine Effects of Transplanted Myoblasts and Relaxin on Post-Infarction Heart Remodelling. *J Cell Mol Med , 11* (5), 1087-1100.

Ghadge, S. K., Mühlstedt, S., Özcelik, C., & Bader, M. (2011). SDF-1α as a Therapeutic Stem Cell Homing Factor in Myocardial Infarction. *Pharmacol Ther , 129* (1), 97-108.

Glimm, H., Oh, I.-H., & Eaves, C. J. (2000). Human Hematopoietic Stem Cells Stimulated to Proliferate in vitro Lose Engraftment Potential During Theri S/G2/M Transit and Do Not Reenter G0. *Blood , 96* (13), 4185-4193.

Gnecchi, M., Danieli, P., & Cervio, E. (2012). Mesenchymal Stem Cell Therapy for Heart Disease. *Vascul Pharmacol* , xxx-xxx.

Goldspink, P. H., Montgomery, D. E., Walker, L. A., Urboniene, D., McKinney, R. D., Geenen, D. L., et al. (2004). Protein Kinase Cε Overexpression Alters Myofilament Properties and Composition During the Progression of Heart Failure. *Circ Res , 95* (4), 424-432.

Grajales, L., García, J., Banach, K., & Geenen, D. L. (2010). Delayed Enrichment of Mesenchymal Cells Promotes Cardiac Lineage and Calcium Transient Development. *J Mol Cell Cardiol , 48* (4), 735-745.

Grejier, A. E., & van der Wall, E. (2004). The Rold of Hypoxia Inducible Factor 1 (HIF-1) in Hyopxia Induced Apoptosis. *J Clin Pathol , 57* (10), 1009-1014.

Hei, Z., Zhang, A., Wei, J., Gan, X., Wang, Y., Luo, G., et al. (2012). Lipopolysaccharide Effects on the Proliferation of NRK52E Cells via Alternations in Gap-Junction Function. *J Trauma Acute Care Surg , 73* (1), 67-72.

Hidesama, O., Bradfute, S. B., Gallardo, T. D., Nakamura, T., Gaussin, V., Mishina, Y., et al. (2003). Cardiac Progenitor Cells from Adult Myocardium: Homing, Differentiation, and Fusion after Infarction. *Proc Natl Acad Sci U S A , 100* (21), 12313-12318.

Hill, J. M., Dick, A. J., Raman, V. K., Thompson, R. B., Yu, Z. X., Hinds, K. A., et al. (2003). Serial Cardiac Magnetic Resonance Imaging of Injected Mesenchymal Stem Cells. *Circulation , 108*, 1009-1014.

Honczarenko, M., Le, Y., Swierkowski, M., Ghiran, I., Glodek, A. M., & Silberstein, L. E. (2006). Human Bone Marrow Stromal Cells Express a Distinct Set of Biologically Functional Chemokine Receptors. *Stem Cells , 24* (4), 1030-1041.

Jones, J. R., Mata, J. F., Yang, Z., French, B. A., & Oshinski, J. N. (2002). Left Ventricular Remodeling Subsequent to Reperfused Myocardial Infarction: Evaluation of a Rat Model Using Cardiac Magnetic Resonance Imaging. *J Cardiovasc Magn Reson , 4* (3), 317-326.

Joshi, C. N., Martin, D. N., Shaver, P., Madamanchi, C., Muller-Borer, B. J., & Tulis, D. A. (2012). Control of Vascular Smooth Muscle Cell Growth by Connexing 43. *Front Physiol , 3*, 220.

Kleinbongard, P., Baars, T., & Heusch, G. (2012, June 14). Calcium Antagonists in Myocardial Ischemia/Reperfusion–Update 2012. *Wien Med Wochenschr* , Epub ahead of print.

Koninckx, R., Hensen, K., Daniëls, A., Moreels, M., Lambrichts, I., Jongen, H., et al. (2009). Human Bone Marrow Stem Cells Co-Cultured with Neonatal Rat Cardiomyocytes Display Limited Cardiomygenic Plasticity. *Cytotherapy , 11* (6), 778-792.

Kucia, M., Dawn, B., Hunt, G., Guo, Y., Wysoczynski, M., Majka, M., et al. (2004). Cells Expressing Early Cardiac Markers Reside in the Bone Marrow and Are Mobilized into the Peripheral Blood after Myocardial Infarction. *Circ Res , 95* (12), 1191-1199.

Kunze, A., Congreso, M. R., Hartmann, C., Wallraff-Beck, A., Huttmann, K., Bedner, P., et al. (2009). Connexin Expression by Radial Glia-Like Cells is Required for Neurogenesis in the Adult Dentate Gyrus. *Proc Natl Acad Sci U S A , 106*, 11336-11341.

Kushner, F. G., Hand, M., Smith, S. C., King, S. B., Anderson, J. L., Antman, E. M., et al. (2009). 2009 Focused Updates: ACC/AHA Guidelines for the Management of Patients With ST-Elevation Myocardial Infarction (updating the 2004 Guideline and 2007 Focused Update) and ACC/AHA/SCAI Guidelines on Percutaneous Coronary Intervention. *Circulation , 120* (22), 2271-2306.

Laflamme, M. A., Myerson, D., Saffitz, J. E., & Murry, C. E. (2002). Evidence for Cardiomyocyte Repopulation by Extracardiac Progenitors in Transplanted Human Hearts. *Circ Res , 90* (6), 634-640.

Lapidot, T., & Kollet, O. (2002). The Essential Roles of the Chemokine SDF-1 and Its Receptor CXCR4 in Human Stem Cell Homing and Repopulation of Transplanted Immune-Deficiend NOD/SCID and NOD/SCID/B2m(null) Mice. *Leukemia , 16* (10), 1992-2003.

Laugwitz, K.-L., Moretti, A., Lam, J., Gruber, P., Chen, Y., Woodard, S., et al. (2005). Postnatal isl1+ Cardioblasts Enter Fully Differentiated Cardiomyocyte Lineages. *Nature , 433* (7026), 647-653.

Leri, A., Anversa, P., & Frishman, W. (Eds.). (2007). *Cardiovascular Regeneration and Stem Cell Therapy* (1 ed.). Singapore: Blackwell Publishing.

Leung, D. S., Unsicker, K., & Reuss, B. (2002). Expression and Developmental Regulation of Gap Junction Connexins Cx26, Cx32, Cx43 and Cx45 in the Rat Midbrain-Floor. *Int J Dev Neurosci , 20*, 63-75.

Li, W., Ma, N., Ong, L. L., Nesselmann, C., Klopsch, C., Ladilov, Y., et al. (2007). Bcl-2 Engineered MSCs Inhibited Apoptosis and Improved Heart Function. *Stem Cells , 25*, 2118-2127.

Lin, J. H., Weigel, H., Cotrina, M. L., Liu, S., Bueno, E., Hansen, A. J., et al. (1998). Gap-Junction-Mediated Propagation and Amplification of Cell Injury. *Nat Neurosci , 1*, 494-500.

Liu, H., Xue, W., Ge, G., Luo, X., Li, Y., Xiang, H., et al. (2010). Hypoxic Preconditioning Advances CXCR4 and CXCR7 Expression by Activating HIF-1α in MSCs. *Biochem Biophys Res Commun , 401* (4), 509-515.

Maass, K., Chase, S. E., Lin, X., & Delmar, M. (2009). Cx43 CT Domain Influences Infarct Size and Susceptibility to Ventricular Tachyarrhythmias in Acute Myocardial Infarction. *Cardiovasc Res , 84* (3), 361-367.

Maeda, S., & Tsukihara, T. (2011). Structure of the Gap Junction Channel and Its Implications for Its Biological Functions. *Cell Mol Life Sci , 68* (7), 1115-1129.

Martin, C. M., Meeson, A. P., Robertson, S. M., Hawke, T. J., Richardson, J. A., Bates, S., et al. (2004). Persistent Expression of the ATP-binding Cassette Transporter, Abcg2, Identifies Cardiac SP Cells in the Developing and Adult Heart. *Dev Biol , 265* (1), 262-275.

Meşe, G., Richard, G., & White, T. W. (2007). Gap Junctions: Basic Structure and Function. *J Invest Dermatol , 127* (11), 2516-2524.

Mohanty, S., Bose, S., Jain, K. G., Bhargava, B., & Airan, B. (2011, September 6). TGFβ1 Contributes to Cardiomyogenic-Like Differentiation of Human Bone Marrow Mesenchymal Stem Cells. *Int J Cardiol* , xxx-xxx.

Muller, P., Pfeiffer, P., Koglin, J., Schäfers, H.-J., Seeland, U., Janzen, I., et al. (2002). Cardiomyocytes of Noncardiac Origin in Myocardial Biopsies of Human Transplanted Hearts. *Circulation , 106* (1), 31-35.

Muller-Borer, B. J., Cascio, W. E., Anderson, P. A., Snowwaert, J. N., Frye, J. R., Desai, N., et al. (2004). Adult-Derived Liver Stem Cells Acquire a Cardiomyocyte Structural and Functional Phenotype ex vivo. *Am J Pathol , 165* (1), 135-145.

Muñoz-Pinedo, C. (2012). Signaling Pathways that Regulate Life and Cell Death: Evolution of Apoptosis in the Context of Self-Defense. *Adv Exp Med Biol , 738*, 124-143.

Nagasawa, T., Nakajima, T., Tachibana, K., Iizasa, H., Bleul, C. C., Yoshie, O., et al. (1996). Molecular Cloning and Characterization of a Murine Pre-B-Cell Growth-Stimulating Factor/Stromal Cell-Derived Factor 1 Receptor, A Murine Homolog of the Human Immunodeficiency Virus 1 Entry Coreceptor Fusin. *Proc Natl Acad Sci U S A , 93* (25), 14726-14729.

Nahrendorf, M., Hu, K., Fraccarollo, D., Hiller, K.-H., Haase, A., Bauer, W. R., et al. (2003). Time Course of Right Ventricular Remodeling in Rats with Experimental Myocardial Infarction. *Am J Physiol Heart Circ Physiol , 284* (1), H241-H248.

National Research Council. (1996). *Guide for the Care and Use of Laboratory Animals.* Washington, DC: The National Academies Press.

Nikjoo, H., & Khvostunov, I. K. (2003). Biophysical Model of the Radiation-Induced Bystander Effect. *Int J Radiat Biol , 79* (1), 43-52.

O'Connell, T. D., Ni, Y. G., Lin, K.-M., Han, H., & Yan, Z. (2003). *Isolation and Culture of Adult Mouse Cardiac Myocytes for Signaling Studies.* AfCS Research Reports.

Ørn, S., Manhenke, C., Anand, I. S., Squire, I., Nagel, E., Edvardsen, T., et al. (2007). Effect of Left Ventricular Scar Size, Location and Transmurality on Left Ventricular Remodeling with Healed Myocardial Infarction. *Am J Cardiol , 99* (8), 1109-1114.

Pearson, R. A., Luneborg, N. L., Becker, D. L., & Mobbs, P. (2005). Gap Junctions Modulate Interkinetic Nuclear Movement in Retinal Progenitor Cells. *J Neurosci , 25*, 10803-10814.

Peixoto, P. M., Ryu, S. Y., Pruzansky, D. P., Kuriakose, M., Gilmore, A., & Kinnally, K. W. (2009). Mitochondrial Apoptosis is Amplified Through Gap Junctions. *Biochem BiophysRes Commun , 390*, 38-43.

Peled, A., Petit, I., Kollet, O., Magid, M., Ponomaryov, T., Byk, T., et al. (1999). Dependence of Human Stem Cell Engraftment and Repopulation of NOD/SCID Mice on CXCR4. *Science , 283* (5403), 845-848.

Pillekamp, F., Halbach, M., Reppel, M., Pfannkuche, K., Nazzal, R., Nguemo, F., et al. (2009). Physiological Differences between Transplanted and Host Tissue Cause Functional Decoupling after in vitro Transplantation of Human Embryonic Stem Cell-Derived Cardiomyocytes. *Cell Physiol Biochem , 23*, 65-74.

Pillekamp, F., Halbach, M., Reppel, M., Pfannkuche, K., Nazzal, R., Nguemo, F., et al. (2009). Physiological Differences Between Transplanted and Host Tissue Cause Funtional Decoupling after in vitro Transplantation of Human Embryonic Stem Cell-Derived Cardiomyocytes. *Cell Physiol Biochem , 23* (1-3), 65-74.

Qiao, H., Surti, S., Choi, S. R., Raju, K., Zhang, H., Ponde, D. E., et al. (2009). Death and Proliferation Time Course of Stem Cells Transplanted in the Myocardium. *Mol Imaging Biol , 11* (6), 408-414.

Quaini, F., Urbanek, K., Beltrami, A. P., Finato, N., Beltrami, C. A., Nadal-Ginard, B., et al. (2002). Chimerism of the Transplanted Heart. *N Engl J Med , 346* (1), 5-15.

Ramachandran, S., Xie, L. H., John, S. A., Subramaniam, S., & Lal, R. (2007). A Novel Role for Connexin Hemichannel in Oxidative Stress and Smoking-Induced Cell Injury. *PLoS One , 2*, e712.

Ramesh, B., Bishi, D. K., Rallapalli, S., Arumugam, S., Cherian, K. M., & Guhathakurta, S. (2012, March 7). Ischemic Cardiac Tissue Conditioned Media Induced Differentiation of Human Mesenchymal Stem Cells into Early Stage Cardiomyocytes. *Cytotechnology* , xxx-xxx.

Ramkisoensing, A. A., Pijnappels, D. A., Swildens, J., Goumans, M. J., Fibbe, W. E., Schalij, M. J., et al. (2012). Gap Junctional Coupling with Cardiomyocytes is Necessary but Not Sufficient for Cardiomyogenic Differentiation of Cocultured Human Mesenchymal Stem Cells. *Stem Cells , 30* (6), 1236-1245.

Ratajczak, M. Z., Kim, C. H., Abdel-Latif, A., Schneider, G., Kucia, M., Morris, A. J., et al. (2012). A Novel Perspective on Stem Cell Homing and Mobilization: Review on Bioactive Lipids as Potent Chemoattractants and Cationic Peptides as Underappreciated Modulators of Responsiveness to SDF-1 Gradients. *Leukemia , 26* (1), 63-72.

Reaume, A. G., de Sousa, P. A., Kulkarni, S., Langille, B. L., Zhu, D., Davies, T. C., et al. (1995). Cardiac Malformation in Neonatal Mice Lacking Connexin43. *Science , 267*, 1831-1834.

Redel, A., Jazbutyte, V., Smul, T. M., Lange, M., Eckle, T., Eltzschig, H., et al. (2008). Impact of Ischemia and Reperfusion Times on Myocardial Infarct Size in Mice In Vivo. *Exp Biol Med , 233* (1), 84-93.

Roger, V. L., Go, A. S., Llyod-Jones, D. M., Benjamin, E. J., Berry Jarett, D., Borden, W. B., et al. (2012). Heart Disease and Stroke Statistics—2012 Update: A Report from the American Heart Association. *Circulation , 125* (1), e2-e220.

Rose, R. A., Jiang, H., Wang, X., Helke, S., Tsoporis, J. N., Gong, N., et al. (2008). Bone Marrow-Derived Mesenchymal Stromal Cells Express Cardiac Specific Markers, Retain the Stromal Phenotype, and Do Not Become Functional Cardiomyocytes In Vitro. *Stem Cells , 26* (11), 2884-2892.

Rota, M., Kajstura, J., Hosoda, T., Bearzi, C., Vitale, S., Esposito, G., et al. (2007). Bone Marrow Cells Adopt the Cardiomyogenic Fate in vivo. *Proc Natl Acad Sci U S A , 104*, 17783-17788.

Rozental, R., Morales, M., Mehler, M. F., Urban, M., Kremer, M., Dermietzel, R., et al. (1998). Changes in the Properties of Gap Junctions During Neuronal Differentiation of Hippocampal Progenitor Cells. *J Neurosci , 18*, 1753-1762.

Ruiz-Meana, M., & Garcia-Dorado, D. (2009). Pathophysiology of Ischemia-Reperfusion Injury: New Therapeutic Options for Acute Myocardial Infarction. *Rev Esp Cardiol , 62* (2), 199-209.

Sano, S., Nakagawa, Y., Yamaguchi, R., FujisawaY, Satake, E., Nagata, E., et al. (2012). Carbenoxolone Alters the Morphology of Adipose Tissues and Downregulates Genes Involved in Adipogenesis, Glucose Transport and Lipid Metabolism in High-Fat Diet-Fed Mice. *Horm Metab Res , 44* (1), 15-20.

Sharma, M., Afrin, F., Satija, N., Tripathi, R. P., & Gangenahalli, G. U. (2011). Stromal-Derived Factor-1/CXCR4 Signaling: Indispensable Role in Homing and Engraftment of Hematopoietic Stem Cells in Bone Marrow. *Stem Cells Dev , 20* (6), 933-946.

Siegel, G., Krause, P., Wöhrle, S., Nowak, P., Ayturan, M., Kluba, T., et al. (2012, March 13). Bone Marrow-Derived Human Mesenchymal Stem Cells Express Cardiomyogenic Proteins But Do Not Exhibit Functional Cardiomyogenic Differentiation Potential. *Stem Cells Dev* , xxx-xxx.

Sjostedt, S., & Bezak, E. (2012). Non-Targeted Effects of Ionising Radiation and Radiotherapy. *Australas Phys Eng Sci Med , 33* (3), 219-231.

Sordi, V., Malosio, M. L., Marchesi, F., Mercalli, A., Melzi, R., Giordano, T., et al. (2005). Bone Marrow Mesenchymal Stem Cells Express a Restricted Set of Functionally Active Chemokine Receptors Capable of Promoting Migration to Pancreatic Islets. *Blood , 106* (2), 419-427.

Stagg, M. A., Coppen, S. R., Suzuki, K., Varela-Carver, A., Lee, J., Brand, N. J., et al. (2006). Evaluation of Frequency, Type, and Function of Gap Junctions between Skeletal Myoblasts Overexpressing Connexin43 and Cardiomyocytes: Relevance to Cell Transplantation. *FASEB J , 20* (6), 744-746.

Thygesen, K., Alpert, J. S., & White, H. D. (2007). Universal Definition of Myocardial Infarction. *Circulation , 116* (22), 2634-2653.

Uemura, R., Xu, M., Ahmad, N., & Ashraf, M. (2006). Bone Marrow Stem Cells Prevent Left Ventricular Remodeling of Ischemic Heart Through Paracrine Signaling. *Circ Res , 98*, 1414-1421.

Villars, F., Guillotin, B., Amedee, T., Dutoya, S., Bordenave, L., Bareille, R., et al. (2002). Effect of HUVEC on Human Osteoprogenitor Cell Differentiation Needs Heterotypic Gap Junction Communication. *Am J Physiol Cell Physiol , 282*, C775-C785.

Wang, T., Xu, Z., Jiang, W., & Ma, A. (2006). Cell-to-Cell Contact Induces Mesenchymal Stem Cell to Differentiate into Cardiomyocyte and Smooth Muscle Cell. *Int J Cardiol , 109* (1), 74-81.

Wen, J., Zhang, J.-Q., Huang, W., & Wang, Y. (2012). SDF-1α and CXCR4 as Therapeutic Targets in Cardiovascular Disease. *Am J Cardiovasc Dis , 2* (1), 20-28.

Williams, A. R., & Hare, J. M. (2011). Mesenchymal Stem Cells: Biology, Pathophysiology, Translational Findings and Therapeutic Implications for Cardiac Disease. *Circ Res , 109* (8), 923-940.

Wobus, A. M., Kaomei, G., Shan, J., Wellner, M.-C., Rohwedel, J., Guanju, J., et al. (1997). Retinoic Acid Accelerates Embryonic Stem Cell-Derived Cardiac Differentiation and Enhances Development of Ventricular Cardiomyocytes. *J Mol Cell Cardiol , 29* (6), 1525-1539.

Wu, Y., Ip, J. E., Huang, J., Zhang, L., Matsushita, K., Liew, C. C., et al. (2006). Essential Role of ICAM-1/CD18 in Mediating EPC Recruitment, Angiogenesis, and Repair to the Infarcted Myocardium. *Circ Res , 99*, 315-322.

Wynn, R. F., Hart, C. A., Corradi-Perini, C., O'Neill, L., Evans, C. A., Wraith, J. E., et al. (2004). A Small Proportion of Mesenchymal Stem Cells Strongly Expresses Functionally Active CXCR4 Receptor Capable of Promoting Migration to Bone Maroow. *Blood , 104* (9), 2643-2645.

Xu, M., Uemura, R., Dai, Y., Wang, Y., Pasha, Z., & Ashraf, M. (2007). In vitro and in vivo Effects of Bone Marrow Stem Cells on Cardiac Structure and Function. *J Mol Cell Cardiol , 42*, 441-448.

Xue, T., Cho, H. C., Akar, F. G., Tsang, S. Y., Jones, S. P., Marban, E., et al. (2005). Functional Integration of Electrically Active Cardiac Derivatives from Genetically Engineered Human Embryonic Stem Cells with Quiescent Receipient Ventricular Cardiomyocytes: Insights into the Development of Cell-Based Pacemakers. *Circulation , 111*, 11-20.

Yagi, H., Soto-Gutierrez, A., Parekkadan, B., Kitagawa, Y., Tompkins, R. G., Kobayashi, N., et al. (2010). Mesenchymal Stem Cells: Mechanisms of Immunomodulation and Homing. *Cell Transplant , 19* (6), 667-679.

APPENDICES

APPENDIX A: Protocol approval letter (12-052)

UIC UNIVERSITY OF ILLINOIS AT CHICAGO

Office of Animal Care and
Institutional Biosafety Committees (MC 672)
Office of the Vice Chancellor for Research
206 Administrative Office Building
1737 West Polk Street
Chicago, Illinois 60612-7227

April 23, 2012

David L. Geenen
Medicine/Cardiology
M/C 715

Dear Dr. Geenen:

The protocol indicated below was reviewed at a convened ACC meeting in accordance with the Animal Care Policies of the University of Illinois at Chicago on **3/20/2012**. *The protocol was not initiated until final clarifications were reviewed and approved on* **4/23/2012**. *The protocol is approved for a period of* ***3*** years with annual continuation.

Title of Application: Cardiac Muscle Regeneration in Heart Failure

ACC Number: 12-052

Initial Approval Period: 4/23/2012 to 3/20/2013

Current Funding: ***Currently protocol NOT matched to specific funding source. Modification will need to be submitted prior to Just in time or acceptance of award to match protocol to external funding source. All animal work proposed in the funding application must be covered by an approved protocol.***

Performance Site: ***UIC is the only performance site currently approved for this protocol.***

This institution has Animal Welfare Assurance Number A3460.01 on file with the Office of Laboratory Animal Welfare (OLAW), NIH. **This letter may only be provided as proof of IACUC approval for those specific funding sources listed above in which all portions of the funding proposal are matched to this ACC protocol.**

In addition, all investigators are responsible for ensuring compliance with all federal and institutional policies and regulations related to use of animals under this protocol and the funding sources listed on this protocol. Please use OLAW's "*What Investigators Need to Know about the Use of Animals*" (http://grants.nih.gov/grants/olaw/InvestigatorsNeed2Know.pdf) as a reference guide. Thank you for complying with the Animal Care Policies and Procedures of UIC.

Sincerely yours,

Bradley Merrill, PhD
Chair, Animal Care Committee

BM/*mbb*

APPENDIX B: Protocol approval letter (08-077)

UNIVERSITY OF ILLINOIS
AT CHICAGO

Office of Animal Care and Institutional Biosafety Committees (MC 672)
Office of the Vice Chancellor for Research
206 Administrative Office Building
1737 West Polk Street
Chicago, Illinois 60612-7227

November 26, 2008

David L. Geenen
Medicine/Cardiology
M/C 715

Dear Dr. Geenen:

The protocol indicated below has been reviewed in accordance with the Institutional Biosafety Committee Policies of the University of Illinois at Chicago and was approved on **11/13/2008** for **3** years. *The protocol was not initiated until final clarifications were reviewed and approved on **11/26/2008** **with the following conditions.***

Title of Application: Chemokine Receptor 4 Expression in Mesenchymal Stem Cells

IBC Number: 08-077

Condition 1: The enclosed report indicates the training status for bloodborne pathogen (BBP) training. Only those personnel who have been trained and whose training has not expired are approved for work that may involve exposure to bloodborne pathogens. Please note that federal regulations require yearly training for BBP.

Condition 2: Mice will be housed in BSL2 for one week following injection of cells transfected with adenovirus. Personnel working with mice will need to undergo BRL/COMRB BSL2 training prior to initiation of work with transfected cells and mice.

You may forward this letter of acceptable IBC verification of your research protocol to the funding agency considering this proposal. **Please be advised that investigators must report significant changes in their research protocol to the IBC office via a letter addressed to the IBC chair prior to initiation of the change. If a protocol changes in such a manner as to require IBC approval, the change may not be initiated without IBC approval being granted.**

Thank you for complying with the UIC's Policies and Procedures.

Sincerely,

Randall C. Jaffe, Ph.D.
Chair, Institutional Biosafety Committee

RCJ/*mbb*

Enclosures

Cc: IBC file, Santipongse Chatchavalvanich

VITA

Santipongse Chatchavalvanich

EDUCATION

2006–2012 Ph.D., Physiology and Biophysics, College of Medicine
University of Illinois at Chicago, Chicago, Illinois

1996–2002 M.D., Faculty of Medicine Siriraj Hospital
Mahidol University, Bangkok, Thailand

RESEARCH AND PROFESSIONAL EXPERIENCE

2006–2012 Graduate Student
David L. Geenen, Ph.D., Assistant Professor
Department of Physiology and Biophysics
University of Illinois at Chicago, Chicago, Illinois

2005–2006 Postdoctoral Scholar
Konstantin G. Birukov, M.D., Ph.D., Assistant Professor
Section of Pulmonary and Critical Care Medicine
Department of Medicine
University of Chicago, Chicago, Illinois

2004–2005	Postdoctoral Fellow
	Konstantin G. Birukov, M.D., Ph.D., Assistant Professor
	Division of Pulmonary and Critical Care Medicine
	Department of Medicine
	Johns Hopkins University, Baltimore, Maryland

TEACHING EXPERIENCE

2002–2004	Instructor
	Department of Physiology
	Faculty of Medicine Siriraj Hospital, Bangkok, Thailand

HONORS AND AWARDS

2009–2010	American Heart Association Predoctoral Fellowship
	(Midwest Affiliate)
2012	Third Place, Annual Stem Cell and Regenerative Medicine Program
	Outstanding Research Award in Stem Cell and Regenerative Medicine

MEMBERSHIPS

American Heart Association

The Medical Council of Thailand

The Physiological Society of Thailand

PUBLICATIONS

Birukova, A. A., **Chatchavalvanich, S.**, Oskolkova, O., Bochkov, V. N., & Birukov, K. G. (2007). Signaling pathways involved in OxPAPC-induced pulmonary endothelial barrier protection. Microvasc Res, 173-181.

Birukova, A. A., **Chatchavalvanich, S.**, Rios, A., Kawkitinarong, K., Garcia, J. G., & Birukov, K. G. (2006). Differential regulation of pulmonary endothelial monolayer integrity by varying degrees of cyclic stretch. Am J Pathol, 1749-1761.

Birukova, A. A., Fu, P., **Chatchavalvanich, S.**, Burdette, D., Oskolkova, O., Bochkov, V. N., & Birukov, K. G. (2007). Polar head groups are important for barrier-protective effects of oxidized phospholipids on pulmonary endothelium. Am J Physiol Lung Cell Mol Physiol, L924-L935.

Nonas, S., Birukova, A. A., Fu, P., Xing, J., **Chatchavalvanich, S.**, Bochkov, V. N., . . . Birukov, K. G. (2008). Oxidized phospholipids reduce ventilator-induced vascular leak and inflammation in vivo. Crit Care, R27.

Nonas, S., Miller, I., Kawkitinarong, K., **Chatchavalvanich, S.**, Gorshkova, I., Bochkov, V. N., . . . Birukov, K. G. (2006). Oxidized phospholipids reduce vascular leak and inflammation in rat model of acute lung injury. Am J Respir Crit Care Med, 1130-1138.

Singleton, P. A., **Chatchavalvanich, S.**, Fu, P., Xing, J., Birukova, A. A., Fortune, J. A., . . . Birukov, K. G. (2009). Akt-Mediated Transactivation of the S1P1 Receptor in Caveolin-Enriched Microdomains Regulates Endothelial Barrier Enhancement by Oxidized Phospholipids. Circ Res, 978-986.

ABSTRACTS

Chatchavalvanich, S., Geenen, D. L. Early Cell-Cell Coupling Contributes to Loss of Transplanted Stem Cell Retention and Efficacy. Poster Presentation, Basic Cardiovascular Sciences 2012 Scientific Sessions, New Orleans, LA, July, 2012.

Chatchavalvanich, S., Birukova, A. A., Garcia, J. G. N., Birukov, K. G. Signal Transduction and Gene Expression in Magnitude-dependent Mechanochemical Regulation of Lung Endothelial Barrier. Poster Discussion Session, 2006 American Thoracic Society (ATS) International Cponference, San Diego, CA, May, 2006.

Chatchavalvanich, S., Nonas, S., Miller, I., Kawkitinarong, K., Gorshkova, I., Bochkov, V. N., Leitinger, N., Natarajan, V., Garcia, J. G. N., Birukov, K. G. Oxidized Phospholipids Reduce Vascular Leak and Inflammation in Rat Model of Acute Lung Injury. Poster Presentation, 2006 Combined Annual Meeting of Central Society for Clinical Research (CSCR) and Midwestern Section American Federation for Medical Research (MWAFMR), Chicago, IL, April, 2006.